THESIS

This is to certify that the

dissertation entitled

THE EFFECT OF OVERLOAD ON THREE
DIFFERENT KINDS OF STEEL

presented by

MOHAMMAD GHOBADI

has been accepted towards fulfillment
of the requirements for

Ph.D. degree in Metallurgy

John F. Martin
Major professor

Date 2/2/84

THE EFFECT OF OVERLOAD ON THREE DIFFERENT KINDS OF STEEL

By

Mohammad Ghobadi

A DISSERTATION

Submitted to

Michigan State University

in partial fulfillment for the requirements

for the degree of

DOCTOR OF PHILOSOPHY

Department of Metallurgy, Mechanics and Materials Science

1984

ABSTRACT

THE EFFECT OF OVERLOAD ON THREE DIFFERENT KINDS OF STEEL.

By

Mohammad Ghobadi

Axial strain controlled tests were performed on plain carbon steels (1018, 1020, and 1030 steels) specimens of three different geometries in order to determine the effect of initial and periodic overloading on fatigue properties and microstructures. The overload was applied in the range that was expected to have a significant effect, the maximum strain amplitude being one percent. To study the effect of cycling on the microstructure, some of the specimens were polished and etched, and plastic replicas were taken at regular intervals during the fatigue test.

Initial overstrain resulted in a decrease of the fatigue life of all specimens. For 1020 and 1030 specimens periodic overstrain resulted in even shorter life, while 1018 specimens were not affected by periodic overstrain.

Processed replicas showed that fatigue microcracks initiate and propagate more rapidly in the coarser grains of 1020 and 1030 specimens compared with 1018 specimens.

TABLE OF CONTENTS

LIST OF TABLES

LIST OF FIGURES

CHAPTER 1

INTRODUCTION

The term fatigue is used to describe the behavior of a material that is subjected to a cyclically varying load of sufficiently large magnitude such that the material fails. What constitutes failure depends on the problem, but in general, failure means the fracture of the component. At any rate, some detectable change in mechanical behavior of the material must take place.

Generally speaking, fatigue consists of three stages: crack initiation, crack growth, and fracture. These stages sometimes overlap. In the conventional fatigue test, a particular type of specimen is subjected to a cyclic load with constant stress or strain amplitude and its life, i.e., the number of cycles to failure, is determined. In practice, conditions are different. For example a mechanism, especially a high speed one, is usually subjected to a loading program which varies continuously with time. In such circumstances, it is very likely that a member will be subjected to a very high stresses in some portion of the loading program while experiencing idling or rest intervals at some other part of the program. The stress history built up is thus a very complicated one. The harmful or beneficial effects of such a complex loading program on a member cannot be related to any level of stress. More sophisticated tests are thus required, and much work has been done in this direction. Before describing these, a few introductory remarks are in order.

Nearly all machine, engine and structural components are subjected to loads which result in stresses higher than their rated stresses. Such high loads are to a great extent occasional and are called overloading.

The effects of overloading depend on the magnitude of overload or overstrain and, in the case of cyclic overload, on the number of cycles. It has been observed in practice and confirmed by laboratory investigation that overloading usually decreases the strength of metals[1] and machine components which have been most highly overloaded are bound to fail during further service at normal loads.

The term overload as defined above is not precise enough, so the following definition will be adopted in this work. A specimen is said to have been overloaded (or overstrained) if the elastic strain is negligible in comparison with plastic strain. The following definitions are also used. If the specimen is subjected to an overload at the beginning of the experiment, it is said to have been initially overstrained. Periodic overstrain means that the specimen is overstrained repeatedly during the experiment such that two successive overstrains are separated by a block of cyclic straining with a lower amplitude. The term no-overstrain is, of course, self explanatory. Overstraining, or overloading, and its effects on the fatigue life are not well understood. Consequently, no quantitative and generally accepted rules are available[2]. But as design stresses are raised and the service life of many components is increased, the influence of occasional cycles of overload has become increasingly important[2,3].

The results published to date indicate that, for several materials, application of short initial blocks of high strain cycles result in a reduction of the fatigue life at subsequent low strain levels. On the other hand, periodic overstraining, especially during fatigue crack propagation, has a beneficial effect since it usually slows down the propagation process[4,5]. But this is not always the case. There is evidence that the crack propagation rate under periodic overstraining is 100 times higher than the rate under steady strain condition[1]. Such an overload or overstrain can cause considerable reduction in fatigue life[6].

The results referred to above are clearly phenomenological. No serious attempt has been made to examine the microstructural changes. In the work reported here, microstructural examination has been undertaken and correlation between the microstructural changes and observed phenomena attempted.

In this investigation three different kinds of specimens, smooth round hour-glass, thick-sheet hour-glass, and thin-sheet hour-glass profile, were prepared for fatigue testing to failure at room temperature. The specimens were made from the following grades of low carbon alloy structural steels: 1018, 1032, and 1020, respectively. These were chosen because of their wide use in structures and machinery. Furthermore, their microstructures are relativly simple, thus making the metalographical examinations easier. The experimental program consisted of three series of tests for each kind of specimens, namely: no overstrain, initial overstrain and periodic overstrain.

Since the surface grains are weaker compared with those inside the specimen, the changes start on the surface of the specimen. Because the initial changes in surface appearance, which result from fatigue action, are apparently extremely minute, methods which could reveal very small changes in surface appearance were employed. It was possible to display changes at an early stage, and to follow the course of these changes to the final, complete failure of the specimen. This was accomplished by using polished fatigue specimens, a simple plastic replica technique, and optical and electron microscope examinations.

The parameters under study were initial overloads and periodic overloads. Their effects on the fatigue life of three steels were demonstrated. The investigation consisted of both phenomological studies and direct microscopic observations of the fatigue process.

An attempt was made to compare the effects of periodic overstraining and initial overstraining with the case of non-overstraining on the life of each specimens.

CHAPTER 2

GENERAL REVIEW

In this chapter a brief review of litreature is presented and some of the results obtained in previous investigations is briefly discussed.

Fatigue is the main cause of most mechanical failures encountered in engineering practice. In the study of this phenomenon, it is convenient to treat the engineering and metallurgical aspects separately.

2.1 ENGINEERING CONSIDERATION OF FATIGUE

Systematic investigations of fatigue began with the work of A. Wöhler in 1852[7] and has been pursued intensively ever since. Much of the early work on fatigue is concerned with the determination of the fatigue (or endurance) limit. This is the maximum value of uniaxial cyclic stress below which no failure will occur. As mentioned in the introduction, the concept of endurance limit, while of importance, is not adequate. This is because the loading of most structural and machine elements are far more complex than the simple loading conditions under which the usual fatigue tests are performed. Furthermore, as will be discussed, the endurance limit itself depends on the loading history. It is thus clear that for a better understanding of the fatigue phenomenon, the effects of factors influencing it must be studied. The list of such factors is rather extensive and thus all of them cannot be discussed here. In the following, the most important of these factors will be considered and the results,that are reported in the literature briefly discussed.

The factors to be discussed are mean stress, initial overstrain, and periodic overstrain. The effect of loading history on the endurance limit and the question of fluctuating load amplitudes will be briefly discussed.

2.2 MEAN STRESS

In any real life fatigue problem, some mean stress or mean strain is present. In many cases, both mean stress and mean strain are present. It is well-known that the mean stress influences the fatigue life. For instance, tensile mean stresses shorten the fatigue life, while compressive mean stresses lengthen it. The process by which this comes about is not well understood, but alternate hypotheses abound. It has been suggested that stable stress-strain behavior, the rate of crack initiation, the size of the shear crack required to start a normal mode crack, the rate of propagation, and the crack size necessary to cause rupture are all influenced by the mean stress[3,6,8]. But this hypothesis has not been accepted by everyone. Some have argued that the amplitude of shear stress is the only factor influencing crack initiation and that mean stress has no effect[8]. It is widely believed that, for crack propagation, a tensile stress must be present. Therefore, during compressive cycling, a crack may initiate but it cannot propagate.

Since (for constant amplitude) the critical crack size is inversely proportional to the maximum tensile stress, one sees that the number of cycles required to produce a crack of critical size is smaller with a tensile mean stress than with zero or compressive mean stress.

The damage caused by occasional mean stress blocks is similar to that which results from initial overstrains provided that these blocks cause appreciable deformation[8]. Therefore, a loading with a compressive mean stress applied for a short block will cause the same damage as a few high strain cycles. Watson and Topper[3] have shown that, for short overload blocks, the sign of the mean stress has very little effect.

Topper and Sandor[6] conducted two experiments. In the first one the specimens were subjected to a stress pattern consisting of blocks of fully reversed cycles (i.e. no mean stress) followed by one cycle with some tensile mean stress. In the second experiment the specimens were cycled under a constant tensile mean stress. The total number of cycles in both experiments were the same. Comparison of the results were showed that the damage suffered by the specimen in the first experiment was half the damage suffered by the ones in the second experiment. This shows that most of the plastic straining caused by mean stress occurs during the first cycle. In other words, the remaining cycles do not have a very significant effect and hence their removal will not reduce the amount of damage appreciably.

In the presence of mean stresses, the experimental data show significant deviations from damage summation calculations (based on completely reversed strain-life data with constant amplitude)[9]. The present state of knowledge is not sufficient to make any quantitative predictions regarding the effects of mean stress on fatigue damage. The work of Topper et al[3] indicates that, at strain levels high enough to cause appreciable repeated plastic straining, the effect of mean stresses is somewhat diminished and damage summations are nearly one. However, when large plastic strains are followed by strains in the elastic range, the effect of mean stresses is appreciable and values show considerable deviations from one.

2.3 INITIAL AND PERIODIC OVERLOAD

A machine or structural element is occasionally subjected to loads which result in appreciable amounts of plastic strain. This, as pointed out in the Introduction, is called overloading. The plastic strain thus developed has a considerable effect on the fatigue properties and has thus attracted the attention of many investigators. A comprehensive study of initial overloading has been done by Kommer[10-12]. His conclusions may be summarized as follows. For a given cycle ratio, a high initial overstress followed by a lower stress (in some cases) show equal damage to endurance life at the high and low stresses.

On the other hand, if the initial overstress and cycle ratio is low, an actual increase of the normal endurance life at subsequent higher stresses can be observed. Furthermore, it has been shown that, in the case of steel, specimens of higher tensile strength and lower ductility are more sensitive to damage than those of lower strength and higher ductility[12]. Finally, it has been demonstrated that a low initial overstress will cause equal damage to endurance life at a subsequent higher stress, while a high initial overstress can cause much more than equal damage to endurance life at a subseqent lower stress. The work of Watson et al[13] concerning the effects of overstraining on the fatigue life of five different kinds of steels: SAE-1015 steel, CSA G4012, 950X, VAN-80 and AOS-1122; has shown that as a result of overstraining the fatigue life is drastically reduced near the fatigue limit. For three of these steels, the damaging effect is reduced with the increase in succeeding strain levels. SAE-1015 suffers the most damage as a result of overstraining, while VAN-80 appears to be unaffected by it. However, there is a considerable body of literature which shows that the fatigue life is improved when high amplitude pre-load or pre-strain is applied. Results, reported in a paper by Belyaev[2] on the effect of overloading on the fatigue life, indicate that prolonged overloading causes the failure of the component while a short overloading may result in its hardening.

Turning next to the effects of periodic overstrain, there is some evidence that periodic overloading can result in higher fatigue resistance under variable amplitude conditions.

The results obtained by Schijve[5] from work on Aluminum 2024-T3 Alclod and 7075-T6 Clad sheet show that an increase in the maximum stress increases the subsequent life-to-failure. Ditschum[4] has observed that periodic overstraining of ferrovac E leads to a higher fatigue life compared with the material that has been subjected only to an initial overstrain. On the other hand, the fatigue life of this material is only slightly increased if it undergoes constant amplitude cycling.

The work of Watson et al[14] on periodic overloads on mild steels has shown that, in the absence of residual stresses, periodic high overstrains cause appreciable fatigue damage and reduction of life. This can be explained by the fact that overstrain accelerates Stage I, and to a lesser extent, Stage II of crack growth.

2.4 EFFECT OF LOAD HISTORY ON THE FATIGUE PROPERTIES

As mentioned previously, fatigue properties are extremely history-dependent. Bennet[15] investigated this history dependence by subjecting a series of specimens to initial overload and then retesting them at a second stress level and observing the relative number of cycles to failure. On the basis of his experiments, Bennet reached the conclusion that, when a specimen is loaded at different stress levels, the apparent rate of damage depends on the value of both stresses. He observed that, if the damage caused by one stress level is measured by the damage occuring at a subsequent stress level, the overall damage is dependent on both stress levels. Specifically, if the initial stress is higher than the stress applied subsequently, the damage suffered is higher and it decreases later. The opposite is the case when the specimen is first subjected to a low stress and then to a higher one. These and other results obtained by Bennet and Kommers lead to the conclusion that the fatigue limit is a function of stress history of the component. More generally, load history must be taken into account when determining the fatigue properties of a material. Dolan et al[16] performed a number of tests to failure on SAE-2340, SAE-1045 and 75S-T aluminum alloy on both notched and unnotched polished specimens. They reached the following conclusions. For ferrous metals, the fatigue limit is highly dependent on stress history, and it is therefore not well-defined. Generally, repetitions of an understress alternated with repetitions of a stress 10 to 20 percent above the original fatigue limit, result in an appreciable increase in fatigue life. This can be interpreted as an increase in fatigue limit.

Recent investigations have shed some light on the problems encountered in complex history analysis. It is now recognized that difficulties encountered are mostly due to the fact the sequence effects were not properly taken into account in the early work in this area since much of this work was concerned with determining the effect of overloading on the fatigue limit[8,17]. The results obtained from these investigations have indicated both beneficial and detrimental effects, and this has led to confusion.

As was pointed out in the Introduction, the crack initiation and propagation which leads to the fracture of a component is of great importance in the study of fatigue. These phenomena are explained in terms of metallurgical concepts. The remainder of this chapter is devoted to a brief examination of these concepts and their significance.

2.5 METALLURGICAL ASPECTS OF FATIGUE

The process of crack nucleation starts with slip. In some grains the slip bands form very fine cracks which can be seen only at very high magnification. As the body undergoes cyclical loading, the cracks grow and combine into a few major cracks which can be seen with the unaided eye. The growth of a crack (or cracks) continues until a critical size is reached and fracture occurs suddenly. The speed at which these processes take place depends on the magnitude of the stress. If stress is increased, the speed would likewise be increased.

Crack initiations follow the occurrence of slip in grains[18]. It is evident that the microstructure of a metal has great influence on its behavior under cyclic loading. It should also be realized that the microstructure of a metal can be altered by cyclic deformations. These alterations may have great influence on the fatigue performance of a material.

Most structural metals are made up of a large number of ordered crytals or grains. Such materials are called polycrystalline. Two different grains are separated by the grain boundaries, which have a great influence on the behavior of metals under different operating conditions. It is interesting that, while grain boundaries are regions where the lattice is imperfect, they are not necessarily regions of weakness.

It is well-known that the grains are anisotropic and their mechanical properties are, in general, different. Since neighboring grains have different orientations, the slip planes are not parallel. As a result, slip is hindered when the metal is strained into the plastic range. The grains at a free surface are less-constrained than the grains in the interior of the metals. Accordingly, plastic deformation in surface grains takes place at a lower stress than in internal grains[19]. Thus, surface grains behave in a more ductile manner. Since, in most cases, the stress is maximum at the surface[19], it follows that surface grains deform more than the grains in the interior. It is well-known that fatigue cracks originate at the free surface. Furthermore the surface is both a favored place for dislocation movement and a place for the formation of slip-band grooves. The orientation of some grains is such that the places of slip and planes of maximum applied shear stress coincide. In fatigue experiments, slip appears first in those crystals in which the resolved shear stress on slip planes has the highest value[20]. In ductile metals, dislocations in each grain move along crystallographic planes and thereby cause slip. Thus, within each grain, there are one or more planes sliding relative to each other. Slip occurs both in monotonic and cyclic loading[21]. Although the slip lines produced by these two types of loading are in many ways similar, there are some subtle differences.

The most remarkable difference is that slip bands appear in groups or striations which are more-or-less evenly spaced in each grain. These striations first appear after a few thousand cycles. As the cyclic loading continues, they become broader and more pronounced. This broadening goes on until either the bands cover the surface of a particular grain or failure by cracking occurs. If examined under an electron microscope, the slip bands in a specimen subjected to a steady stress, are seen to be straight and parallel whereas those in a specimen subject to fatigue, appear to be curved and generally shorter. This can be clearly seen in Figure 2-1. In general, most of the directions of the slip lines are the trace of crystallographic plane. It is interesting that the slip bands produced by fatigue hardly ever cross the grains, although striations (or grouped bands) sometimes extend from one grain boundary to another.

Using electron microscopy, it has been shown[19] that both slip band intrusions and extrusions occur on the surface of a metal subject to fatigue loading. Figure 2-2 shows a typical extrusion schematically[22]. Slip band intrusions act as stress raisers causing high stress concentrations and a natural location for crack initiation. Shear stresses are the main controlling factor in this type of slip. If the gross stress (or strain) is raised or the material is subjected to a larger number of cycles, the number of slip bands and their lengths increase. It was noted previously that the slip lines are, for the most part, contained within each grain. As the number of cycles is increased, more and more slip lines appear and the slip bands themselves thicken. These "thick" bands are the source of fatigue cracks. It is worth noting that slip band intrusion is a local phenomenon occurring at regions of high stress and strain while most of the grains of the component may be free of any slip, even at fracture. The removal of several microns from the surface of the component by electropolishing eliminates most of the slip bands. Some of these slip band do remain and become more distinct. These have been called persistent slip bands. The number of these persistent slip bands increases as the cycling goes on. For most metals and

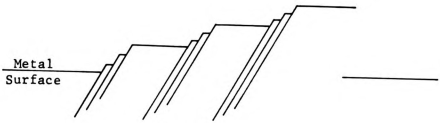

(a) Steady stress

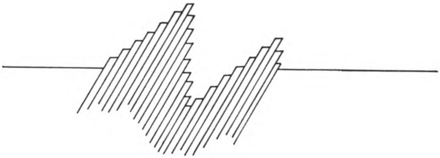

(b) Cyclic stress

Figure 2-1 Slip in ductile metals due to external loads.
(a) Static, steady stress. (b) Cyclic stress.

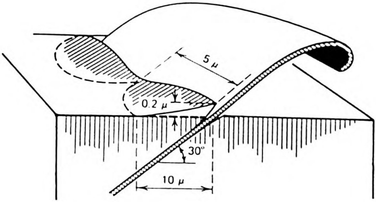

Figure 2-2 Schematic Extrusion in a slip band.

alloys there is an apparent fatigue limit associated with the formation of persistent slip bands. If the stress is not high enough for their formation, no fracture takes place[23]. It has been observed that, in a large number of materials, the fatigue cracks initiate in these persistent slip bands. Very little is known about the mechanism of slip band production and crack initiation apart from the fact that cracks always start on the slip planes, which have the highest resolved shear stress.

The fatigue life of a component can be significantly increased by removal of persistant slip bands. In some cases, the life of a component has been extended indefinitely by intermittent cycling and electropolishing. These observations strengthen the widely-held view that fatigue is very much a surface phenomenon and its early stages are controlled by surface conditions.

CHAPTER 3

3.1 FATIGUE DAMAGE ANALYSIS TECHNIQUES

The accurate prediction of fatigue life of metalic components has long preoccupied fatigue researchers. Various properties of metals, such as ultimate strength, hardness, true monotonic fracture ductility and strength, and cyclic stress-strain properties have been used as indices of fatigue life.

Use of these properties, in conjunction with empirical formulas, permits an estimation of the approximate account of the phenomenological fatigue damage that occurs on smooth specimens subjected to completely-cyclic loading.

For a given material, one can plot a S-N curve which is a diagram showing the variation of stress versus the number of cycles to failure. Using this diagram, the endurance limit and the fatigue life of the specimen can be determined.

While an S-N curve provides useful information, it is inadequate for practical problems since, in most cases, a component is subjected to more than one stress level. The question, then, is how to account for varying stress levels in determining the fatigue life of the component.

To answer this question, a number of "cumulative damage" theories have been proposed. In one such theory, it is assumed that no matter how stress varies from one cycle to the next, the damage will accumulate. Damage at each stress level is defined as the number of cycles divided by the number of cycles that result in failure at that stress level. Under a complex loading, failure will occur when the sum of the damage increments reaches one. It is clear that one needs a complete S-N curve for each individual cycle in order to predict the fatigue life under a complex loading.

It is reasonable to assume that, at any particular stress value, each cycle contributes an equal amount of damage and, furthermore, that the cumulative damage under cyclic loading and the net work absorbed are proportional. These are the assumptions on which one of the most widely used damage accumulation rules, the so called Miner's rule[24], is based. To derive this, let W and N_f represent the net work absorbed and the number of cycles at failure for some stress level. Denoting the net work absorbed by the specimen as w_i and the number of cycles as n_i for the same stress level, one has

$$w_i/W = n_i/N_f \tag{3-1}$$

with

$$\sum w_i = W \quad \text{or}$$

$$\sum w_i/W = 1. \tag{3-2}$$

Substituting into this from (3-1), we have:

$$\sum n_i/N_{f_i} = 1 \tag{3-3}$$

where N_{f_i}, $i = 1,\ldots, k$, are fatigue lives at given load levels, and n_i, $i=1,\ldots,k$, are the number of cycles acting at each load level.

In addition to assumptions already mentioned, Miner's rule assumes that the load is completely reversible with no mean stress. Furthermore, the damage which occurs is independent of the loading history. Moreover, there is no sequential effect.

Unfortunately, none of these assumptions are quite true. For instance, experiments contradict the last assumption regarding the order of amplitude change. Given identical block sizes and amplitudes, the high-to-low causes more damage than the low-to-high one. That it should be so is reasonable and can be explained. The high loads initiate cracks which then propagate at lower loads, but smaller loads cannot initiate cracks as rapidly as the high loads.

Despite its shortcomings, the linear damage accumulation theory yields fairly accurate results when its basic underlying assumptions are nearly satisfied.

3.2 STRESS-STRAIN HYSTERESIS LOOPS

The stress-strain hysteresis loop, shown schematically in Figure 3-1, is the best means of describing the cyclic behavior of metals. In a hysteresis loop, the total strain range ($\Delta\varepsilon$) is twice the strain amplitude ($\Delta\varepsilon/2$), and the total stress range ($\Delta\sigma$) is twice the stress amplitude ($\Delta\sigma/2$). The total strain amplitude can be represented as the sum of its elastic and plastic components:

$$\Delta\varepsilon/2 = \Delta\varepsilon_e/2 + \Delta\varepsilon_p/2. \tag{3-4}$$

Using Hook's law one can write

$$\Delta\varepsilon_e = \Delta\sigma/E \tag{3-5}$$

where E is Young's modulus and hence

$$\Delta\varepsilon/2 = \Delta\sigma/2E + \Delta\varepsilon_p/2. \tag{3-6}$$

3.3 CYCLIC HARDENING AND SOFTENING

Application of a completely reversed cyclic load to a metal results in either hardening or softening depending on its initial condition and the load amplitude. These phenomena are called cyclic

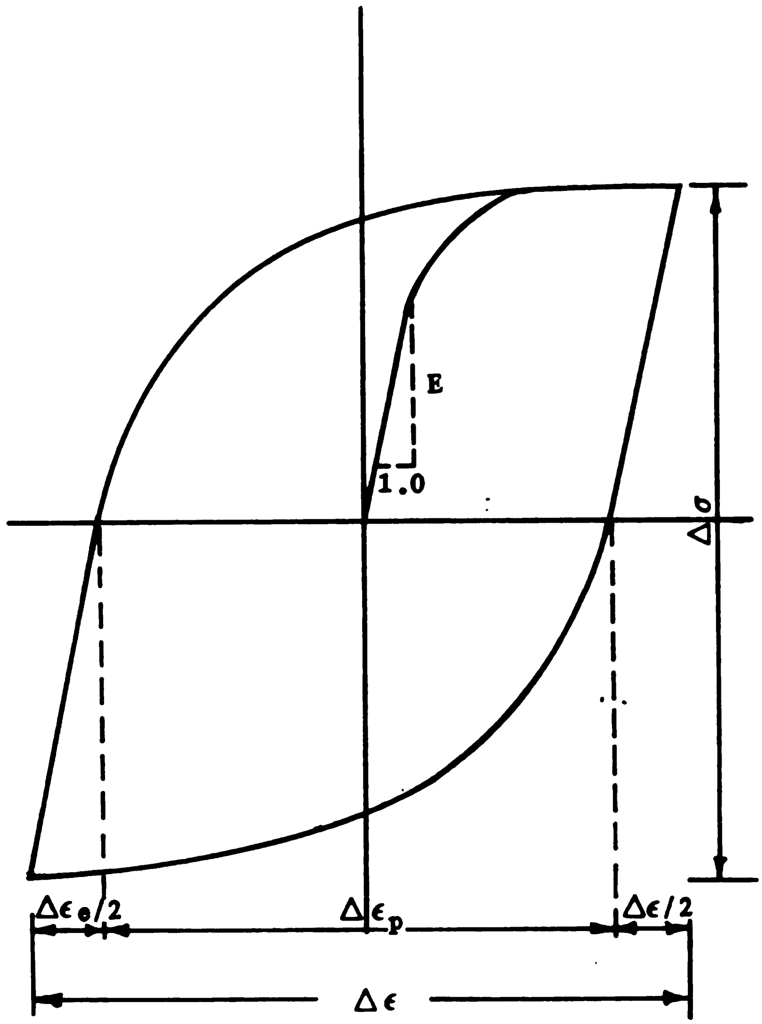

Figure 3-1 Schematic of a Stress-Strain Hysteresis Loop.

hardening or softening. After a period of cyclic hardening and softening, an intermediate strength level is attained. This represents a cyclically stable condition. Fatigue hardening is more complicated than the work-hardening encountered in the familiar static tests. This complication is mainly due to the reversal and repetition of loads. Fatigue tests can be carried out under stress or strain control. The behavior of the material, however, would be different as can be seen from the Figures 3-2 and 3-3[25,26]. These Figures show cyclic stress-strain behavior of an initially annealed metal. Annealed metals have the characteristic of getting harder when they are subjected to high strain (or stress) cycling and becoming softer when subjected to low strain (or stress) cycling. In Figure 3-2 the cyclic behavior under stress control is depicted. It can be seen that, as the material softens, the strain amplitude increases. Figure 3-2(b) shows the hardening procedure. Figure 3-3 on the other hand shows the behavior of the material under strain control. One can get a fatigue curve by drawing the maximum stress against the number of cycles in a strain-controlled test. If the specimen is initially work-hardened, it would soften and cyclic softening would result.

Fatigue softening-hardening characteristics can be shown on curves that indicate the variations of stress versus cycles of loading. This curve, which depends on the initial condition of the material, also shows its equilibrium fatigue behavior. Stable stress and strain amplitudes can be related by a power law of the form[27]

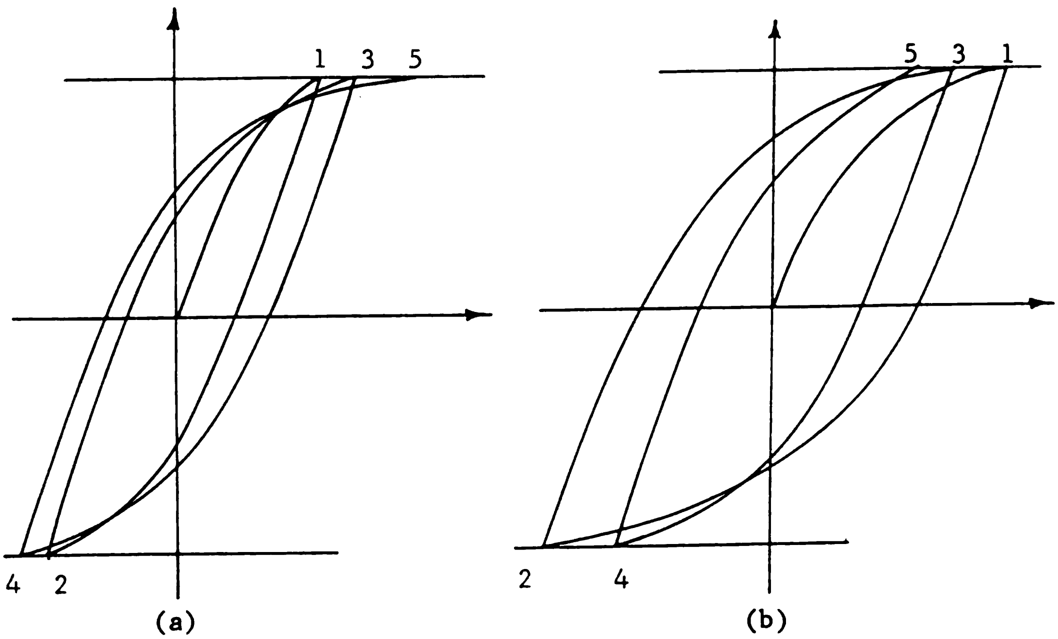

Figure 3-2 Stress-Strain Loops for Stress Control
(a) Cyclic Sofening (b) Cyclic Hardening.

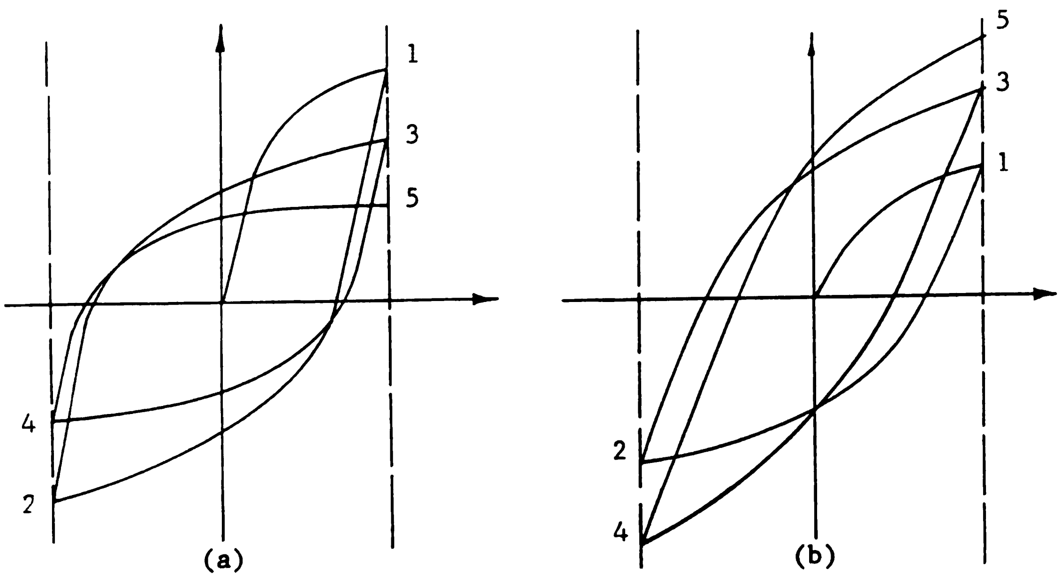

Figure 3-3 Stress-Strain Loops for Strain Control
(a) Cyclic Softening (b) Cyclic Hardening.

$$\Delta\sigma/2 = K' \ (\Delta\varepsilon_p/2)^{n'} \tag{3-7}$$

in which K' is the cyclic strength coefficient and n' the cyclic strain hardening exponent.

3.4 STRAIN LIFE ANALYSIS

In experiments carried out at different strain ranges, it has been observed that if a log-log plot of the stable plastic amplitude, $\Delta\varepsilon_p/2$, versus the number of reversals to failure, $2N_f$, is drawn, one will generally get a band of points narrowly scattered about a straight line. The plastic strain-life data can be related in the following form:

$$\Delta\varepsilon_p/2 = \varepsilon_f' \ (2N_f)^c \tag{3-8}$$

where ε_f' is the fatigue ductility coefficient and $2N_f$ is the number of reversals to failure. In a similar fashion a log-log plot of stable stress amplitude, $\Delta\sigma/2$, versus the number of reversals to failure, $2N_f$, could be drawn. This again yields a straight line.

From this plot the stress amplitude and life can be related by the formula:

$$\Delta\sigma/2 = \sigma_f' \ (2N_f)^b. \tag{3-9}$$

Dividing (3-4) by the Young's modulus, E, one gets:

$$\Delta\varepsilon_e/2 = (\sigma_f'/E)\ (2N_f)^b \qquad (3\text{-}10)$$

which gives the elastic-strain amplitude in terms of fatigue-strength coeficient, σ_f', and the fatigue strength exponent, b.

Substitution of (3-9) and (3-10) into (3-4) yields:

$$\Delta\varepsilon/2 = (\sigma_f'/E)\ (2N_f)^b + \varepsilon_f'\ (2N_f)^c. \qquad (3\text{-}11)$$

The above equation, called the strain-life relation, is the foundation of the cyclic strain-based approach to fatigue.

In Figure 3-4 the heavy curve represents equation (3-11), while the two straight lines show the elastic strain versus $2N_f$ and plastic strain versus $2N_f$. The data to be used for drawing these graphs are obtained from testing smooth specimens to failure under fully reversed constant amplitude strain control.

The application of the formulas discussed here will be found in Chapter 6 in connection with the experimental data.

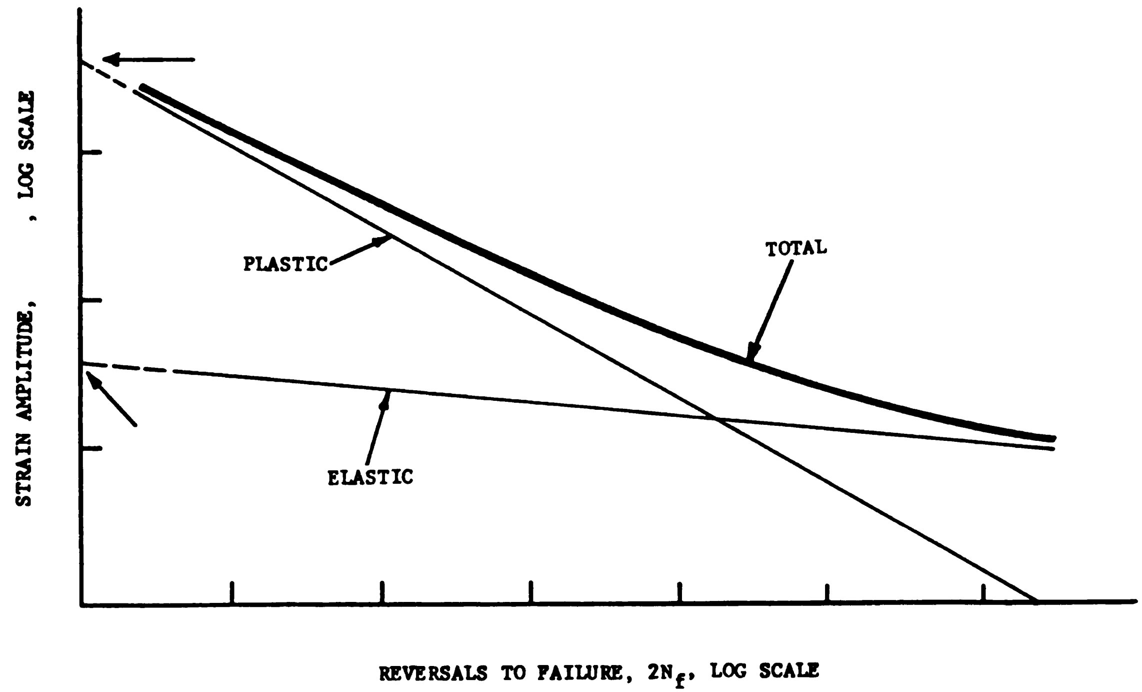

Figure 3-4 Strain-Life Curves showing Total, Elastic and Plastic Components.

CHAPTER 4

MATERIAL AND SPECIMENS

For the investigations reported here, three widely-used low carbon steels were chosen. These were 1018, 1020, and 1030. Detailed information regarding the chemical compositions and mechanical properties of these materials is given in Tables 4-1 and 4-2, respectively.

The specimens used were of three different types:

1) Thick-sheet hour-glass specimens. These were made from 1030 sheet steel of 7.62 mm (0.03 inch) thickness. In order to make the metallographical structure of these specimens as similar to the 1018 and 1020 specimen as possible they were heat-treated. To accomplish this, they were annealed at 850° C for 20 minutes in an electric furnace and left to furnace cool. Figure 4-1 shows the dimensions and geometry of these specimens.

2) Thin hour-glass sheet specimens. These specimens were made from 1020 sheet steel of 1.78 mm (0.070 inch) nominal thickness. This material was cold-rolled and annealed. The gage sections of all the

Table 4-1 Chemical Composition of the Specimens.

	carbon	Manganese	Phoshorus	Sulfur
1018	0.18	0.70	0.20	0.025
1020	0.20	0.41	0.10	0.011
1030	0.30	0.70	0.20	0.025
	Weight%			

Table 4-2 Mechanical Properties of Specimens Material as received.

Material	Tensile Strenght psi	Yield Strength psi	Elongation in 2 in., %	Reduction in area %	Brinell hardness
1018	62	43	20	45	120
1020	58	40	20	45	116
1030	73	51	16	39	142

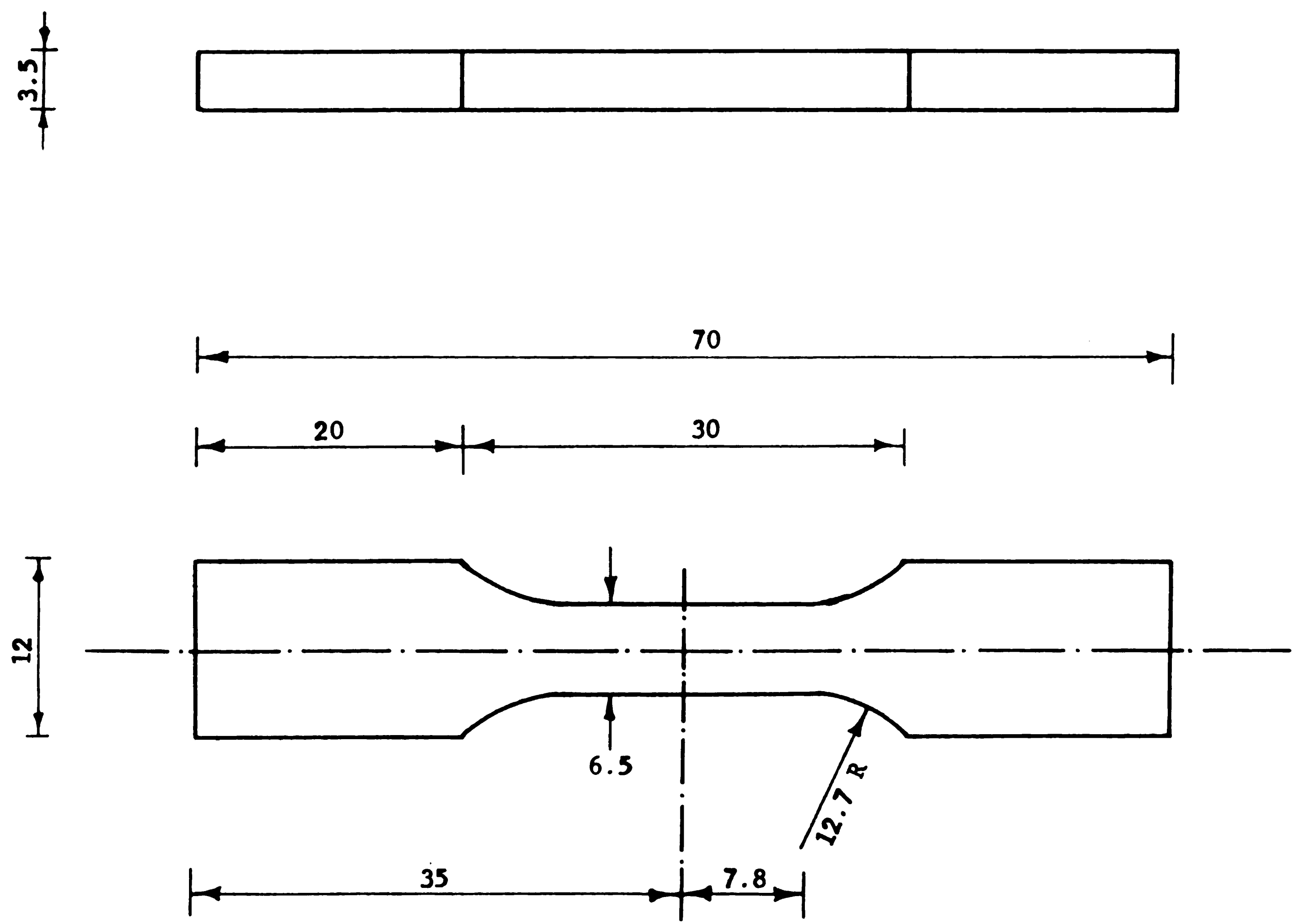

Figure 4-1 Specimen Configuration of Thick Sheet Specimens (1030 Steel).

(All dimensions are in millimeter).

thick-sheet and thin-sheet specimens were parallel to the rolling direction. Figure 4-2 shows the dimensions and geometry of these thin sheet specimens.

3) Bar specimens. These specimens were machined from an extruded bar of 1018 steel of 15.88 mm (0.625 inch) diameter. Figure 4-3 shows the geometry and dimensions of the bar steel specimens. Although machining might have caused some surface hardening, no heat-treatment was done on specimens made of the 1018 and 1020 steels.

The flat side (surface A and B of Figure 4-4) of all 1020 and 1030 specimens, that were chosen for metallographical examination, were polished. The polishing was done in three stages. First, the specimens were manually polished on 180, 240, 320, 400, and 600 grit papers. Then, in the second stage, lapping wheels were used. These wheels were covered with a short-napped felt cloth and impregnated with alumina slurry. Alumina particles of 1.0, 0.3, and 0.05 micron sizes were used for fine polishing. In the second stage of polishing, the A and B surfaces of all specimens were examined with an optical microscope to make sure that no circumferential markings were present. In cases were such markings were found, the polishing was repeated until they were removed. In view of the fact that cracks generally initiate at surface damages and irregularities, and the results obtained from tests on such specimens are questionable, these precautions were very necessary. In order to reduce the likelihood of crack initiation at the corners, all specimen corners were slightly pol-

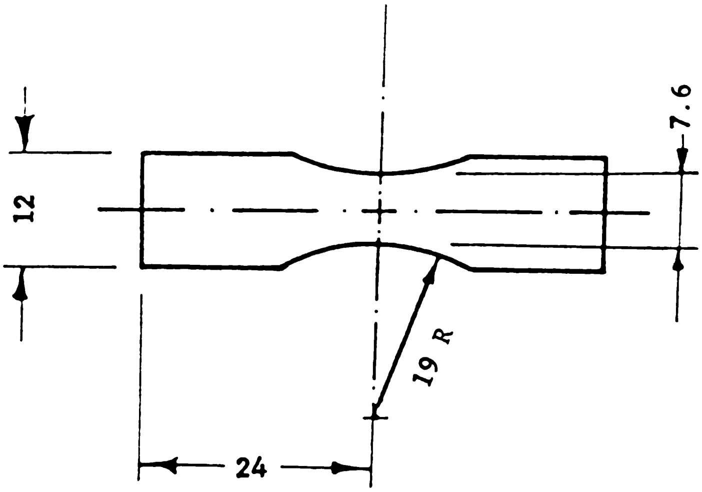

Figure 4-2 Specimen Configuration of Thin Sheet Specimens (1020 Steel).

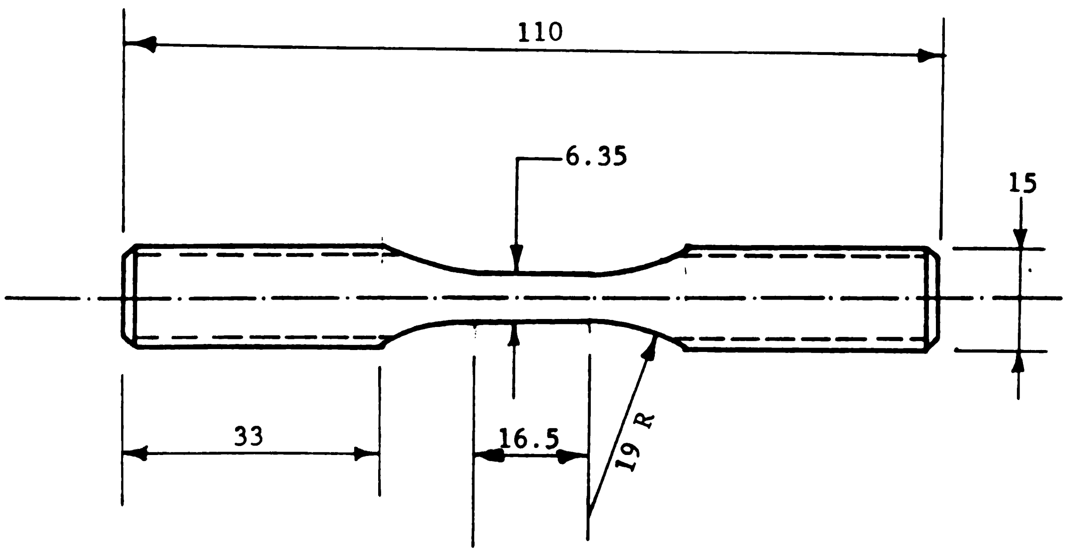

Figure 4-3 Specimen Configuration of Cylindrical Specimens (1018 Steel).

(All dimensions are in millimeter).

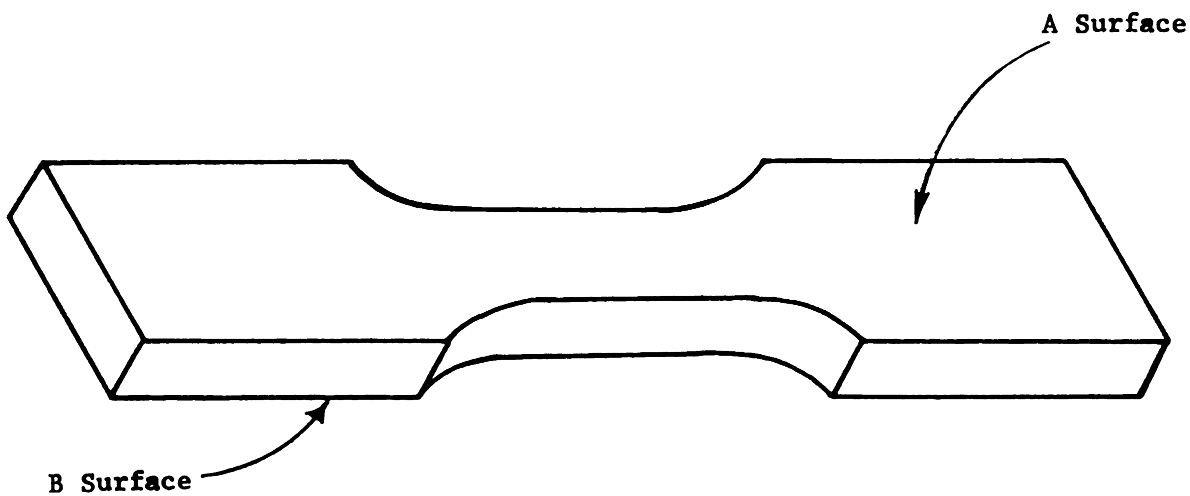

Figure 4-4 Pictorial representation of Thick Sheet Specimens.

ished. Despite this precaution, the cracks initiated at the corners in nearly all specimens tested. Finally, all specimens were electro-polished using a solution of 20 percent perchloric acid and 80 percent glacial acetic acid. The electro-polishing was done at room temperature with a voltage of 10-20 volts. Once the specimens were polished, surface replicas were taken of the whole gage length and were then examined under the microscope and photographed.

In preparing the bar steel specimens, the gage lengths were polished with 600 grit paper followed by 0.3 and 0.05 micron alumina powder. To get a mirror-like surface finish, an electro-chemical reagent of 20 percent perchloric acid and 80 percent glacial acetic acid was employed. The polishing was done with a stainless steel cathode and a voltage of 5 to 8 volts. This took about 2-3 minutes.

After electro-polishing, the following reagent was used: nital, consisting of 5 milliliter nitric acid (HNO_3) and 95 milliliter methyl alcohol(CH_3OH). Specimens were immersed in the nital solution for about thirty seconds at room temperature. This etchant was found to be very effective in delineating both the grain boundaries and slip bands.

To obtain more micorostructural details, the specimens were first etched and then polished and re-etched. In these cases, some surface material had to be removed since the grain boundaries would otherwise have appeared wide upon re-etching.

Treating the specimen in this way gave a very smooth and polished surface in which the smallest change could be seen. It had the added advantage of removing the worked surface layer which is always present in surfaces that have been polished mechanically. This is important since the worked surface may effect the fatigue behavior. Furthermore, as a result of this chemical polishing treatment, many features of the microstructure of the specimen were revealed. The study of these features led to the establishment of the relationship between the structure of the specimen and the starting point of the fatigue cracks.

CHAPTER 5

EXPERIMENTAL TECHNIQUE

The machine used for testing all specimens was an axial loading electro-hydraulic closed loop, servo-controlled mechanical test system with a maximum load capacity of 11 kips (48.928 KN).

The cyclic fatigue data collected for this investigation were generated under completely reversed strain control with zero mean strain. A system of the type used is shown in Figure 5-1. The command signal used in the investigations was a sine function. In each test, the frequency was the highest possible frequency compatible with preservation of amplitude and prevention of the distortion of the hysteresis loop. When taking data, the frequency was lowered to between 0.1 to 0.2 Hz.

To measure strain in the 1018 bar steel specimens and 1032 thick sheet specimens, a clip-on extensometer was directly attached to the specimens. The gage length over which the strain was measured was 0.5 inch.

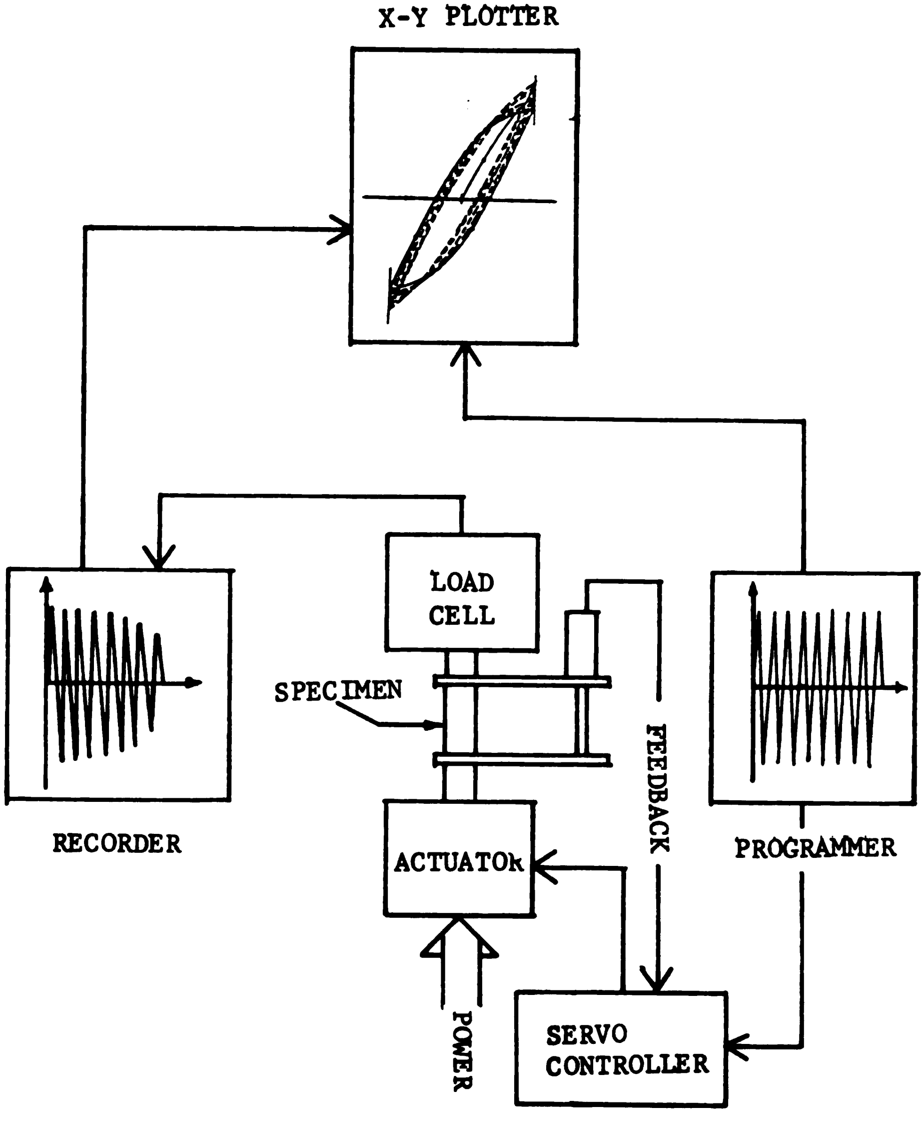

Figure 5-1 An idealized cycling test system which was used for all tests.

To prevent slippage of the knife edges and reduce contact stresses at the points where these were attached to the specimen, a soft plastic tape was wound around the specimens.

Occasionally the extensometer drifted because the knife edges had not settled completely into the plastic tape. In such cases, enough time (10 to 15 minutes) was allowed for the effects of creep to die out.

Because of the relatively small thinness (which creates a problem with buckling) and small gage length of the 1020 sheet steel specimens, the attachment of an extensometer similar to that used for the other two types of specimens was not possible. Instead, a transverse extensometer was attached (Figure 5-2) to measure the transverse strain, ε_{tr}, across the thickness of specimens. The details of contact between the extensometer and the specimens are given in Figure 5-3. It can be seen that on one side of the specimen there is a point contact while the other a flat surface is in contact with the specimen. The gage length was the thickness of the specimens. Axial stress was taken to be equal to the applied load divided by the minimum cross sectional area. The axial strain, which was used as the controlling parameter for all tests, was calculated from the axial stress and transverse strain. The relation between transverse strain ε_{tr} axial stress, σ, and the total axial strain is given by:

$$\varepsilon = (\sigma/E) - (1/\mu_p)\,[\varepsilon_{tr} + \mu_e\,(\sigma/E)] \qquad (5\text{-}1)$$

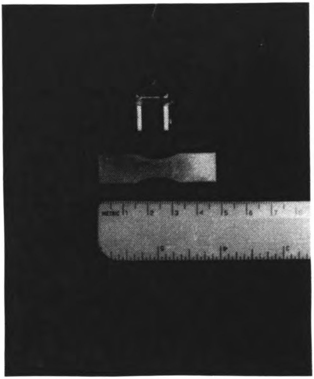

Figure 5-2 Sheet Steel Specimen and Extensometer.

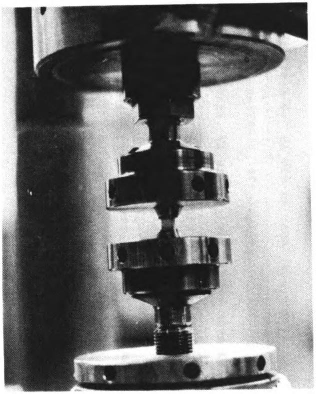

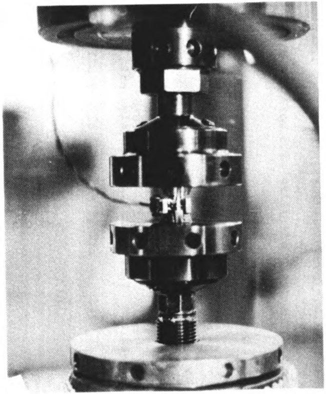

Figure 5-3 (a) Sheet Steel Specimen mounted in load frame.

(b) Sheet Steel Specimen mounted in load fram with extensometer attached.

in which E is the elastic modulus, and μ_e and μ_p are the elastic and plastic Poisson ratios, respectively. The elastic strain component is determined from σ/E, while the plastic strain component is given by:

$$\varepsilon_p = (1/\mu_p) [\varepsilon_{tr} + \mu_e (\sigma/E)]. \tag{5-2}$$

Assuming that no volume change occurred during plastic deformation, the plastic Poisson ratio was assumed to be 0.5 which, upon substitution in Equation (5-1), resulted in:

$$\varepsilon = (\sigma/E) - 2 \varepsilon_{tr} - 2 \mu_e (\sigma/E). \tag{5-3}$$

The controlling parameter throughout the entire test was the total strain given by the above equation whose analog circuit is shown in Figure 5-4. As can be seen, the inputs to the circuit are the load P and transverse strain, ε_{tr}. The circuit contains two variable potentiometers, V1 and V2, which were used to set the circuit such that the final output would be the total strain. To do this, first a dummy load voltage was applied. Since the specimen cross-section area and its Young's modulus were known, V1 was adjusted such that its output would be the elastic strain. Then, with the specimen undergoing cyclic loading in the elastic range under a load-control, potentiometer V2 was adjusted such that its output at amplifier 2 would be zero. This output is the analog of plastic strain. Finally, amplifier 3 gives the sum of elastic and plastic strain, which is the desired controlling parameter, i.e. total strain. A more detailed account can

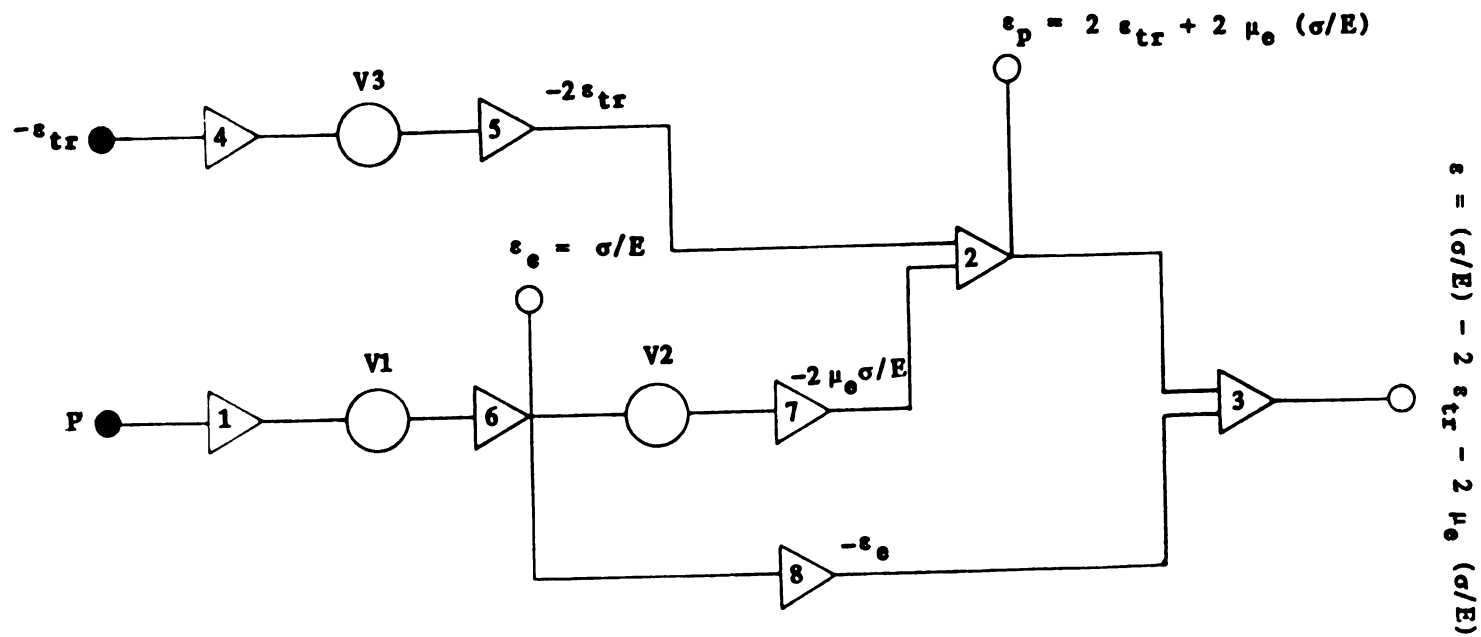

Figure 5-4 Schematic of analog computer strain circuit.

be found in[28].

A load cell mounted in series with the specimens was used to measure loads. In experiments with 1032 flat specimens and 1020 sheet steel specimens wedge type grips were used. The grips were chosen with care so that they would produce sufficient friction to hold the specimens in place throughout the loading program. To prevent buckling of the 1020 sheet steel specimens, a set of shims, as shown in Figure 5-5, were used to support the specimens.

In the presence of small plastic strains, a small misalignment or distortion due to clamping can have a disproportional effect on the results. To eliminate these difficulties, Molten Wood's metal joint grips were used.

Under isothermal conditions and frequencies in the 0.1 to 30 Hz range, the life of a metal is virtually independent of frequency[29]. However, when isothermal conditions cannot be maintained, the heat developed as a result of plastic distortion may cause significant changes in the properties of the metal. Such changes, however, are rarely encountered at room temperature.

An X-Y recorder was used for the permanent recording of the data (see Figure 5-6 for entire test facility). For this purpose, analog signals of load and strain were fed into an analog computer. Here, they were scaled to produce stress and strain on the recorder which

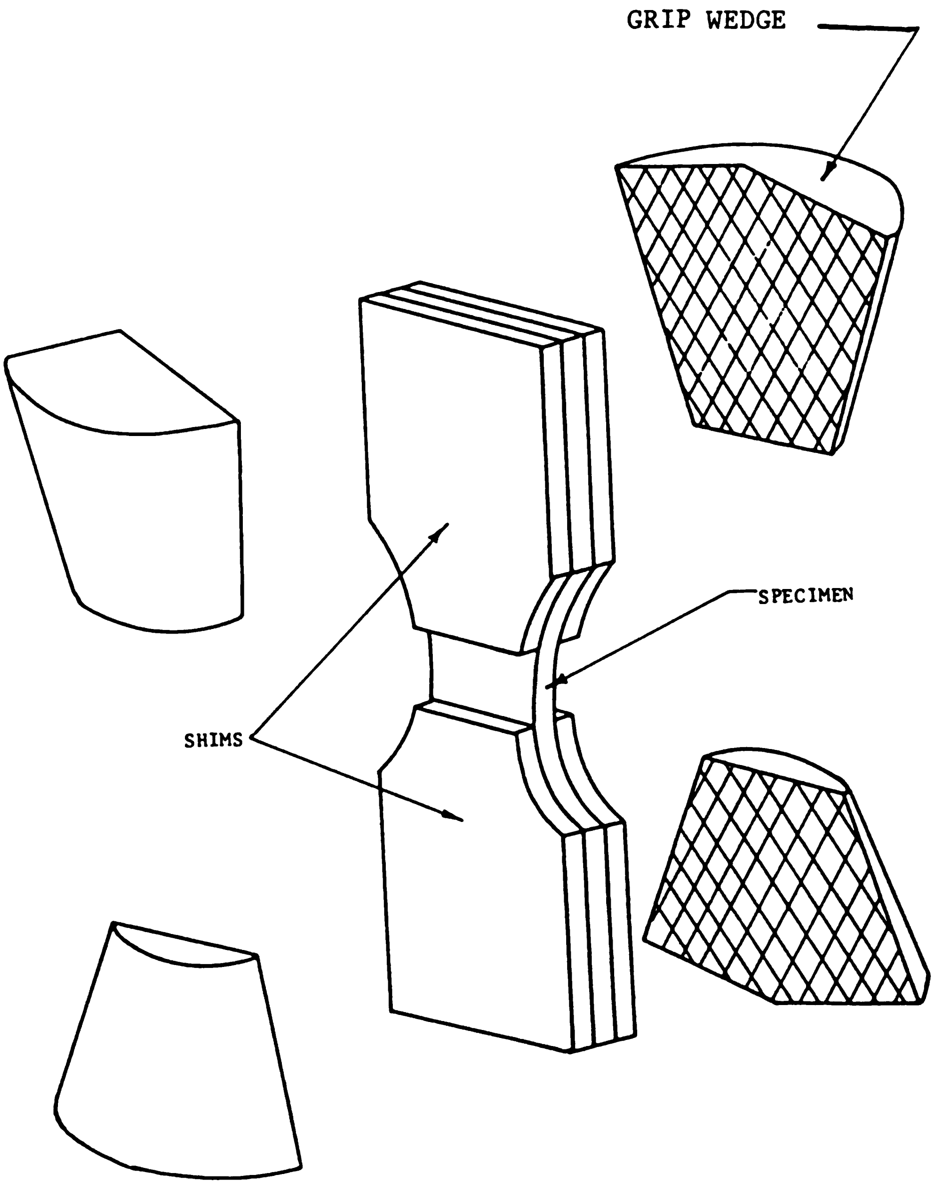

Figure 5-5 Specimen, Grips and Shims for Thin Sheet Steel Specimens.

Figure 5-6 Test facility. From left to right: Load fram, X-Y plotter, MTS control unit and Analog computer.

thus recorded the complete hysteresis loop. To record the stress-strain response of the specimens to overstraining, all such overstrains (initial or periodic) were done at low frequencies between 0.06 to 0.08 Hz. During all tests, the frequency was changed often to allow the application of a large number of cycles within a reasonable time. For monitoring loads and strains in all ranges of frequency, an oscilloscope with variable persistence was used. This ensured that any change in the system which depended on the frequency would be detected.

Where possible, the hysteresis loops were recorded at fixed intervals (namely after 1, 2, 3, 5, 10, 20, 30, 50, 100, ...cycles).

Three different load patterns were used for this study:

1) No overstrain. A constant amplitude completely reversed cyclic strain.

2)Initial overstrain. An initial cyclic overstrain followed by completely reversed cyclic strain.

3) Periodic overstrain. Periodic overstrain between every 100,000 cycles of completely reversed cyclic strain.

For both the initial and periodic overstrains (tests of type 2 and 3), the maximum strain used was ±0.010 (one percent). Each overstrain block consisted of 20 decreasing cycles and was followed by a constant magnitude cycling. Before the start of the test, replicas of the whole gage section area were taken and then the strain gage was mounted.

In experiments with strain control, it often occurs that a specimen continues to cycle after it has been broken into two pieces and the tensile load response has dropped to zero. This causes "hammer damage" and results in inaccuracies in the number of cycles to failure. To prevent this shut-off, a device known as an underpeak detector, which signals the initiation of a crack, was used. Figure 5-7 shows the behavior of a specimen in such a situation.

Studying the changes in the surface of the specimens due to fatigue typically involves the removal and remounting of each specimen during the test. In order to improve the procedure, plastic replicas were found to be ideal since they caused no damage to the surface and were very efficient. The replica procedure consisted of the following steps:

1) electro-polishing the specimen by conventional methods and then making two sets of plastic replicas of the whole gage section of each specimen in the virgin condition;

2) mounting the specimen, cycling it at the specified loading and then repeatedly overstraining, with plastic replicas made before and

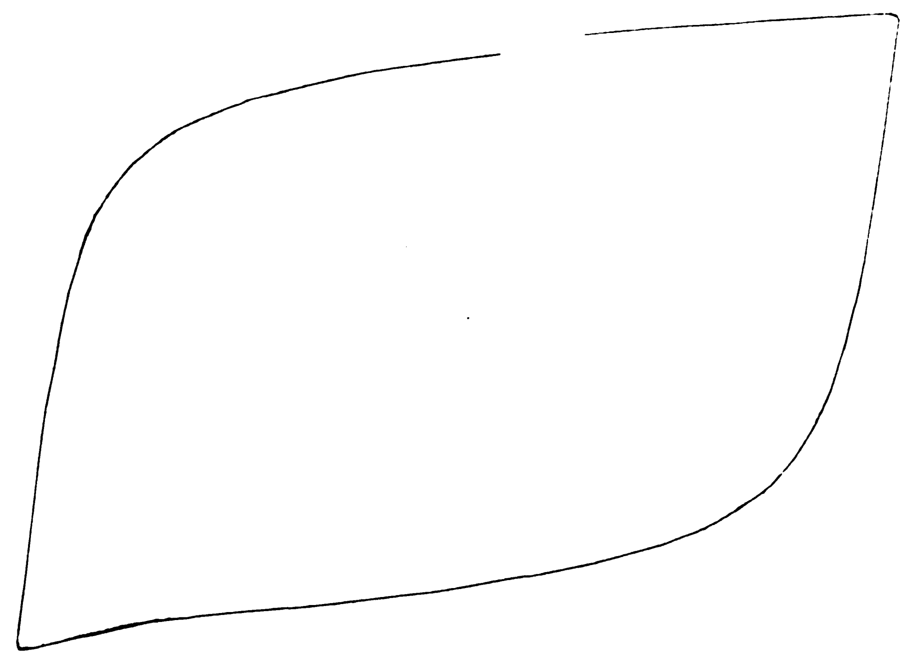

Figure 5-7 Indication of cracked specimen by irregularity in compressive half of hysteresis loop.

after each overstrain (the specimen remains mounted on the machine); and

3) in non-overstrain and initial overstrain cases, replicas were taken after each 100,000 cycles

In all the steps detailed above, the procedure was repeated until failure occurred. In all cases, each replica was allowed to dry (2 to 5 minutes) and then was stripped off, mounted on a glass slide, and labeled. Afterwards the replicas were shadowed with vaporized chromium for observation with both light and electron microscopes. In preparing the replicas, one difficulty was encountered, namely that it was not possible to take a carbon replica directly from the specimen in one stage. This difficulty was overcome by adopting a two-stage procedure. In this procedure, acetone was first applied to the surface of the specimen so that it was completely wet and then a piece of plastic (acetate tape) was immediately laid across. The plastic attached to the specimen took on the surface contours of the specimen. After the plastic dried for about five minutes, it was peeled off with tweezers, mounted on glass slides, and labeled. This constituted our primary replica, but it was not suitable for work under the electron microscope. To obtain a replica suitable for electron microscopy, the primary replica, with the side which had been in contact with the specimen surface upwards, was placed directly under the carbon arc of a vacuum evaporator and carbon was deposited on the replicas. For more details see reference[30].

In the carbon replica thus made, the carbon thickness is more or less constant. This uniformity of thickness results in rather poor contrast under electron microscopy. To remedy this, replicas were shadowed with chromium. The procedure was as follows. As soon as carbon was deposited on the plastic replicas, a coating of chromium was deposited at an angle of almost 45 degrees to the specimen surface. The purpose of this was to cast a shadow containing no chromium behind high spots of the specimen, thus accentuating surface topography and producing better contrast under microscopy.

After shadowing, the composite films (consisting of carbon and plastic) were cut into pieces of appropriate dimensions. The pieces were then placed on grids. The grids had been placed on a piece of filter paper which had been wetted with acetone and inserted into a Petri dish. After the plastic pieces were added to the grids, the Petri dish was covered. Once the plastic had softened, more acetone was added until the filter paper was quite moist. At this stage the lid was replaced and the Petri dish left undisturbed for some time (occasionally overnight) until the plastic had been completely washed away. The secondary replica was then ready. The lid of the Petri dish was removed and the grids and the replica mounted on them were left to dry.

The testing techniques for 1018 and 1030 specimens are fairly standard. The procedure followed for 1020 specimens is different and more time consuming. However, since these specimens have very small thickness and would easily buckle the precautions here are essential. Replica techniques necessitate long preparation time also, but the advantage of obtaining an exact copy of the surface microstructure at any stage of testing justifies the effort.

CHAPTER 6

RESULTS AND DISCUSSION

6.1 FATIGUE TEST RESULTS

In this chapter, first, the results which were obtained are presented and then their significance is briefly discussed.

For each kind of specimen and each type of test, used in this investigation, a table indicating specimen label, modulus of elasticity, value of constant strain amplitude of the stable loops, and reversals to failure was made. Elastic and plastic strain amplitudes in these tables are calculated by the aid of the formulas discussed in Chapter 3. These tables are numbered from 6.1.1 to 6.1.9. In these tables, and throughout the text label "B.S" stands for cylindrical bar specimens made of 1018 steel, "T.S" for thin sheet specimens made of 1020 steel and "F.S" for thick sheet specimens made of 1030 steel.

As mentioned previously, during each test a series of stress-strain loops was recorded after a certain number of cycles. Examples of these are given in Figures 6.1.1 to 6.1.4. Figures 6.1.1 (a) and (b) display the stress-strain response of thick sheet specimen

TABLE 6.1.1

CONSTANT STRAIN AMPLITUDE

BAR STEEL SPECIMENS 1018

Specimen Number	Reference Cycle	Modulus of Elasticity (MPa.)	Total Strain Amplitude	Stress Amplitude (MPa.)	Elastic Strain Amplitude	Plastic Strain Amplitude (Meas.)	Plastic Strain Amplitdue (Calc.)	Reversals to failure
B.S.26	50	201106	0.01650	420.60	0.00209	0.01440	0.01441	216
B.S.18	100	212152	0.01535	384.39	0.00181	0.01335	0.01354	992
B.S. 1	200	206850	0.01040	358.50	0.00173	0.00850	0.00867	1900
B.S. 2	500	209849	0.00780	341.30	0.00163	0.00590	0.00617	2602
B.S. 4	1000	209608	0.00519	303.40	0.00145	0.00356	0.00374	5592
B.S. 7	5000	207691	0.00340	265.50	0.00128	0.00205	0.00212	34350
B.S. 8	20000	206071	0.00231	220.60	0.00107	0.00125	0.00124	139200
B.S. 6	90145	206850	0.00190	186.20	0.00090	0.00080	0.00100	653600
B.S. 9	118020	206326	0.00160	181.00	0.00088	0.00070	0.00072	580000
B.S.10	537600	206850	0.00126	158.60	0.00077	0.00050	0.00049	1500000
*B.S.22	500000	216144	0.00095	139.97	0.00065	0.00025	0.00030	1680458
*B.S.27	15000000	212152	0.00085	139.97	0.00066	0.00015	0.00019	6266184
*B.S.25	300000	216179	0.00100	151.69	0.00070	0.00028	0.00030	1107332

An asterisk(*) in front of a specimen number in Tables 6.1.1 - 6.1.9 indicates that the specimen was subjected to mechanical and electro-polishing for metallographic study.

TABLE 6.1.2

INITIAL OVERSTRIAN

BAR STEEL SPECIMENS 1018

Specimen Number	Reference Cycle	Modulus of Elasticity (MPa.)	Total Strain Amplitude	Stress Amplitude (MPa.)	Elastic Strain Amplitude	Plastic Strain Amplitude (Meas.)	Plastic Strain Amplitdue (Calc.)	Reversals to failure
B.S.15	1000	203403	0.00200	206.85	0.00102	0.00095	0.00098	147054
B.S.14	117440	209553	0.00125	165.60	0.00079	0.00045	0.00046	500000
B.S.17	1818100	201106	0.00105	158.59	0.00079	0.00030	0.00026	4605224
*B.S.20	400000	198645	0.00097	147.55	0.00074	0.00025	0.00023	1971420
*B.S.16	6000000	204126	0.00085	137.49	0.00067	0.00017	0.00018	12000000
*B.S.12	500000	202541	0.00100	144.80	0.00071	0.00030	0.00029	1968588

TABLE 6.1.3

PERIODIC OVERSTRAIN

BAR STEEL SPECIMENS 1018

Specimen Number	Reference Cycle	Modulus of Elasticity (MPa.)	Total Strain Amplitude	Stress Amplitude (MPa.)	Elastic Strain Amplitude	Plastic Strain Amplitude (Meas.)	Plastic Strain Amplitdue (Calc.)	Reversals to failure
B.S.13	100000	202541	0.00135	158.59	0.00078	0.00052	0.00057	324620
B.S.11	200000	206850	0.00120	165.48	0.00080	0.00040	0.00040	560000
B.S.21	912000	209725	0.00110	149.97	0.00072	0.00028	0.00038	1860000
B.S.24	1628000	216076	0.00080	165.48	0.00077	0.00007	0.00003	5560000
*B.S. 3	400000	209580	0.00095	149.97	0.00072	0.00022	0.00023	1417712
*B.S. 5	700000	212835	0.00093	147.55	0.00069	0.00012	0.00024	3000006
*B.S.19	100000	216172	0.00100	159.96	0.00074	0.00028	0.00026	355934
*B.S.23	300000	209684	0.00102	149.97	0.00072	0.00025	0.00030	1129962

TABLE 6.1.4

CONSTANT STRAIN AMPLITUDE

THIN SHEET SPECIMENS 1020

Specimen Number	Reference Cycle	Modulus of Elasticity (MPa.)	Total Strain Amplitude	Stress Amplitude (MPa.)	Elastic Strain Amplitude	Plastic Strain Amplitude (Meas.)	Plastic Strain Amplitdue (Calc.)	Reversals to failure
T.S. 4	50	199955	0.00870	325.79	0.00163	0.00898	0.00707	4154
T.S. 5	50	204195	0.00794	299.93	0.00147	0.00666	0.00647	2520
T.S.14	100	209105	0.00790	291.31	0.00139	0.00632	0.00651	3480
T.S. 6	500	201105	0.00534	291.31	0.00145	0.00393	0.00389	6694
T.S. 7	1000	211070	0.00265	210.30	0.00100	0.00167	0.00165	49380
T.S. 8	20000	219778	0.00200	193.06	0.00088	0.00110	0.00112	126000
T.S. 9	20300	206850	0.00165	171.69	0.00083	0.00078	0.00082	194000
T.S.12	58430	205416	0.00135	142.38	0.00069	0.00065	0.00066	300000
T.S.13	100000	205209	0.00140	153.41	0.00075	0.00060	0.00065	484000
T.S.11	910000	206850	0.00110	137.90	0.00067	0.00038	0.00043	3844640
T.S.24	1020000	203975	0.00080	140.66	0.00069	0.00013	0.00011	4480000
•T.S.16	500000	199955	0.00095	134.45	0.00067	0.00030	0.00028	3221784
•T.S.18	2000000	212594	0.00090	137.90	0.00065	0.00025	0.00025	12695006
•T.S.17	200000	212594	0.00075	127.56	0.00060	0.00015	0.00015	664102
•T.S.15	100000	198231	0.00090	158.58	0.00080	0.00010	0.00010	1063402

TABLE 6.1.5

INITIAL OVERSTRIAN

THIN SHEET SPECIMENS 1020

Specimen Number	Reference Cycle	Modulus of Elasticity (MPa.)	Total Strain Amplitude	Stress Amplitude (MPa.)	Elastic Strain Amplitude	Plastic Strain Amplitude (Meas.)	Plastic Strain Amplitdue (Calc.)	Reversals to failure
T.S.20	5000	206850	0.00110	165.48	0.00080	0.00017	0.00030	767500
T.S.27	100000	193922	0.00105	141.35	0.00073	0.00040	0.00032	633860
T.S.22	1415000	205085	0.00085	132.73	0.00065	0.00022	0.00020	6334260
*T.S.19	500000	211773	0.00095	131.01	0.00062	0.00029	0.00033	129162
*T.S.10	200000	201927	0.00085	137.90	0.00068	0.00017	0.00017	1259924

TABLE 6.1.6

PERIODIC OVERSTRAIN

THIN SHEET SPECIMENS 1020

Specimen Number	Reference Cycle	Modulus of Elasticity (MPa.)	Total Strain Amplitude	Stress Amplitude (MPa.)	Elastic Strain Amplitude	Plastic Strain Amplitude (Meas.)	Plastic Strain Amplitdue (Calc.)	Reversals to failure
T.S.29	106850	212518	0.00110	144.80	0.00068	0.00035	0.00042	444
T.S.30	190000	202796	0.00110	134.45	0.00066	0.00040	0.00044	464880
T.S.25	503750	209484	0.00080	142.04	0.00068	0.00016	0.00012	1074500
T.S.26	100000	210863	0.00082	144.80	0.00069	0.00014	0.00013	1470000
*T.S.21	400000	218344	0.00090	137.19	0.00063	0.00026	0.00027	1425268
*T.S.23	100000	218344	0.00080	127.56	0.00058	0.00022	0.00022	391768

TABLE 6.1.7

CONSTANT STRAIN AMPLITUDE

THICK SHEET SPECIMENS 1030

Specimen Number	Reference Cycle	Modulus of Elasticity (MPa.)	Total Strain Amplitude	Stress Amplitude (MPa.)	Elastic Strain Amplitude	Plastic Strain Amplitude (Meas.)	Plastic Strain Amplitdue (Calc.)	Reversals to failure
F.S. 1	1000	204762	0.00480	278.75	0.00136	0.00340	0.00344	6086
F.S. 3	2000	218750	0.00384	273.25	0.00125	0.00254	0.00259	9866
F.S. 5	5000	205000	0.00287	232.50	0.00113	0.00160	0.00174	27662
F.S. 6	1000	191176	0.00570	290.75	0.00152	0.00395	0.00418	4836
F.S. 7	200	203333	0.00715	295.50	0.00145	0.00565	0.00570	1416
F.S. 8	500	211905	0.00762	304.50	0.00144	0.00595	0.00619	1774
F.S. 9	500	197222	0.00862	277.50	0.00141	0.00657	0.00721	2552
•F.S.10	20000	222222	0.00188	191.25	0.00086	0.00090	0.00102	127162
•F.S.11	50000	215385	0.00129	154.50	0.00072	0.00050	0.00057	186200
•F.S. 2	300000	217241	0.00084	155.50	0.00072	0.00012	0.00012	1567522
•F.S. 4	500000	212500	0.00095	136.50	0.00064	0.00027	0.00031	1644196

TABLE 6.1.8

INITIAL OVERSTRIAN

THICK SHEET SPECIMENS 1030

Specimen Number	Reference Cycle	Modulus of Elasticity (MPa.)	Total Strain Amplitude	Stress Amplitude (MPa.)	Elastic Strain Amplitude	Plastic Strain Amplitude (Meas.)	Plastic Strain Amplitdue (Calc.)	Reversals to failure
F.S.13	300000	212069	0.00092	152.50	0.00072	0.00018	0.00020	1218738
F.S.19	5000000	212838	0.00083	154.00	0.00072	0.00010	0.00011	20907740
*F.S.20	5000000	216552	0.00084	160.50	0.00074	0.00010	0.00010	24412988
*F.S.16	200000	197368	0.00101	145.00	0.00073	0.00025	0.00028	394736
*F.S.21	244000	212500	0.00097	140.00	0.00066	0.00023	0.00031	1062914

TABLE 6.1.9

PERIODIC OVERSTRAIN

THICK SHEET SPECIMENS 1030

Specimen Number	Reference Cycle	Modulus of Elasticity (MPa.)	Total Strain Amplitude	Stress Amplitude (MPa.)	Elastic Strain Amplitude	Plastic Strain Amplitude (Meas.)	Plastic Strain Amplitdue (Calc.)	Reversals to failure
F.S.15	500000	213793	0.00084	157.50	0.00074	0.00010	0.00010	1933892
•F.S.17	500000	210345	0.00084	150.00	0.00071	0.00010	0.00013	2336784
F.S.14	300000	188889	0.00095	158.00	0.00084	0.00012	0.00011	1162156
•F.S.12	200000	210345	0.00101	141.00	0.00067	0.00028	0.00034	781332
•F.S.22	200000	207143	0.00093	137.50	0.00066	0.00025	0.00027	576152
•F.S.18	300000	212500	0.00097	190.00	0.00089	0.00010	0.00008	1254078

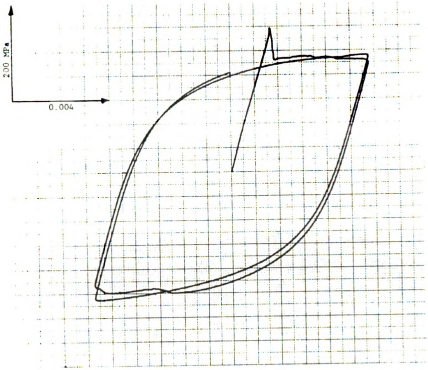

Figure 6.1.1 (a) Stress-Strain response of Specimen F.S.36

(N = 1 and 2).

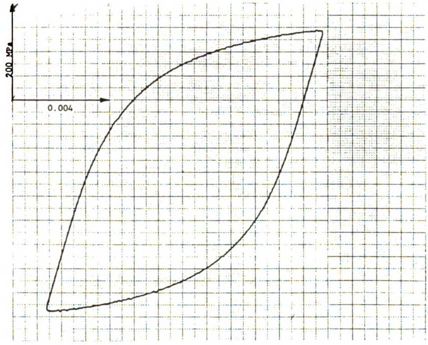

Figure 6.1.1 (b) Stress-Strain response of Specimen F.S.36

(N = 1000).

number 36 (F.S.36) which was subjected to a cyclic load with ±0.006 strain amplitude. The upper yield point of 295 MPa is clearly seen in the first cycle. A hysteresis loop recorded very near to the half-life of this specimen (1000 cycles) appears in Figure 6.1.1 (b). As can be seen in Figure 6.1.1 (a and b) the height of the loops increases with the number of cycles, which indicates that this material undergoes cyclic hardening at this strain amplitude. The stress-strain response of bar steel specimen number 25 (B.S.25) is shown in Figure 6.1.2. It can be seen that the material undergoes cyclic softening at this smaller strain amplitude. It is also seen that the cyclic softening or hardening is prominent in the first 50 percent of the life of the specimen after which a steady state condition is reached for the rest of the specimen's life. Figure 6.1.3 shows a typical stress-strain response of an initially overstrained specimen (specimen F.S.20) and corresponding loops which were recorded during its fatigue life.

Figure 6.1.4 illustrates the hysteresis loops observed during the fatigue test of specimen F.S.14. In this figure, hysteresis loops observed before and after subjecting this specimen to overstrain are shown. The hardening experienced by this material during each overstraining is clearly illustrated in this figure.

As can be seen from Figures 6.1.1 to 6.1.4, if the material undergoes cyclic hardening or softening, then the stress amplitude (height of loops) and elastic and plastic strain amplitudes change

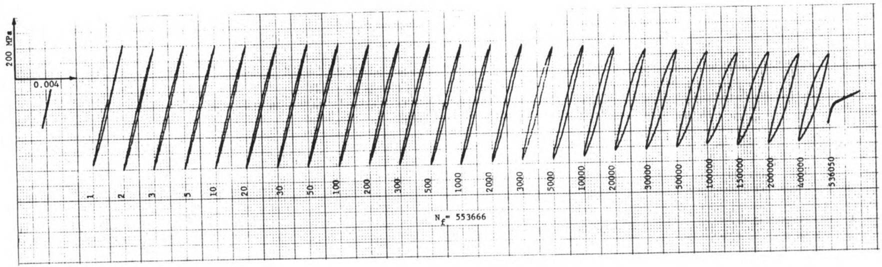

Figure 6.1.2 Stress-Strain response of Specimen B.S.25 During a Constant Strain Test.

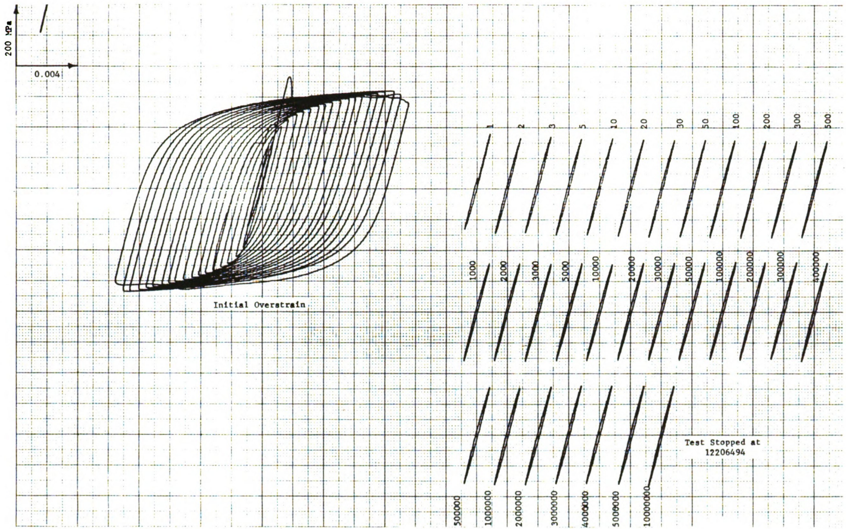

Figure 6.1.3 Stress-Strain response of Specimen F.S.20 During Initial Overstrain Test.

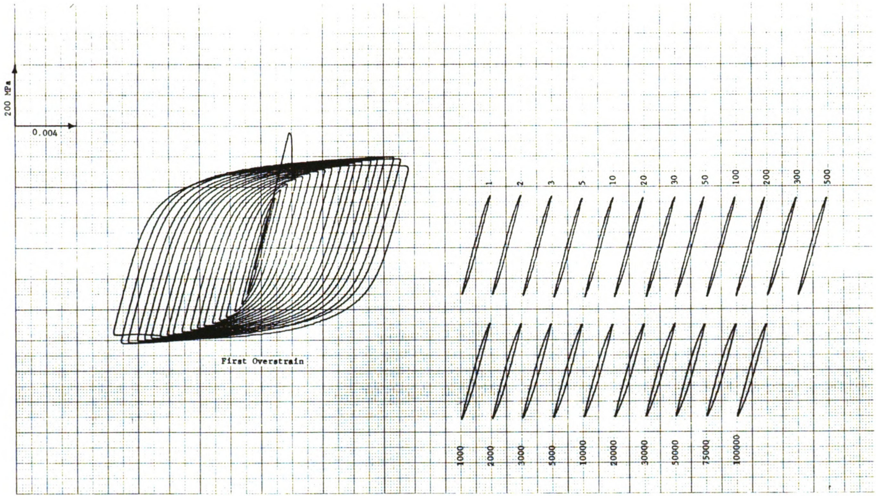

Figure 6.1.4 Stress-Strain response of Specimen F.S.14 During periodic Overstrain Test.

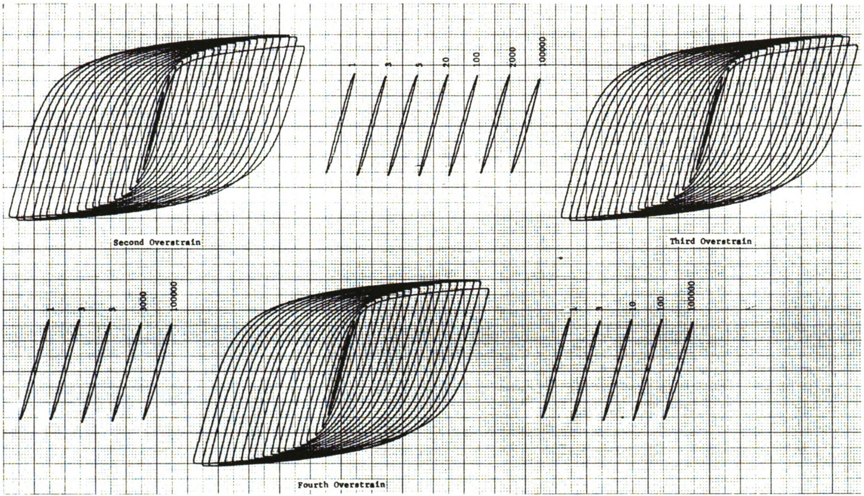

Figure 6.1.4 Continued.

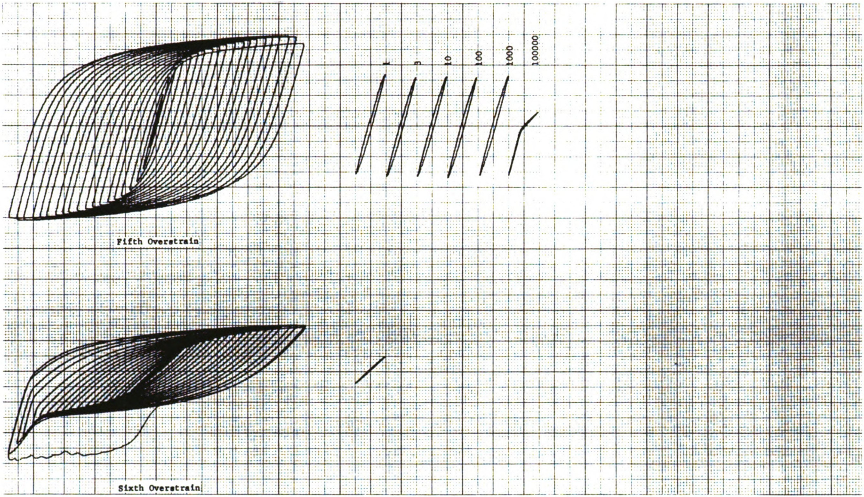

Figure 6.1.4 Continued.

during cycling under the conditions of constant total strain. The height (stress) and the width (total strain) of these loops were measured. From the peak values, the stress amplitude, $\Delta\sigma/2$, and strain amplitude, $\Delta\varepsilon/2$, were calculated. In most cases the elastic modulus, E, was calculated from the first hysteresis loop and used in all subsequent calculations. To obtain the elastic strain, the stress amplitude was divided by the elastic modulus, E. Subtraction of this value from the total strain then yielded the plastic strain (see equations 3-5 and 3-6). Based on the information obtained from these loops, a life table for every specimen, showing the elastic modulus, E, cycles to failure, $2N_f$, the total stress and total strain as well as the calculated elastic and plastic strains for each registered loop were prepared. From these data, figures showing the variations of these quantities with the number of cycles were then drawn. Representative Figures are shown in the graphs included. Figures 6.1.5 to 6.1.10 are plots of complete history of specimens B.S.6, B.S.20, B.S.3, T.S.24, T.S.22, and T.S.25, respectively. Experiments show that the materials under investigation undergo cyclic hardening or softening depending on the strain ranges. The cyclic change of stress amplitude versus reversals (half cycles 2N) of completely reversed strain at different strain amplitudes for three different metals has been shown in Figures 6.1.11 - 6.1.13.

Furthermore, the cyclic hardening (or softening) of the material can be easily determined from these data if one draws the variations of the plastic amplitude versus the reversals. Figure 6.1.14 shows

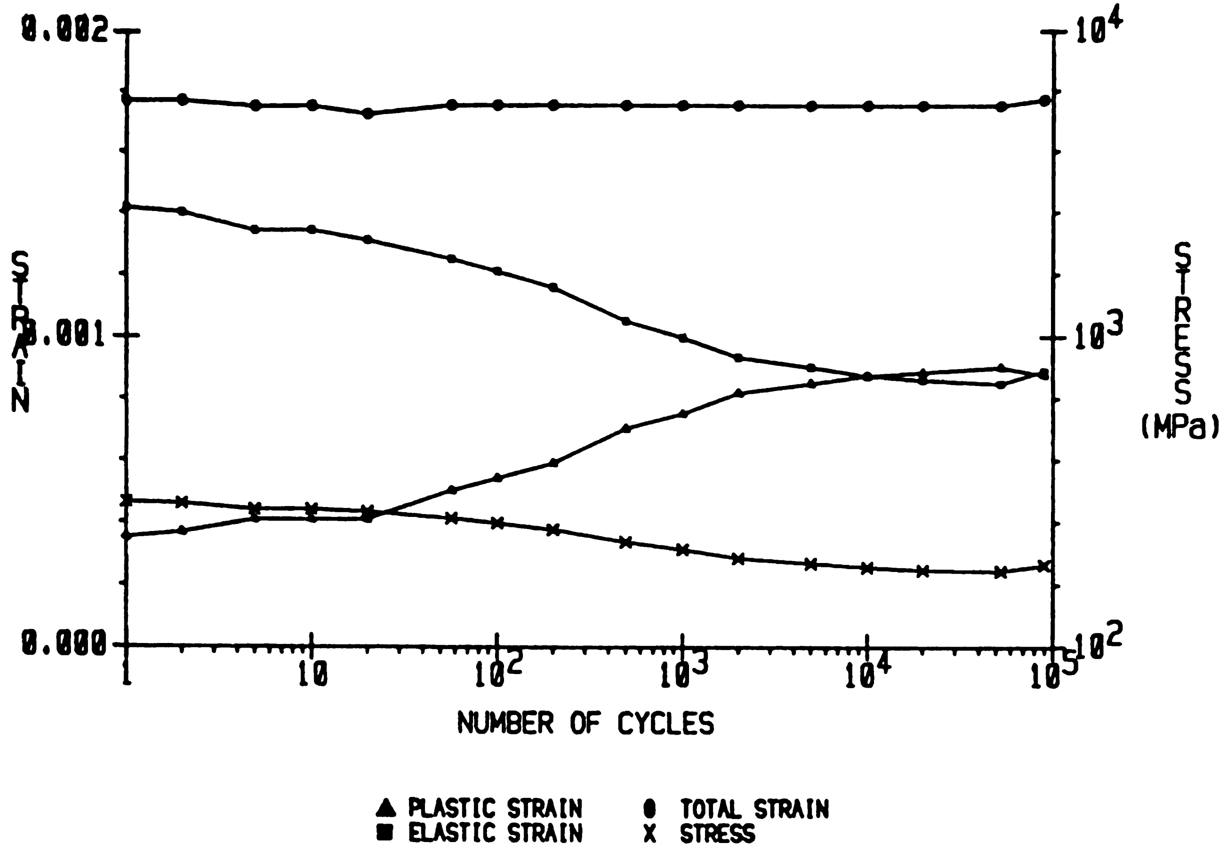

Figure 6.1.5 Life History Plot of Bar Steel Specimen 6 Subjected to Constant Strain cycling.

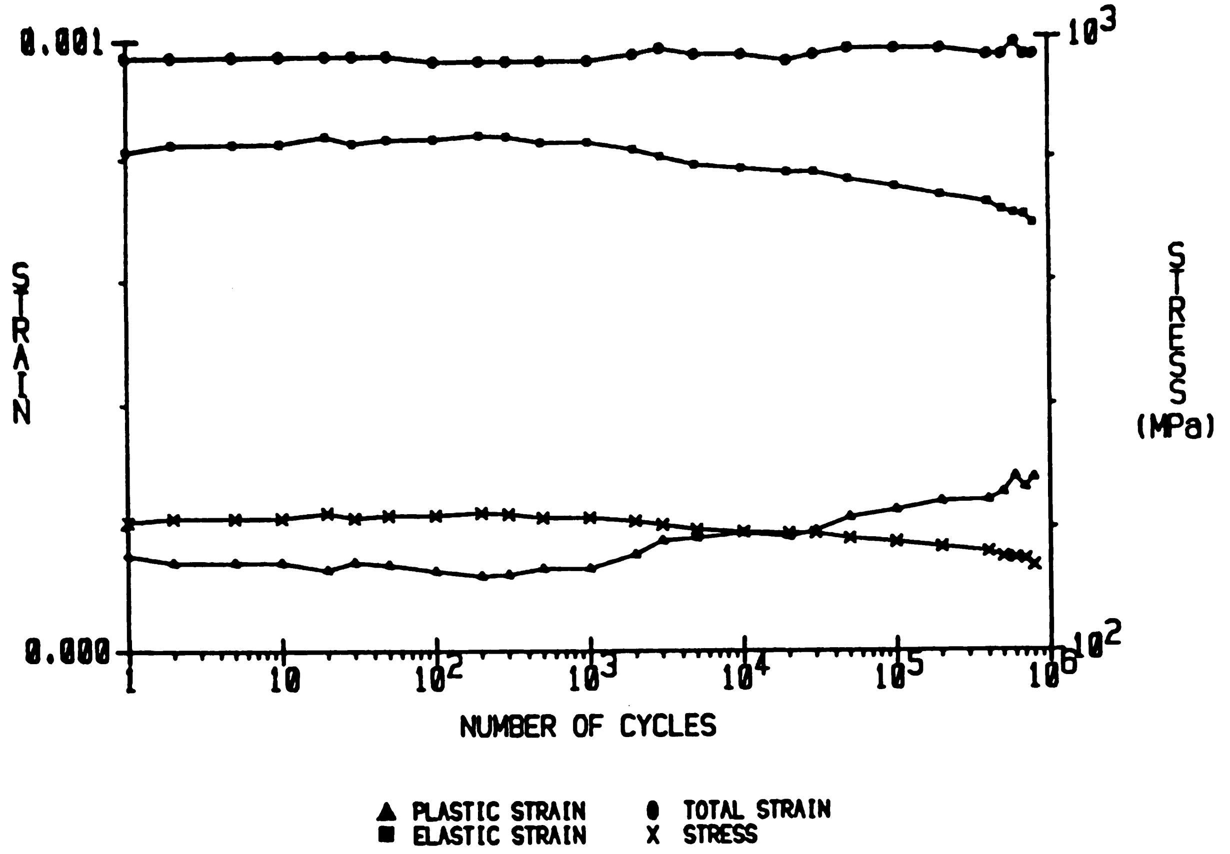

Figure 6.1.6 Life History Plot of Bar Steel Specimen 20 Subjected to Initial Overstraining.

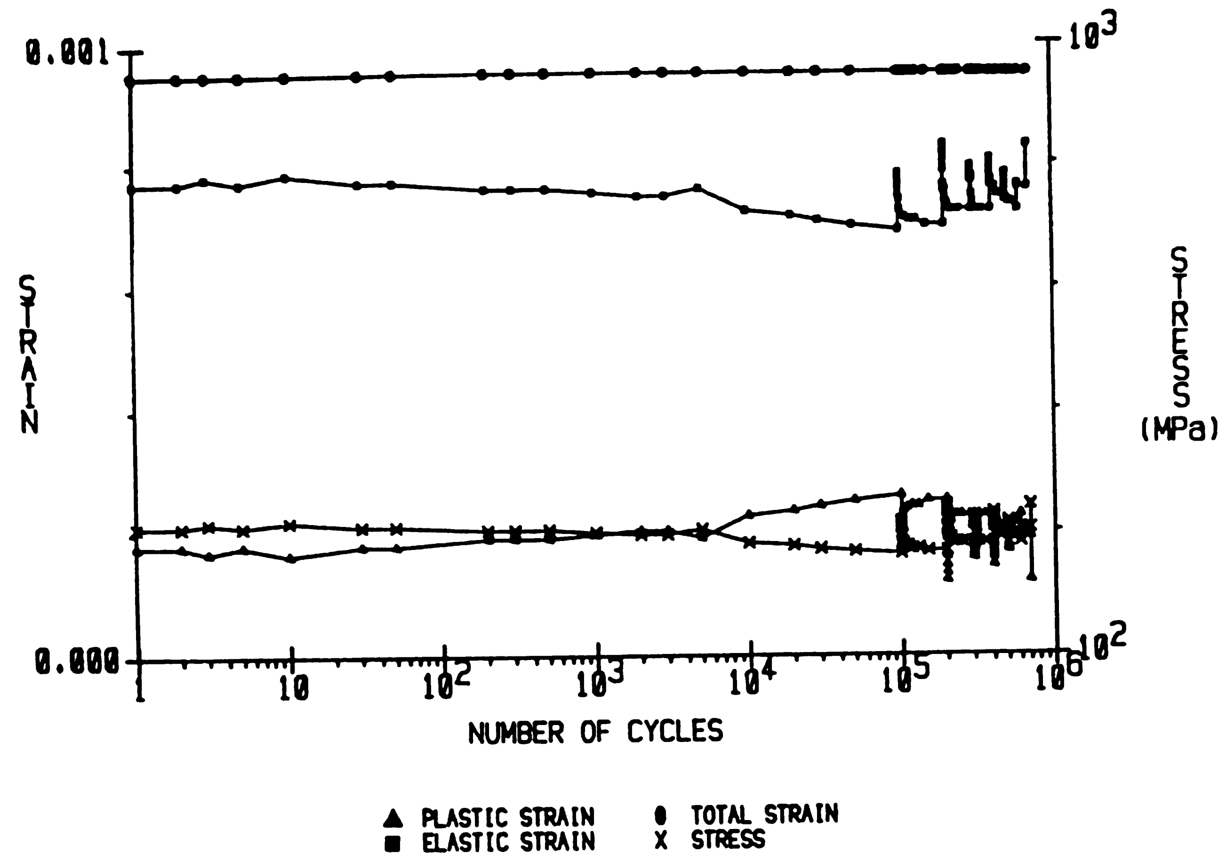

Figure 6.1.7 Life History of Bar Steel Specimen 3 Subjected to Periodic Overstraining.

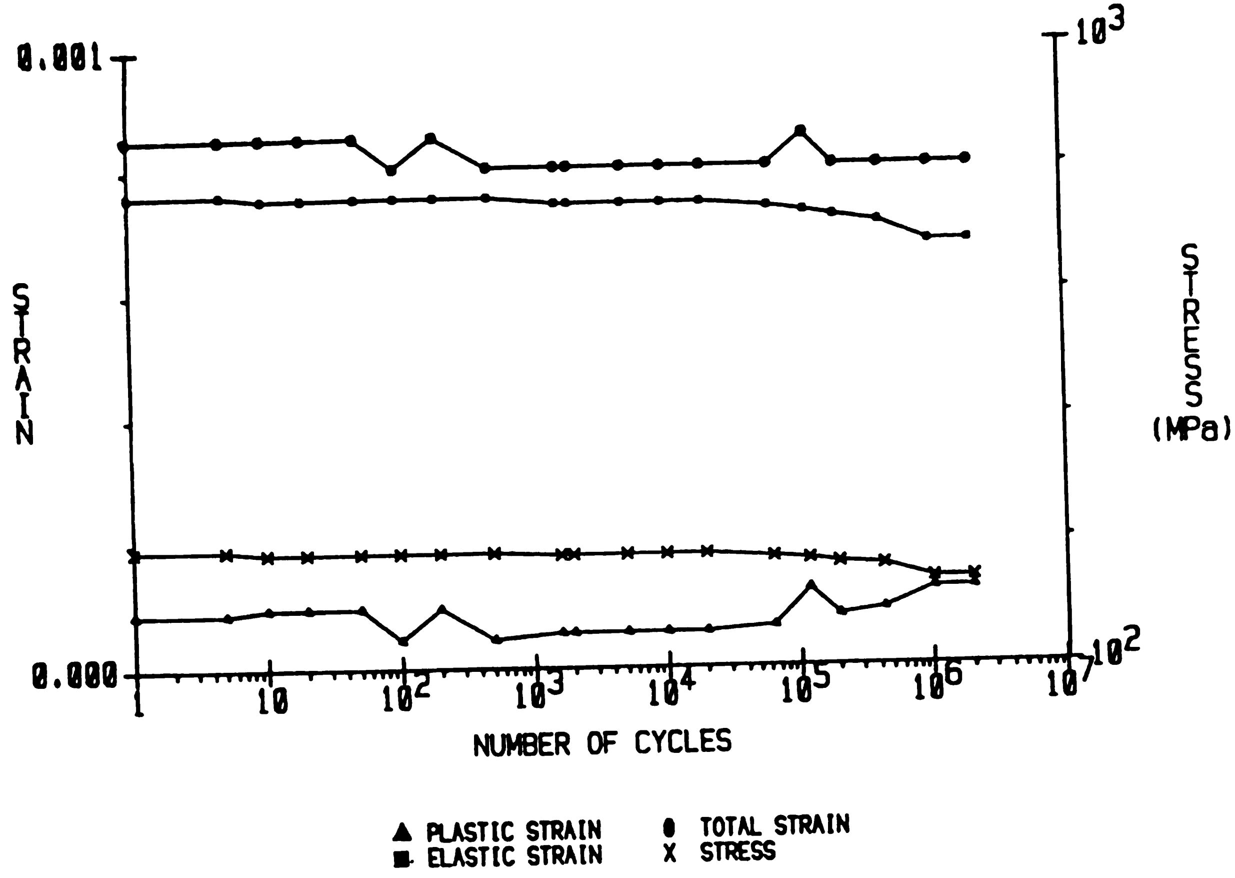

Figure 6.1.8 Life History Plot of Thin Sheet Specimen 24 Subjected to Constant Strain Cycling.

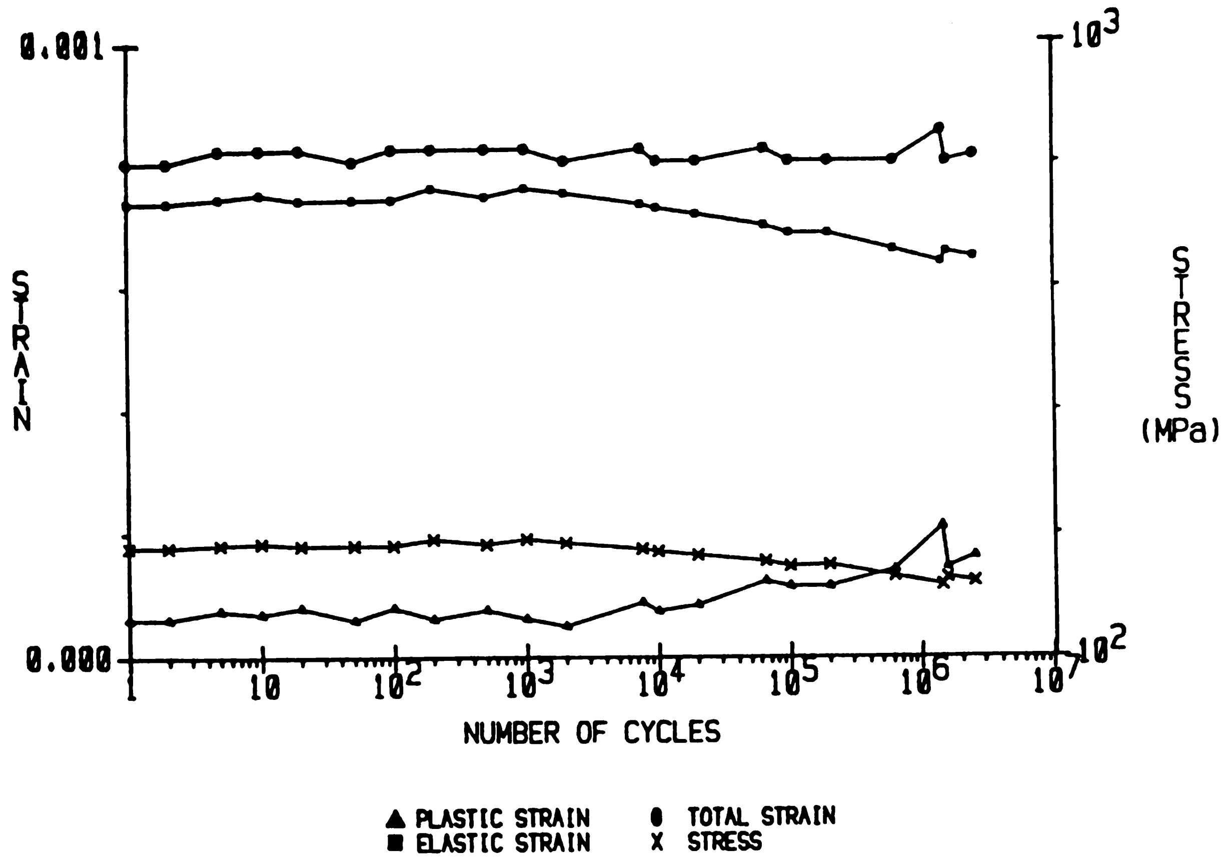

Figure 6.1.9 Life History Plot of Thin Sheet Specimen 22 Subjected to Initial Overstraining.

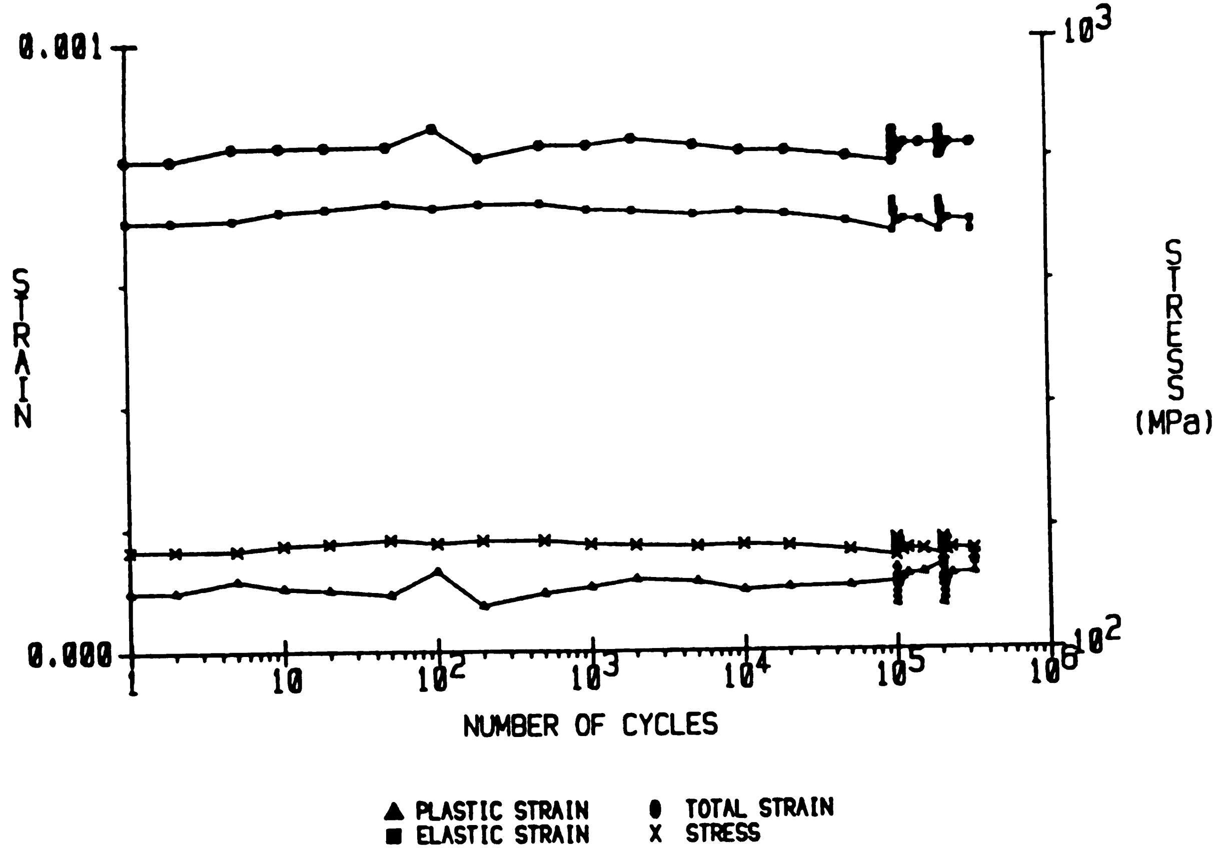

Figure 6.1.10 Life History Plot of Thin Sheet Specimen 25 Subjected to Periodic Overstraining.

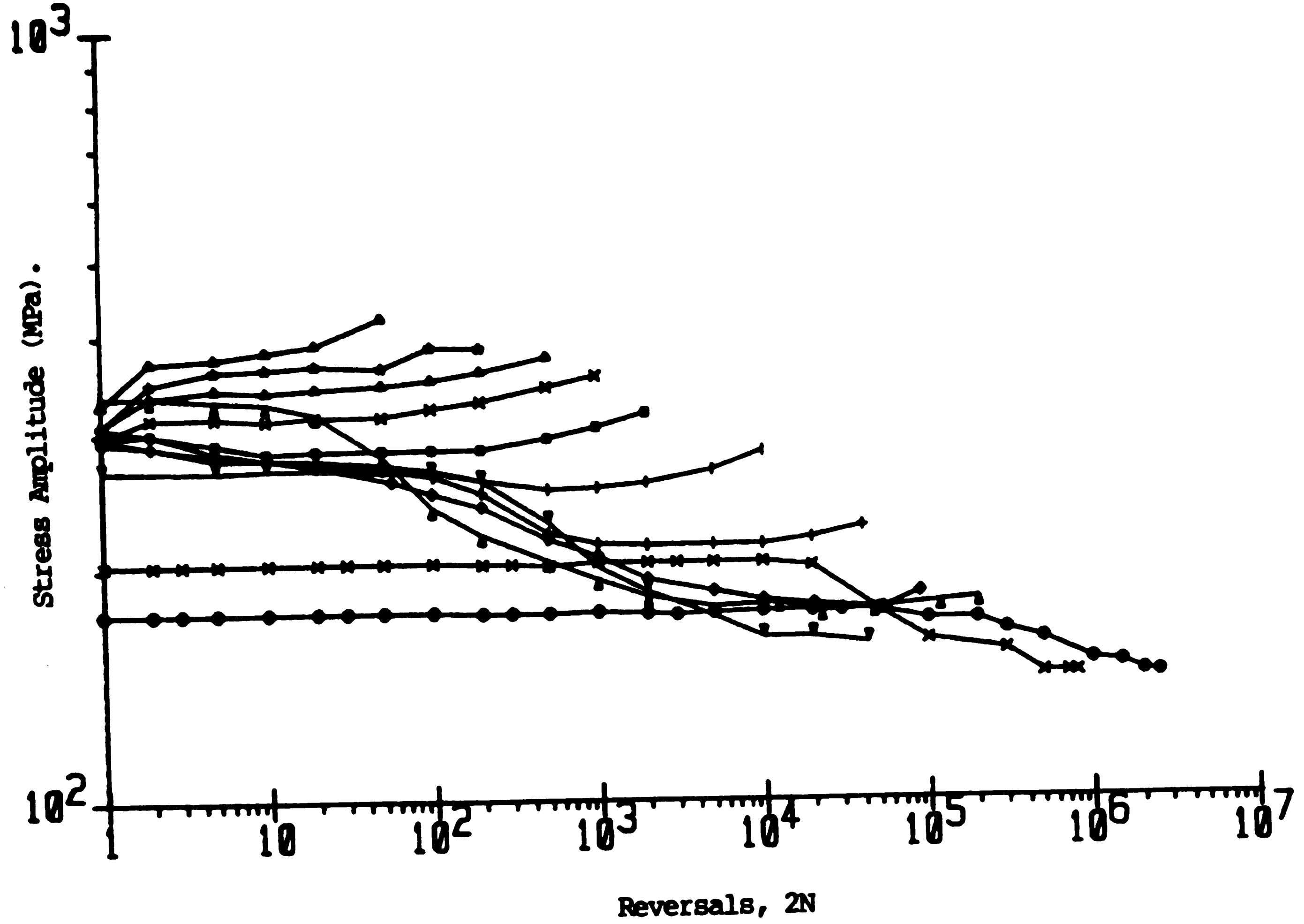

Figure 6.1.11 Stress Amplitude versus Reversals of Bar Steel Specimens for Constant Strain Test.

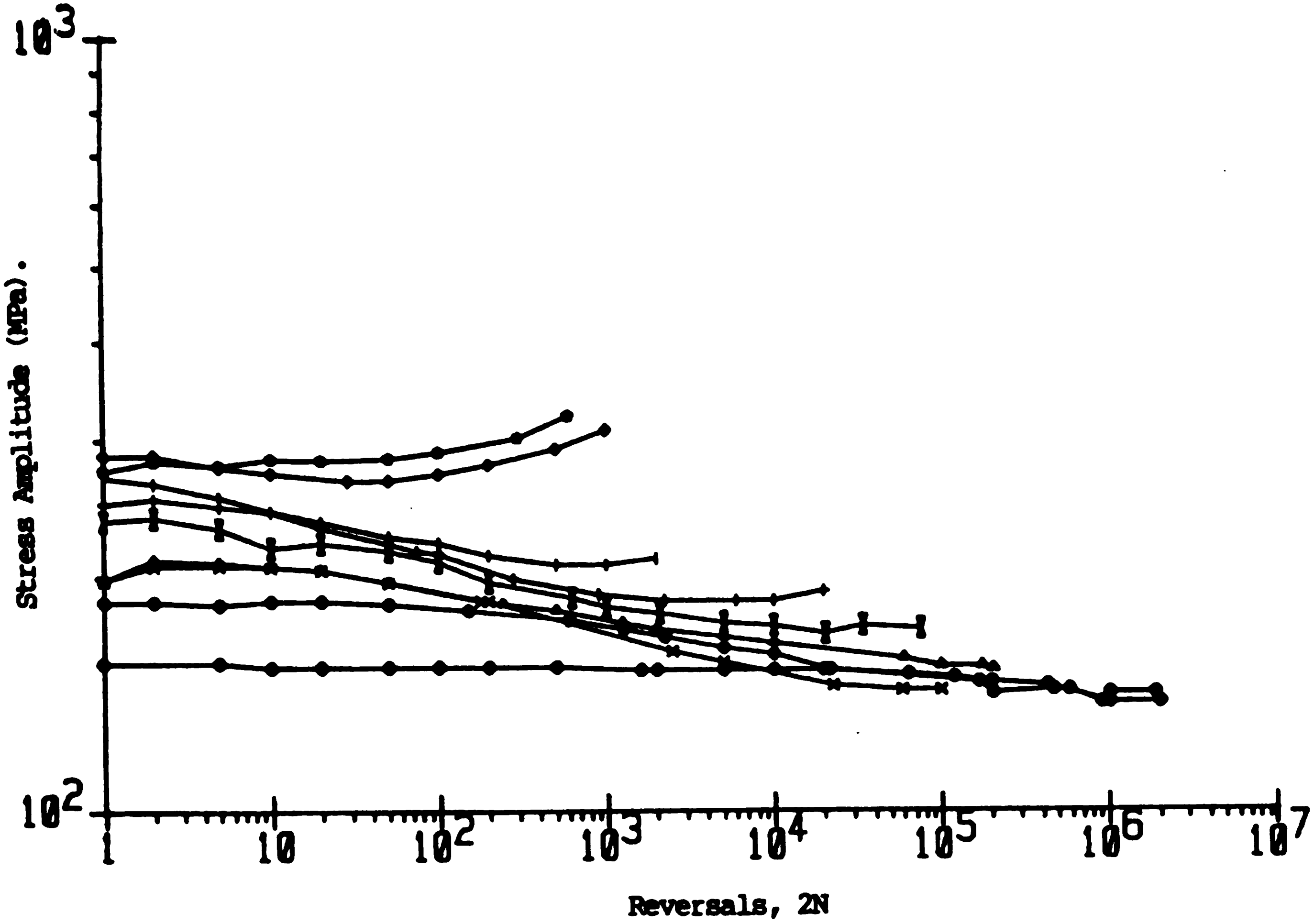

Figure 6.1.12 Stress Amplitude versus Reversals of Thin Sheet Steel Specimens for Constant Strain Test.

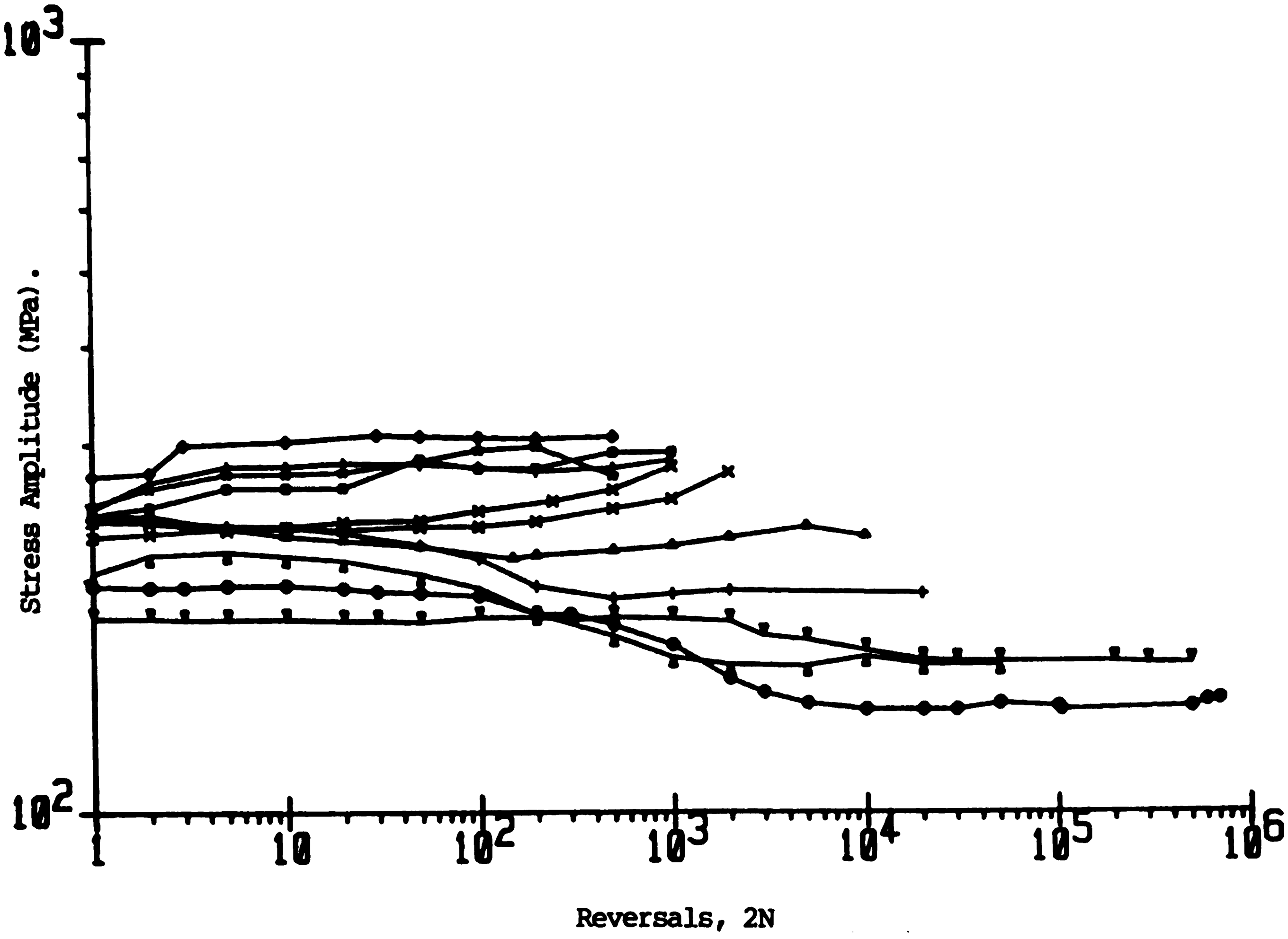

Figure 6.1.13 Stress Amplitude versus Reversals of Thick Sheet

Steel Specimens for Constant Strain Test.

such a curve for bar steel specimen number 25 (B.S.25) which was cycled at a constant strain (0.001 percent). It is evident that this material experienced cyclic softening at this strain amplitude. This occured because the plastic strain was increasing with the number of cycles.

The same trend was observed in the initial overstrain test on the specimen B.S.12. But the increase in the magnitude of the plastic strain was much more rapid which, as expected, resulted in a shorter life to failure (see Figure 6.1.15). In the case of periodically overstrained specimens, the amount of plastic deformation was small compared with the case of initially overstrained specimens. For the same strain amplitude, the life to failure of these specimens was close to specimens that had received no overstraining. Figure 6.1.16 shows the variation of plastic strain amplitude of specimen B.S.21 which was subjected to ±0.0011 percent strain and periodically overstrained. Figure 6.1.17 is an enlargement of the right portion of Figure 6.1.16. As can be seen in this figure, the specimen hardens slightly after each cyclic overstrain and as a result, the amount of plastic strain decreases. However, continued cycling with constant amplitude softens the specimen and it recovers its stable condition. This phenomenon may be due to strain hardening of this material. This explanation is supported by the fact that successive overstrains, and especially cyclic hardening during overstrains, increase the fatigue life of the bar steel specimens subjected to periodic overstraining.

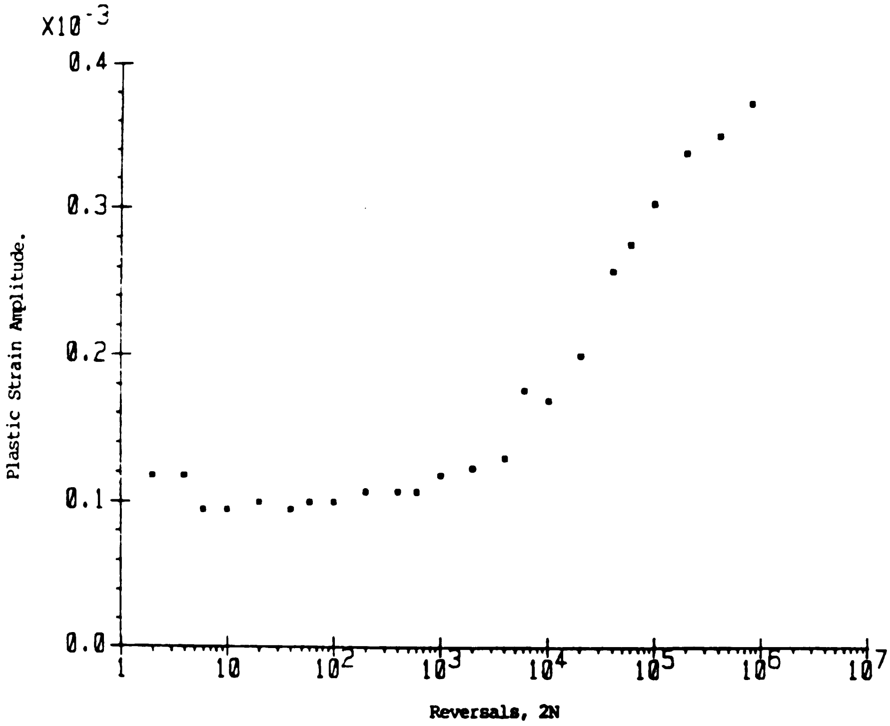

Figure 6.1.14 Plastic Strain history of Specimen B.S.25 Cycled at Constant Strain Amplitude of 0.001

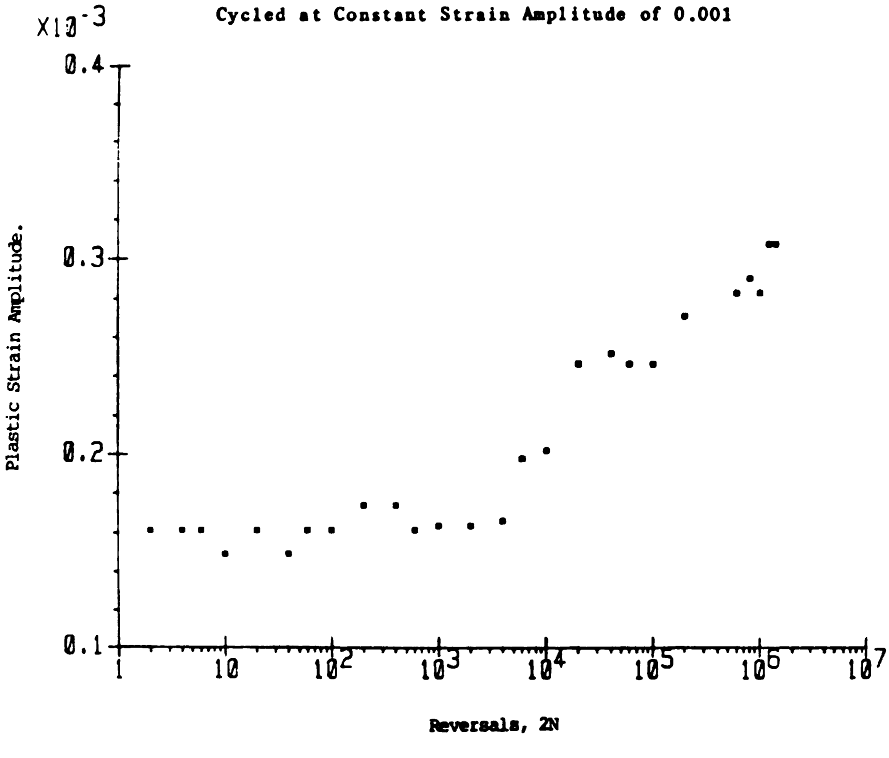

Figure 6.1.15 Plastic Strain history of Specimen B.S.12 which receiving Initial Overstrain followed by 0.001% Strain Amplitude Cycling.

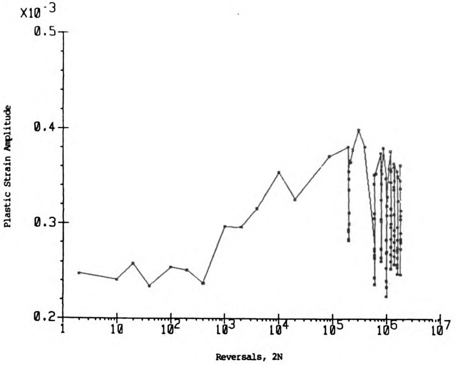

Figure 6.1.16 Plastic Strain history of Specimen B.S.21 which Periodically Overstrained.

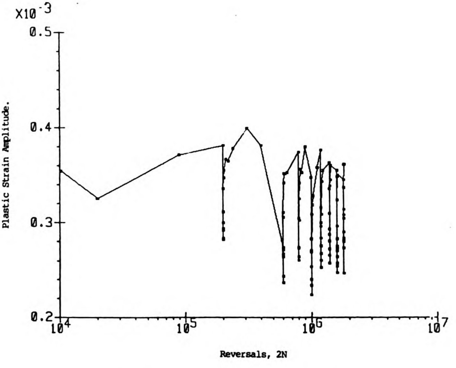

Figure 6.1.17 Right portion of Figure 6.1.16.

The trend was almost the same for 1020 and 1030 specimens. In spite of the fact that these specimens had hardened because of overstraining, the rate of increase in the magnitude of plastic strain for periodic overstrain (recovery of stable condition) was much more rapid compared with the initial overstrain cases. The amount of plastic deformation in the periodically overstrained specimens was relatively high in comparison with those specimens that had either received no overstrain at all or had been initially overstrained. Typical examples of these observations are shown in Figures 6.1.18 to 6.1.25. These observations, coupled with the results of other workers[3,6,8,18], lead to the conclusion that the plastic strain can cause damage resulting in shorter lives. As can be seen from Figure 6.1.14 - 6.1.25 the hysteresis loops for 1018 specimens recover their stable conditions more rapidly than those of 1020 and 1030 specimens.

At approximately half the fatigue life of each specimen a loop was chosen as the representative loop (reference cycle). The reason for this choice was that the stress-strain response could be assumed to have stabilized at this stage. In the case of periodically overstrained specimens, the representative loop at approximately half the fatigue life and just before overstraining was chosen. The corresponding data obtained from these loops were used in plotting the graphs and finding fatigue properties of each material. A summary of the results found from these loops for different types of specimens is presented in Tables 6.1.1 - 6.1.9. Throughout this study, with very few exceptions, a specimen was considered to have failed only when it

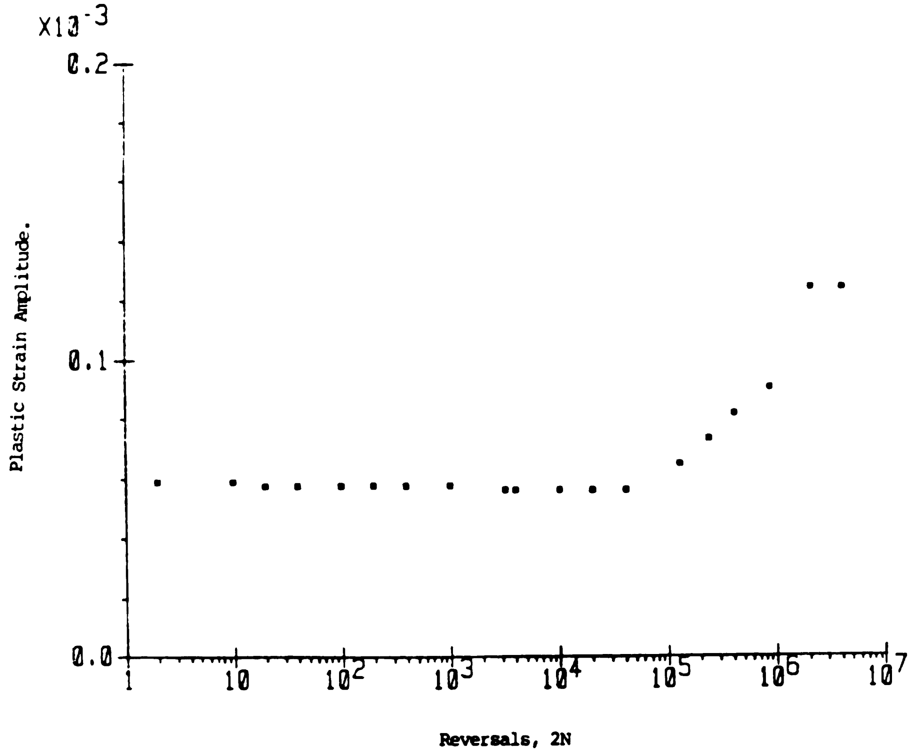

Figure 6.1.18 Plastic strain history of specimen T.S.24 cycled at constant strain amplitude of 0.0008

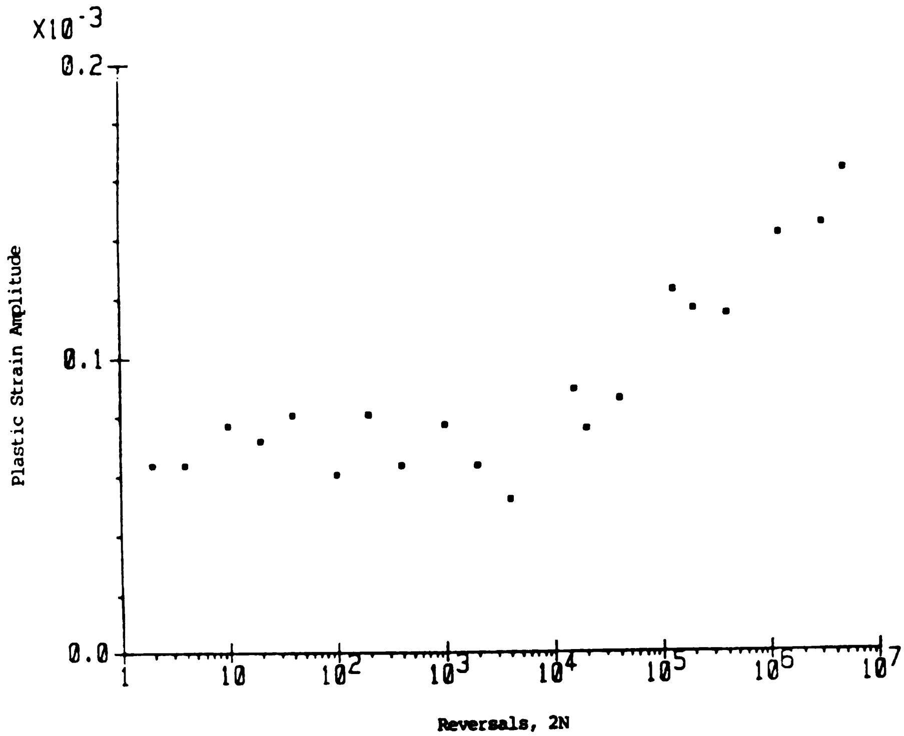

Figure 6.1.19 Plastic strain history of specimen T.S.22 which receiving initial overstrain followed by 0.00085

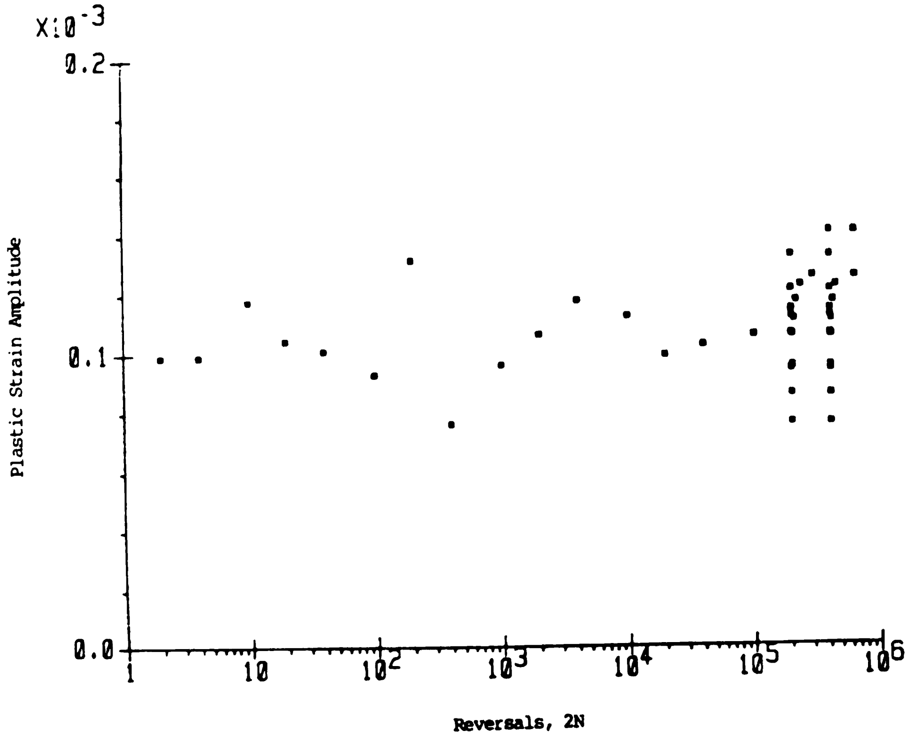

Figure 6.1.20 Plastic strain history of specimenT.S.25 which periodically overstrained.

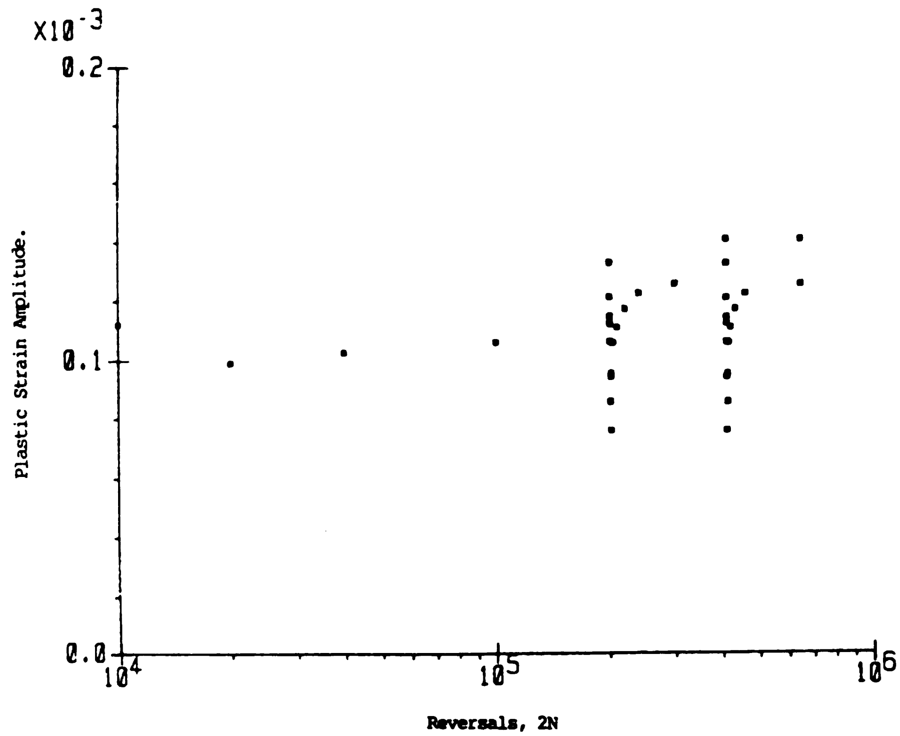

Figure 6.1.21 Right portion of Figure 6.1.20.

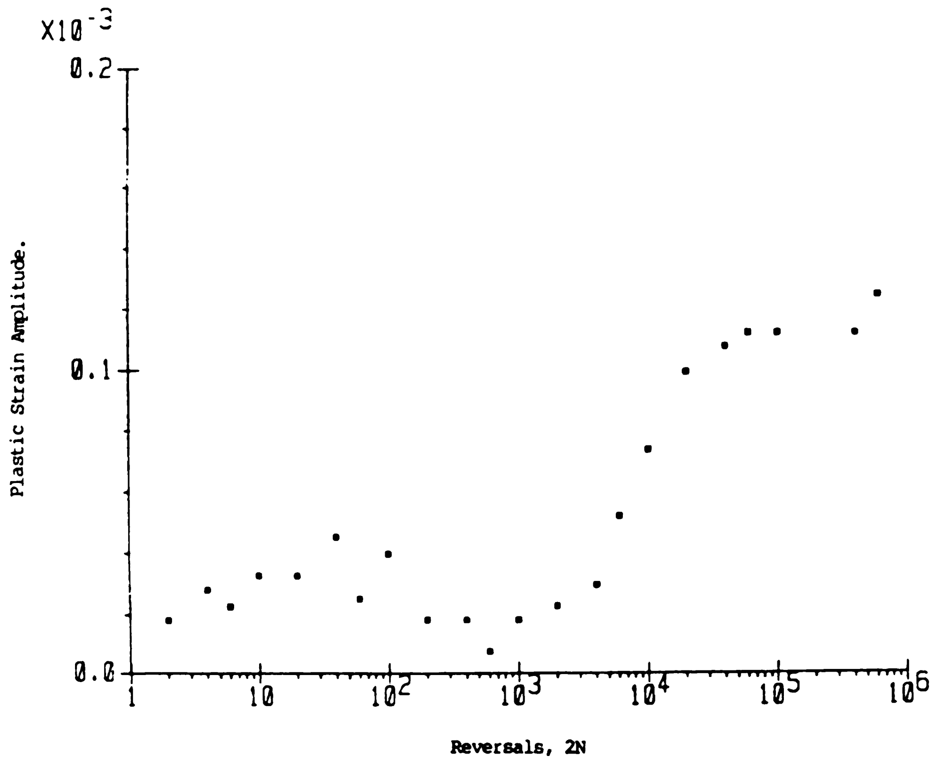

Figure 6.1.22 Plastic strain history of specimen F.S.2 cycled at constant strain amplitude of 0.001

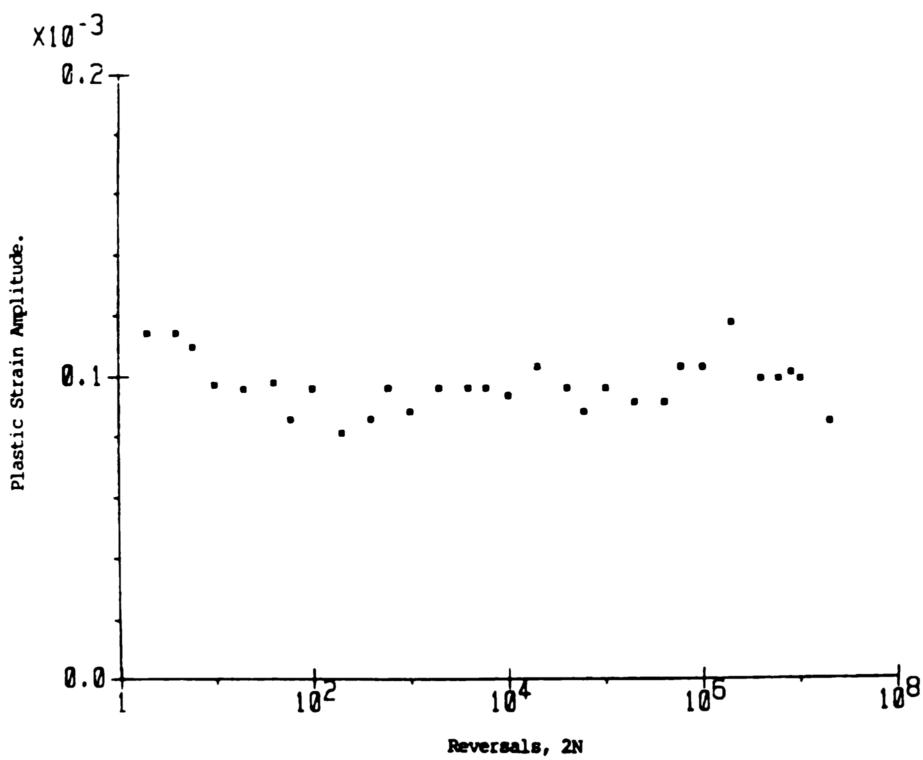

Figure 6.1.23 Plastic strain history of specimen F.S.20 which receiving initial overstrain followed by 0.00084 amplitude cycling.

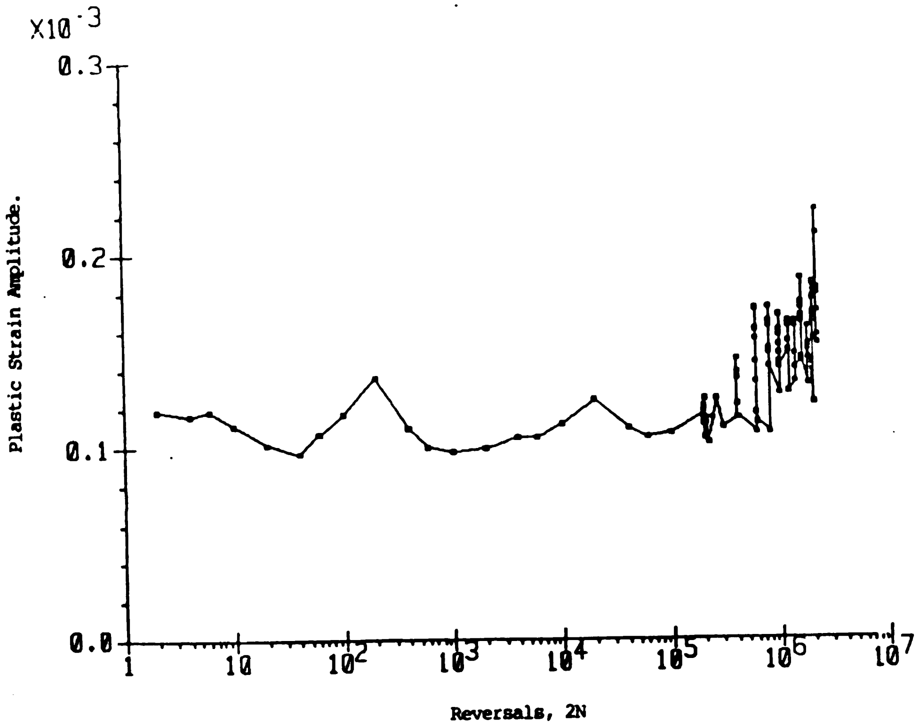

Figure 6.1.24 Plastic strain history of specimen F.S.17 which periodically overstrained.

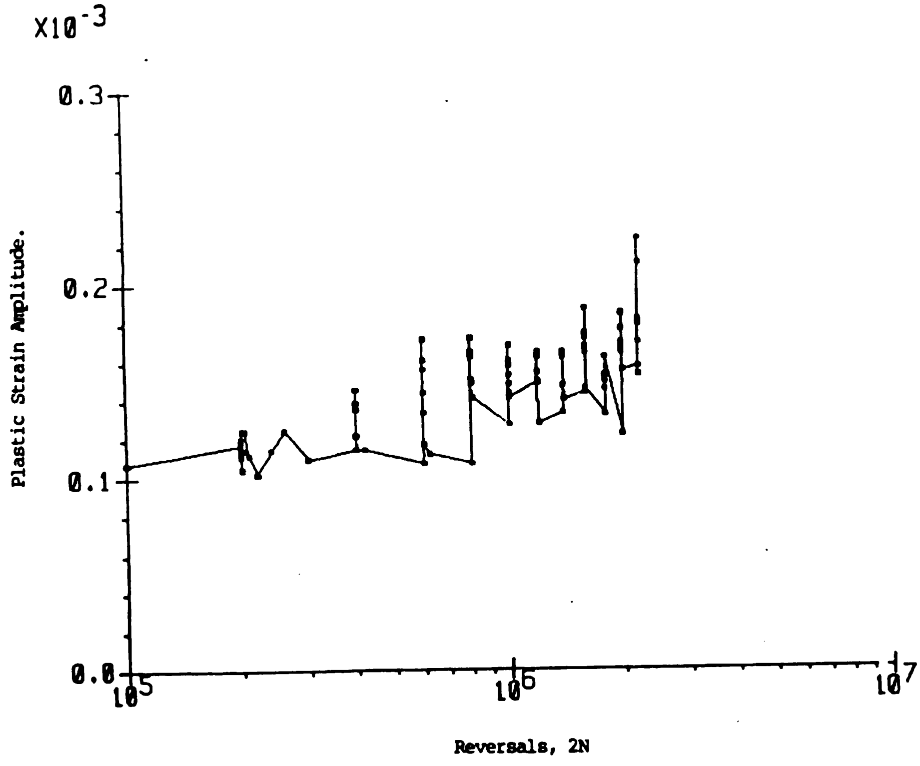

Figure 6.1.25 Right portion of Figure 6.1.24.

had completely separated into two parts.

Figures 6.1.11 - 6.1.13 depicts a stress-strain response that is of a complex nature since, for some specimens, both cyclic hardening and softening is observed. As has already been mentioned, the cyclic stress-strain behavior, that can be obtained from a curve passing through the tips of a set of stable hysteresis loops, would describe the cyclic response. For most metals, the relation between stress amplitude and the plastic strain amplitude (in stable condition) is of the form

$$\Delta\sigma/2 = K' \; (\Delta\varepsilon_p/2)^{n'} \tag{6-1}$$

(i.e. a power law) where K' and n' represent the cyclic strength coefficient and cyclic strain hardening exponent, respectively.

It is obvious that the graph of the above equation in log-log coordinates, is a straight line. The slope of this line represents the cyclic hardening exponent, n'. The data points that characterize each test correspond to the loops which were taken at one-half the fatigue life. Figures 6.1.26 to 6.1.34 show the plots of plastic strain amplitude versus stress amplitude for the three different materials used in this investigation, with three types of cyclic straining. The least-squares method was used to fit a straight line for each set of data. The lines thus obtained are quite distinct in

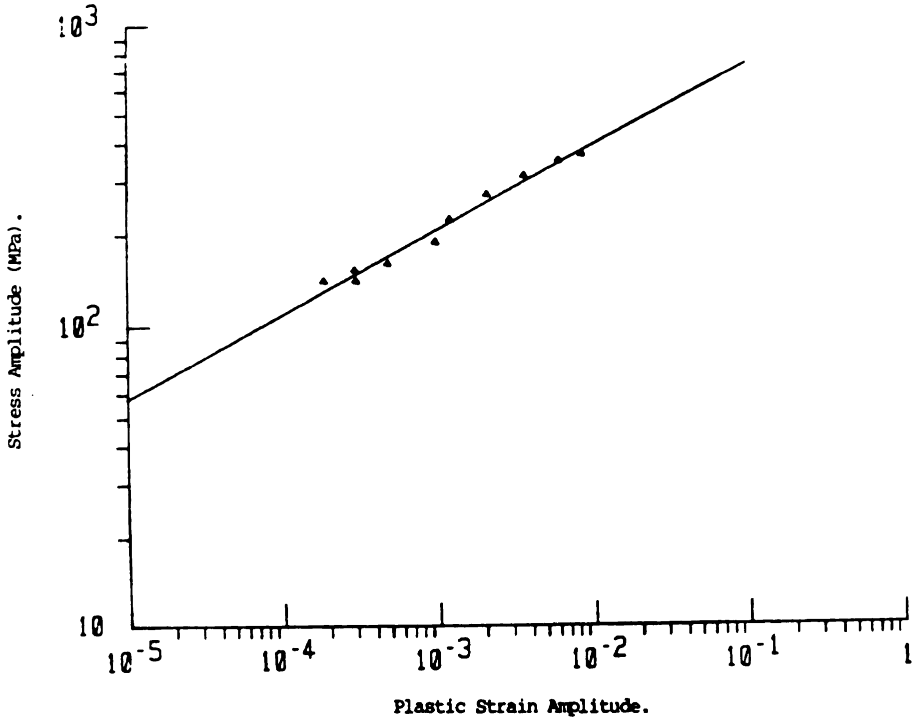

Figure 6.1.26 Stress-plastic strain amplitude from constant strain test results of Bar Steel Specimens.

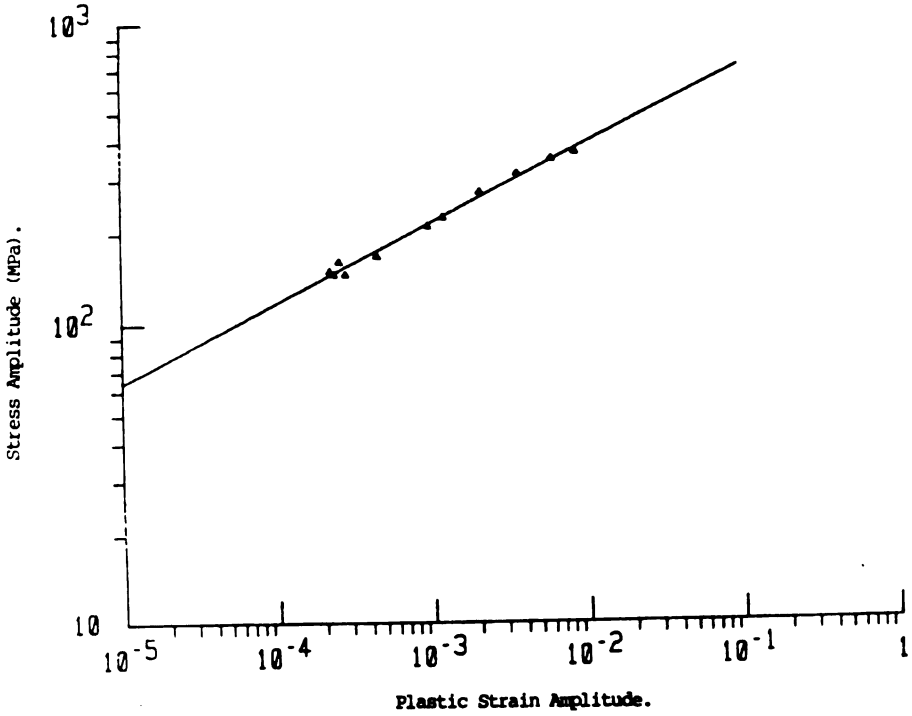

Figure 6.1.27 Stress-plastic strain amplitude data from Bar Steel Specimens subjected to initial overstrains.

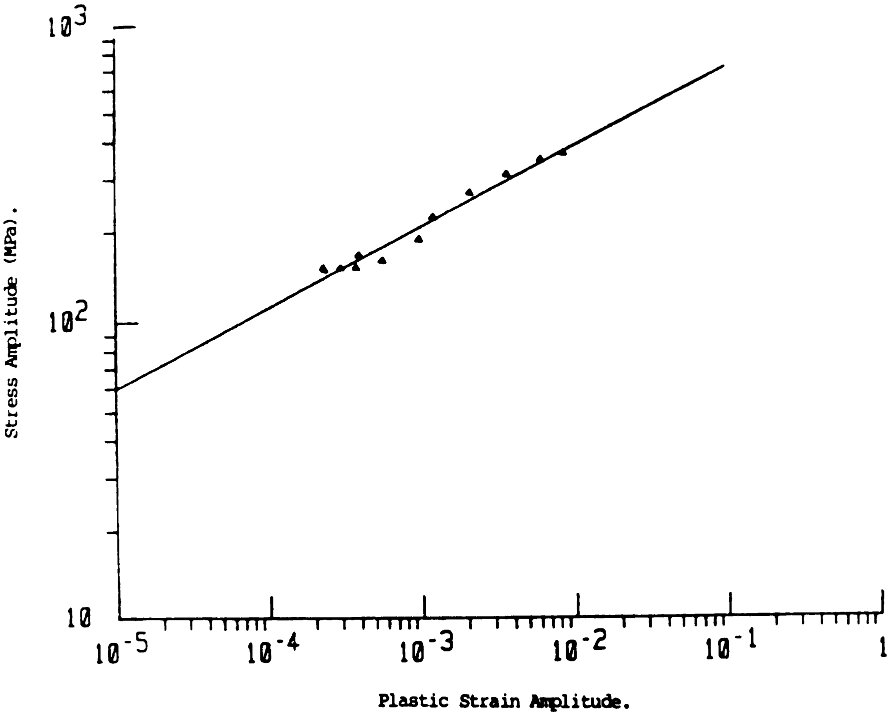

Figure 6.1.28 Stress-plastic strain amplitude data from Bar steel specimens subjected to periodic cyclic overstrains.

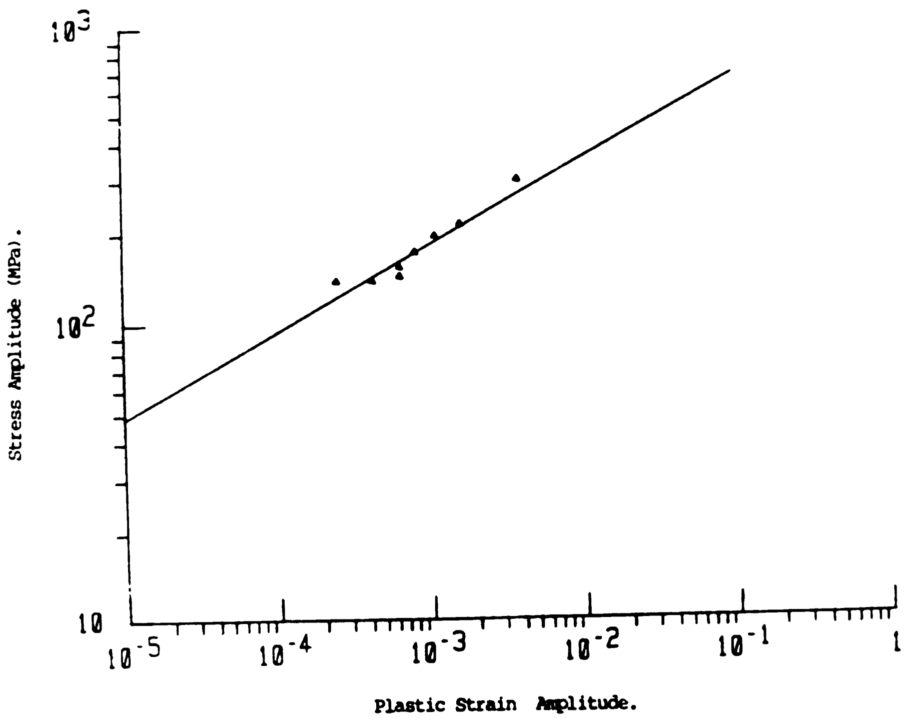

Figure 6.1.29 Stress-plastic strain amplitude from constant strain test of Thin Sheet Steel Specimens.

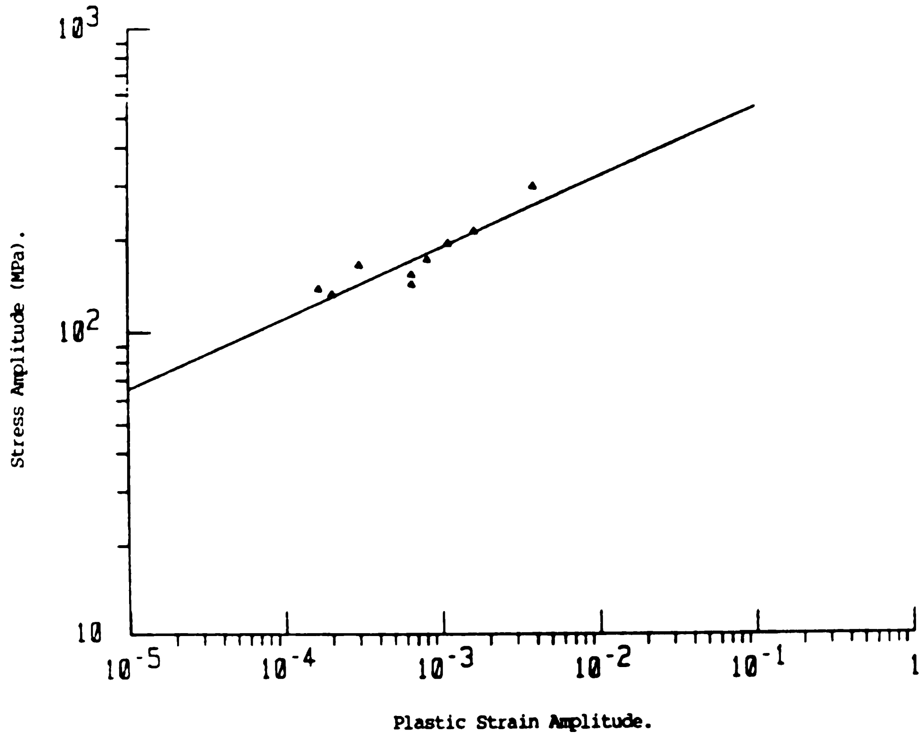

Figure 6.1.30 Stress-plastic strain amplitude data from Sheet Steel Specimens subjected to initial overstrains.

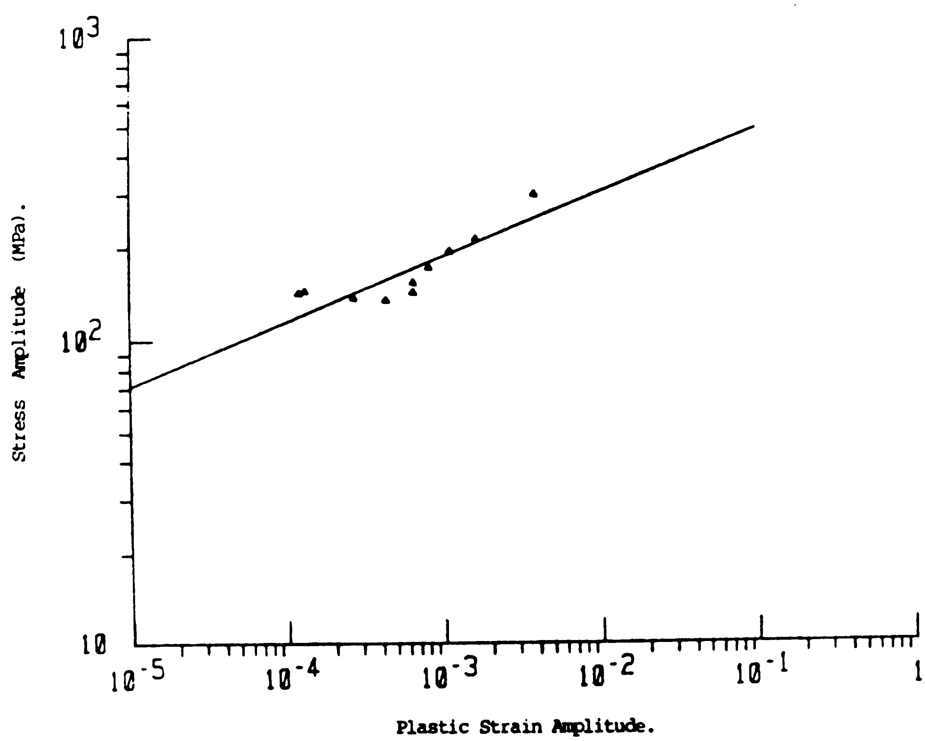

Figure 6.1.31 Stress-plastic strain amplitude data from Sheet Steel Specimens subjected to periodic cyclic overstrains.

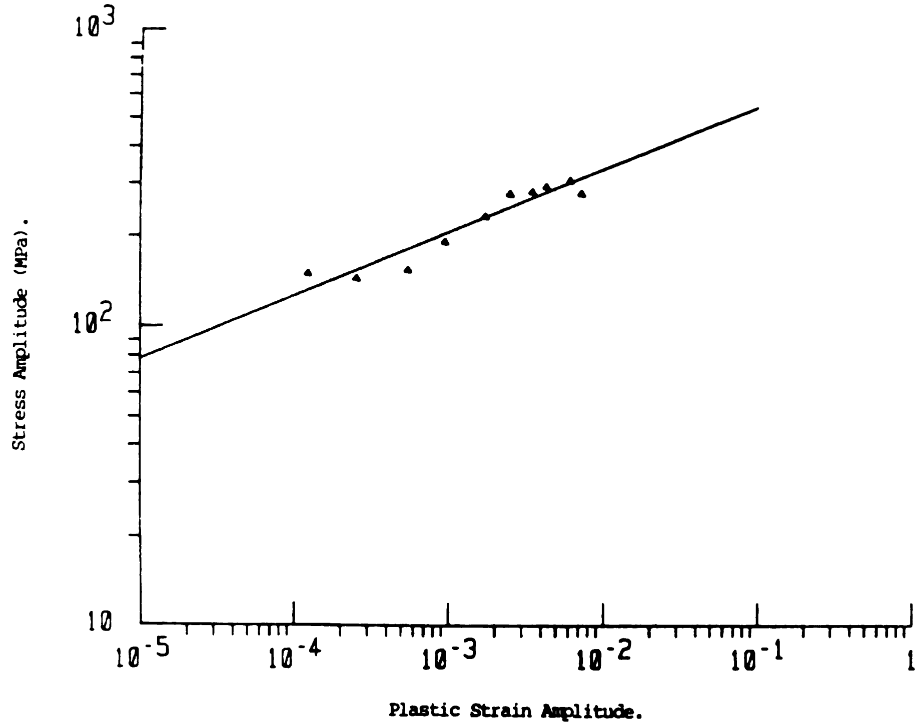

Figure 6.1.32 Stress-plastic strain amplitude from constant strain test of Thick Sheet Steel Specimens.

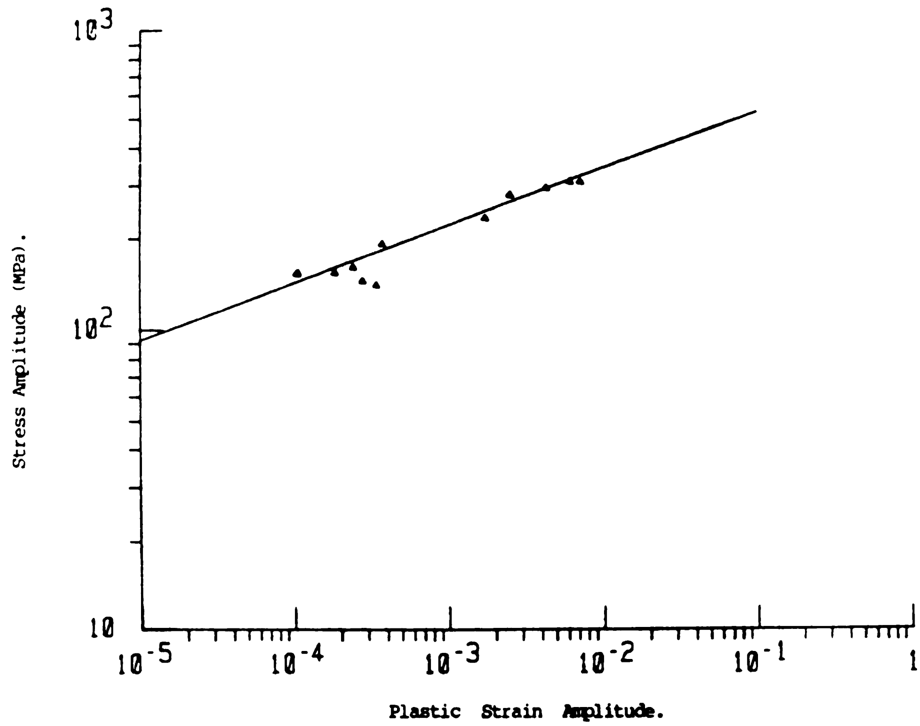

Figure 6.1.33 Stress-plastic strain amplitude data from Thich Sheet Steel Specimens subjected to initial overstrains.

the sense that they have markedly different slopes and intercepts. The obtained data fit the linear log-log relationships relatively well for 1018 and 1020 specimens. For 1030 specimens, the small deviations from the straight line may be attributed to the heat-treatment that was performed on these specimens. A summary of the results obtained from these graphs are shown in Tables 6.1.10 - 6.1.12. The strain hardening exponent obtained was high for cases of non-overstrained specimens (of all three types of material) whereas initial and periodic overstrain decrease the strain hardening exponent. In the case of bar steel, however, periodic overstrain yielded a strain hardening exponent nearly the same as that of the non-overstrained specimens.

From the data of Tables 6.1.1 - 6.1.3, the elastic and plastic strain amplitudes at half life has been plotted versus the reversals ($2N_f$) to failure for bar steel specimens. The least-squares method was used to find the best line showing the variation of elastic strain with life and plastic strain with life. The total strain curve was then found by adding the elastic and plastic strains.

From the plastic line, the fatigue ductility coefficient, ε_f', (the intercept of the plastic line at one reversal) and the fatigue ductility exponent, c, (the slope of the line) were calculated. The fatigue strength coefficient, σ_f', and fatigue strength exponent, b, (the slope) were determined from the elastic line. Figure 6.1.35 shows strain amplitude versus reversals to failure for 1018 specimens which received no overstrain.

TABLE 6.1.10

Cyclic stress-strain and fatigue properties of Bar Steel Specimens.

	No Overstrain	Initial Overstrain	Periodic Overstrain
Cyclic strength coefficient, (MPa)	1345	1259	1299
Cyclic strain hardening exponent	0.274	0.259	0.268
Fatigue Strength coefficient, (MPa)	878	805	887
Fatigue strength exponent	-0.120	-0.114	-0.123
Fatigue ductility coefficient	0.164	0.209	0.189
Fatigue ductility exponent	-0.417	-0.454	-0.438

TABLE 6.1.11

Cyclic stress-strain and fatigue properties of Thin Sheet Steel Specimens.

	No Overstrain	Initial Overstrain	Periodic Overstrain
Cyclic strength coefficient, (MPa)	1281	906	775
Cyclic strain hardening exponent	0.285	0.229	0.208
Fatigue Strength coefficient, (MPa)	667	744	954
Fatigue strength exponent	-0.108	-0.119	-0.140
Fatigue ductility coefficient	0.106	0.362	0.864
Fatigue ductility exponent	-0.382	-0.503	-0.585

TABLE 6.1.12

Cyclic stress-strain and fatigue properties
of Thick Steel Specimens.

	No Overstrain	Initial Overstrain	Periodic Overstrain
Cyclic strength coefficient, (MPa)	871	801	605
Cyclic strain hardening exponent	0.210	0.188	0.152
Fatigue Strength coefficient, (MPa)	743	588	650
Fatigue strength exponent	-0.115	-0.089	-0.103
Fatigue ductility coefficient	0.385	0.191	0.798
Fatigue ductility exponent	-0.533	-0.472	-0.612

The results from the tests, with strain amplitudes more than 0.0012 of no overstrain, have been used in conjunction with the data obtained from the overstrained specimens cycled at amplitudes less than 0.0012, to obtain plots of strain amplitude versus reversals to failure for initial and periodic overstrain cases. This procedure was adopted because the effect of overstrain at short lives is hardly ever noticeable[2,6,32]. Figures 6.1.36 and 6.1.37 show such plots for initial and periodic overstrain cases of 1018 specimens.

From these figures, it is evident that bar steel specimens which when periodically overstrained, exhibit a behavior very similar to specimens with no overstrain. It is also worth noting that the behavior of both types of specimens (no overstrain and periodic overstrain) is distinctly different from that of initially overstrained specimens.

Figures 6.1.38 to 6.1.43 show the graph of stable values of plastic, elastic and total strain taken from Table 6.1.4 - 6.1.9 and plotted versus the reversals to failure for 1020 and 1030 specimens. Comparison of these plots reveal that no appreciable change was observed in the life of specimens which were subjected to initial cyclic overstraining. Periodic cyclic overstraining, on the other hand, caused a sharp decrease in the life of 1030 specimens and a noticeable decline in the life of 1020 specimens. A summary of fatigue properties of the three materials under investigation, based on Figures 6.1.26 - 6.1.43, are shown in tables 6.1.10 - 6.1.12.

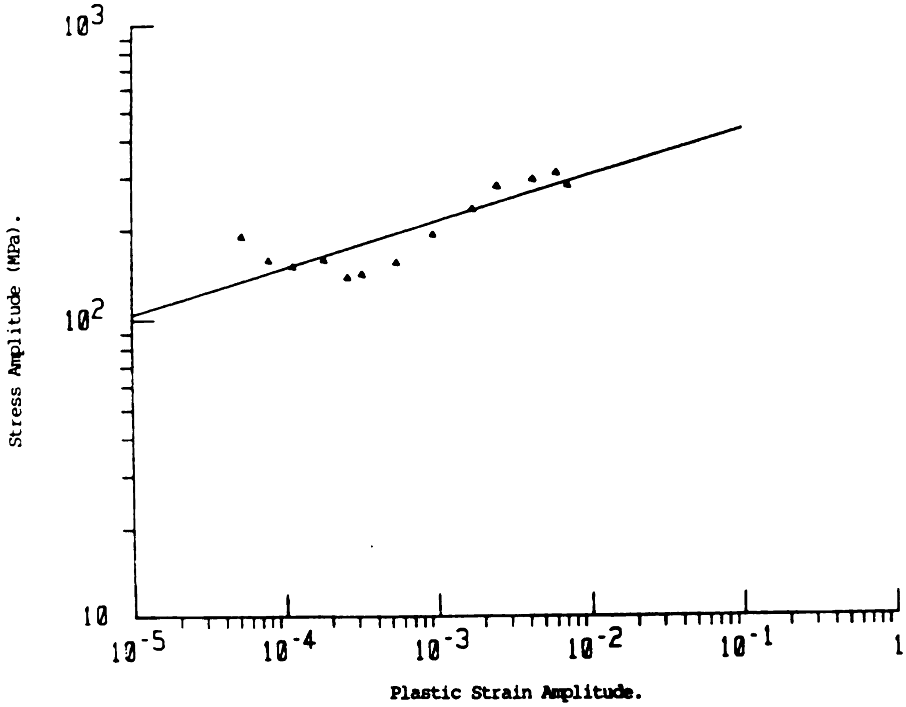

Figure 6.1.34 Stress-plastic strain amplitude data from Thich Sheet steel Specimens subjected to periodic cyclic overstrains.

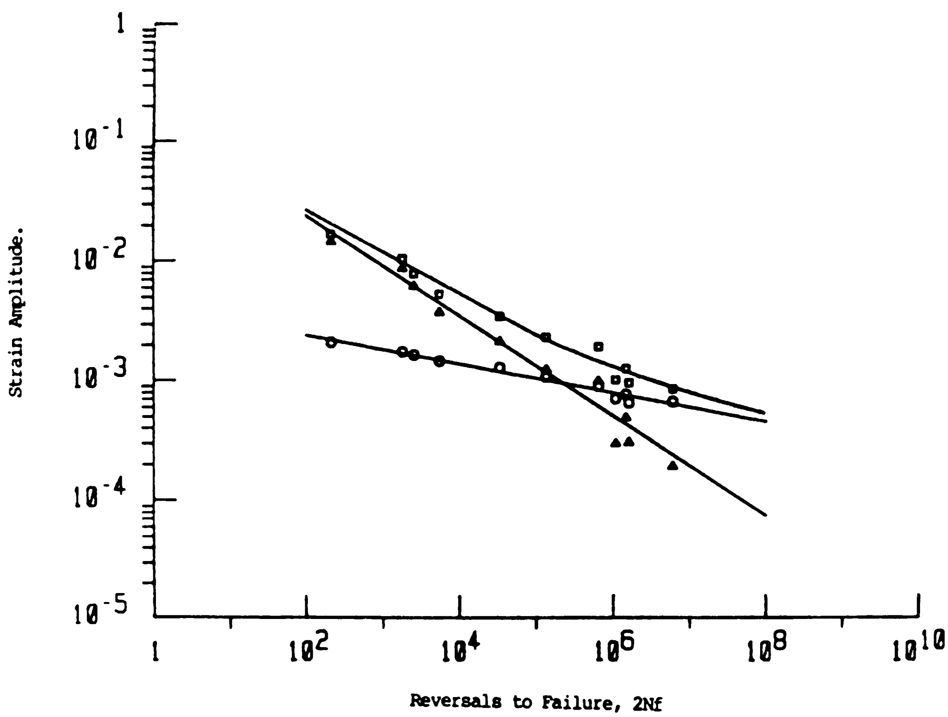

Figure 5.1.35 Strain-reversals to failure for Bar Steel Specimens (no overstraining).

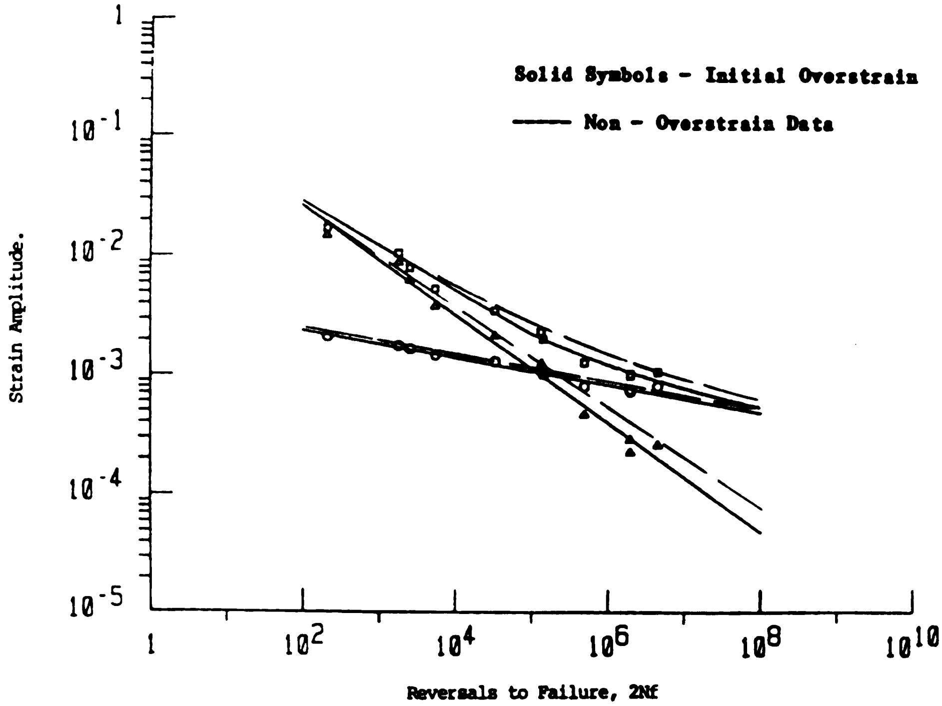

Figure 6.1.36 Strain-reversals to failure for Bar Steel Specimen subjected to initial overstrains.

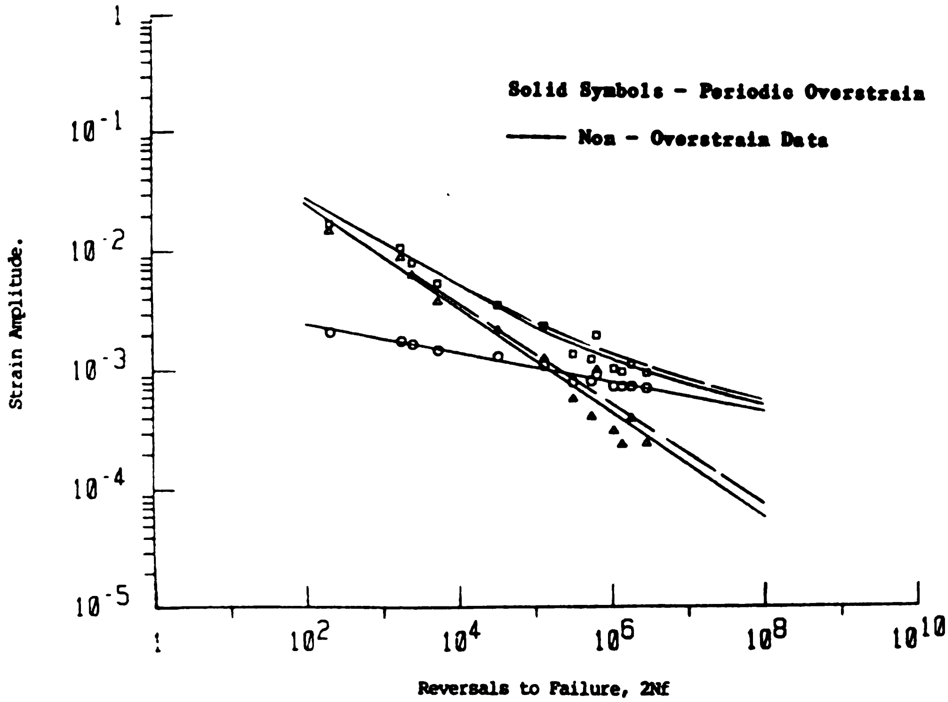

Figure 6.1.37 Strain-reversals to failure for Bar Steel Specimens subjected to periodic cyclic overstrains.

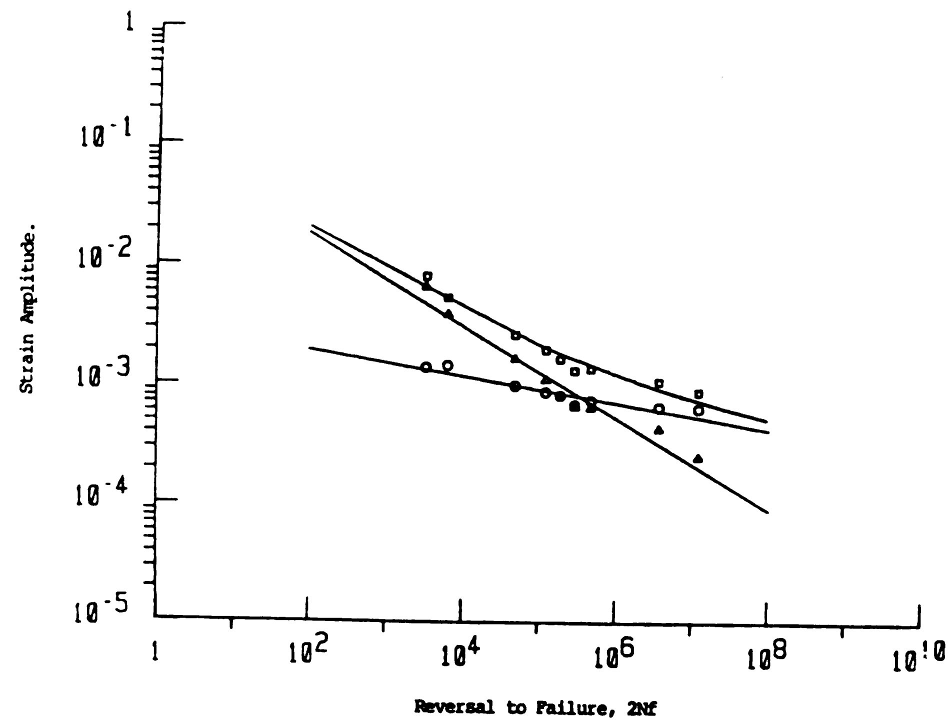

Figure 6.1.38 Strain-reversals to failure data for Sheet Steel Specimens (no overstrain).

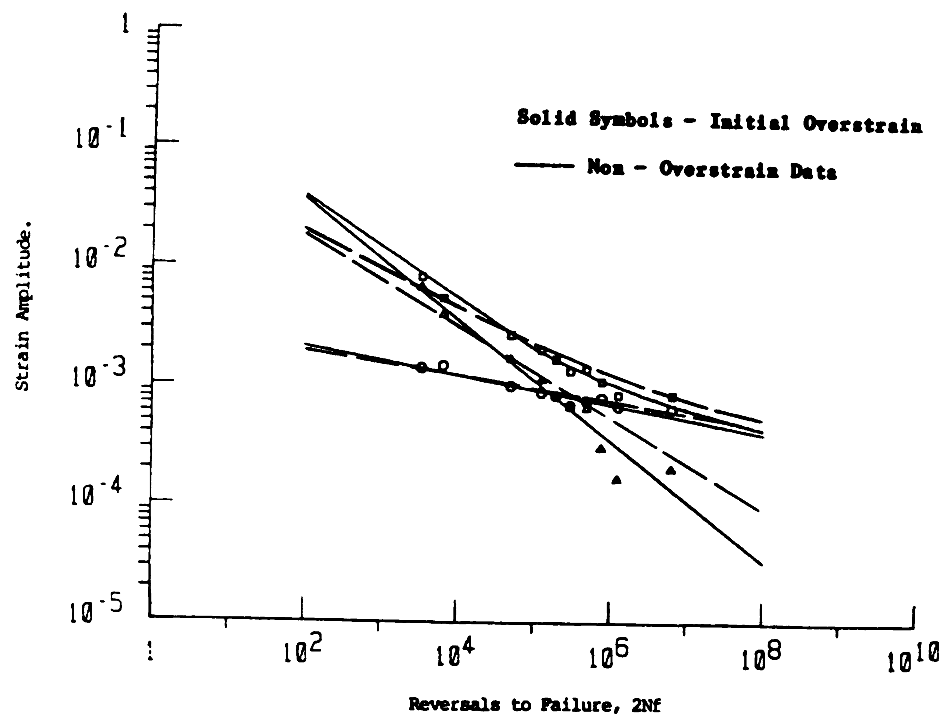

Figure 6.1.39 Strain-reversals to failure data for Sheet Steel Specimens subjected to initial overstrains.

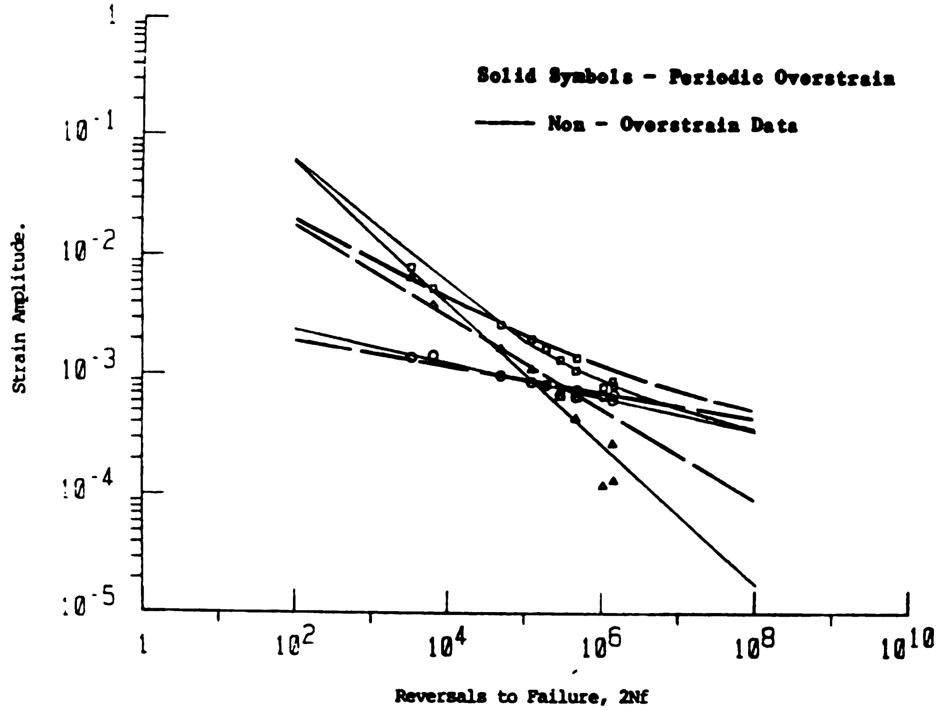

Figure 6.1.40 Strain-reversals to failure data for Sheet Steel Specimens subjected to periodic cyclic overstrains.

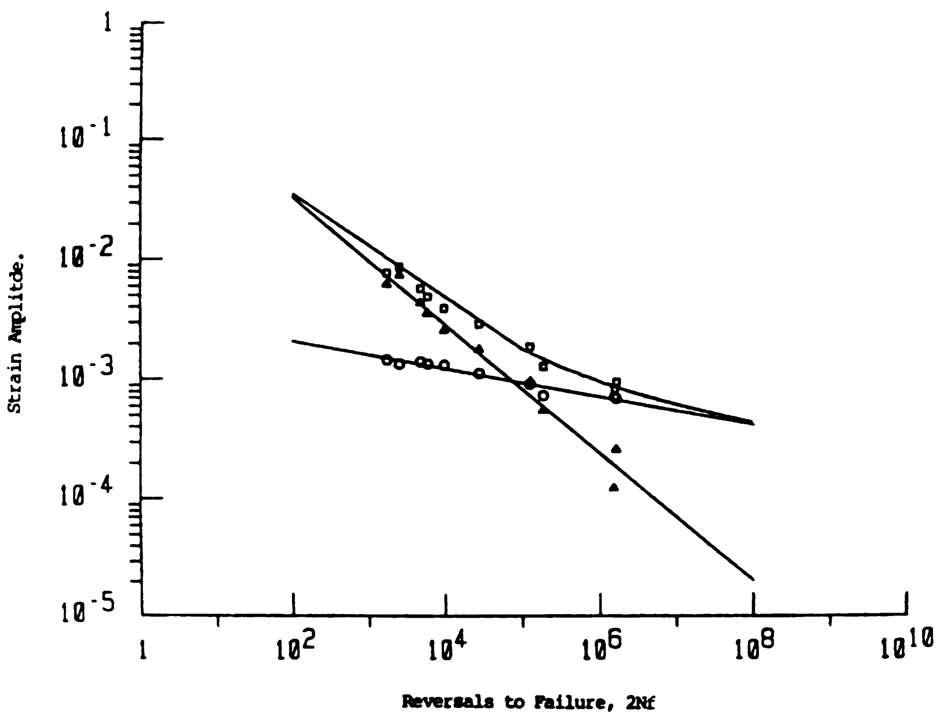

Figure 6.1.41 Strain-reversals to failure data for Thick Sheet Steel Specimens (no overstrain).

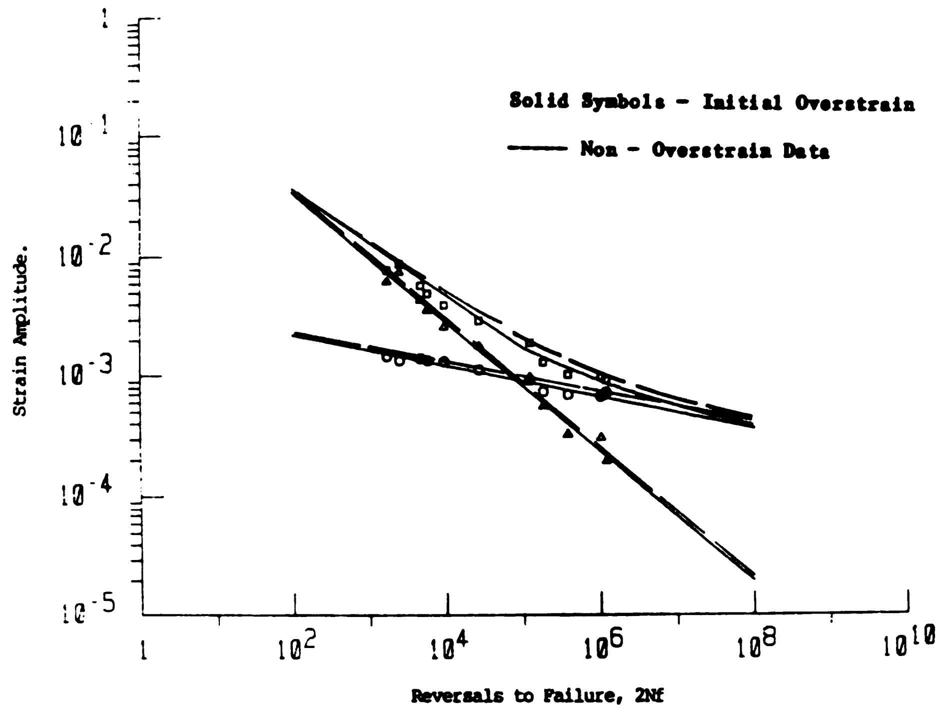

Figure 6.1.42 Strain-reversals to failure data for Thick Sheet Steel Specimens subjected to initial overstrains.

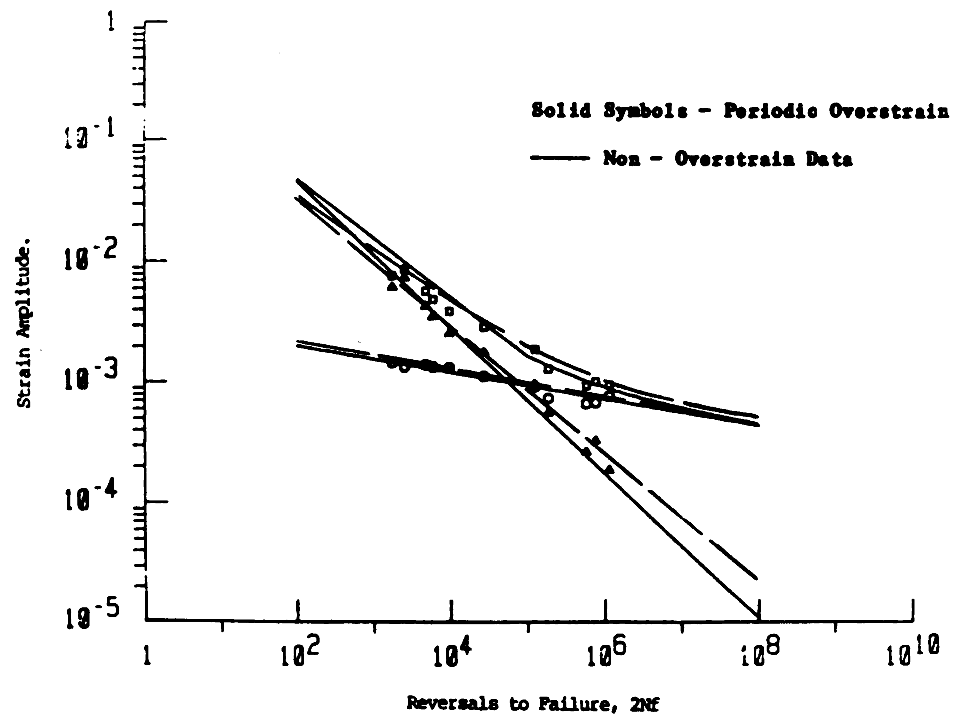

Figure 6.1.43 Strain-reversals to failure data for Thick Sheet Steel Specimens subjected to periodic cyclic overstrains.

The influence of initial and periodic overstraining on the fatigue properties of the materials which were used (as shown in tables 6.1.10 through 6.1.12) and the results of other works[1,2,4,5,13], suggest that the effect of initial and periodic overstraining on a material depends on the condition of the material. In general both initial or periodic overstraining have a detrimental effect on a material but the extent of the effect depends on the material itself.

6.2 SURFACE DAMAGE

Various studies have suggested that the changes associated with damage occurring in a fatigue specimen are continuous. The question of when, in the fatigue life of a specimen, microscopical changes (slip bands, dislocations etc.) occur and how long they last depends on many factors. Chief among these are the stress level and the properties of the material under examination. It is therefore to be expected that all changes may not be observed in a given test or for a given material. Furthermore the type of instrument used, particularly its sensitivity, and the frequency of examination strongly influence the observation of changes which occur.

To assess the effects of various load histories that were imposed in these investigations, the surface damage caused by the cyclic strain was examined. Plastic replicas as described in the procedure section were employed to record the changes which had taken place as a result of fatigue loading. A series of these replicas were taken at different stages (after each 100,000 cycles) of the test and examined by an optical and an electron microscope. Since the replicas recorded the microstructure very accurately, examining them provided the same information that would have come from an examination of the specimens themselves. In this way a permanent record of the microstructure of the specimen during periodic phases of its fatigue life was assembled. Replicas were first made before each test to show the unstrained microstructure of specimens which were chosen for metallographic study. Examples of these microstructures are shown in Figures 6.2.1 to 6.2.5. A description of the various specimens' microstructures as affected by different loadings is provided in the next sub-section.

6.2.1 MICROSTRUCTURE OF NONSTRAINED SPECIMENS

Bar steel specimens, that were made from 1018 annealed steel, show coarse lamellar pearlite, ferrite and bainite containing carbide particles, Figure 6.2.1.

Thin sheet steel specimens and thick sheet steel specimens were made from 1020 and 1030 steel, respectively. The microstructure of thin sheet specimens consists mainly of ferrite, with carbide particles located at grain boundaries, Figure 6.2.2.

The microstructure of the 1030 steel in the as received state is shown in Figure 6.2.3. Evidently the structure is different from the material of the other two specimens. The material was heat-treated

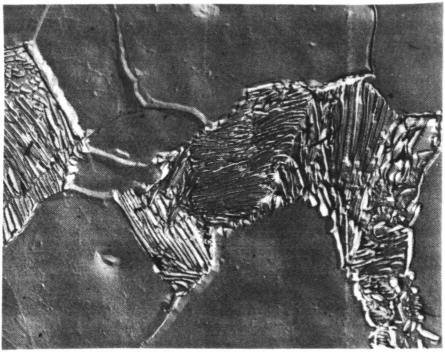

Figure 6.2.1 TEM Replica Micrograph of 1018 Steel Before test (3000X)

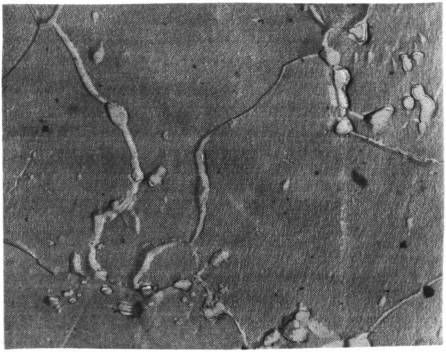

Figure 6.2.2 TEM Replica Micrograph of 1020 Steel Before test (3000X)

(annealed) in order to make it as similar to the other ones as possible. The microstructure of the heat-treated specimen is shown in Figure 6.2.4. The structure of this material after annealing consisted of ferrite and lamellar pearlite.

It should be mentioned that all micrographs were taken from the gage length sections (the rolled side) and after electro-polishing and etching. Figure 6.2.5 shows a typical microstructure of a specimen after mechanical polishing but before electro-polishing. As can be seen in this photo, there are always some scratches after mechanical polishing.

The following three sub-sections describe the metallographical results due to three types of loading. Frequently, while replicas were examined under the electron microscope, the magnification was changed, permitting a particular spot within a grain or changes in neighboring grains to be viewed.

6.2.2 MICROSTRUCTURE OF NON-OVERSTRAINED SPECIMENS

Specimen B.S.27 was subjected to 0.085 percent constant strain. Replicas were taken of the gage surface after each 100,000 cycles until failure. Figure 6.2.6 shows the microstructure of a ferrite grain of this specimen at 10000X after 100,000 cycles. Figure 6.2.7 is a smaller magnification (4500X) of the microstructure of the same specimen after 500,000 cycles which shows several neighboring grains.

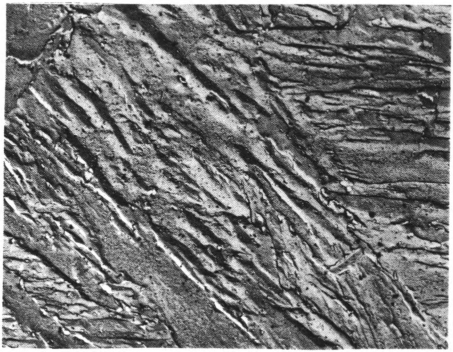

Figure 6.2.3 TEM Replica Micrograph of 1230 Steel as received (3000X)

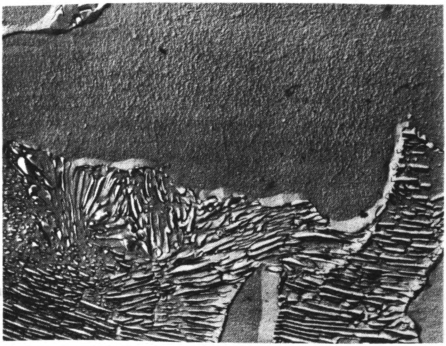

Figure 6.2.4 TEM Replica Micrograph of 1230 Steel After Annealing

(3000X)

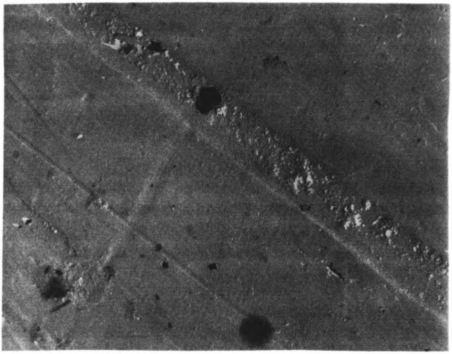

Figure 6.2.5 A typical Micrograph of Specimens After Mechanical Polishing (10000X)

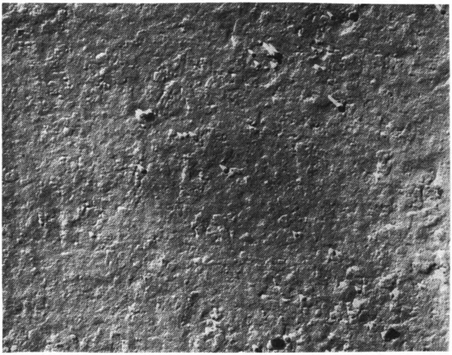

Figure 6.2.6 Microstructure of B.S.27 After 100,000 Cycles (10000X)

No change can be detected from these pictures. As the cycling was continued, however, slip bands were observed in some grains. A typical microstructure of this specimen after 1,000,000 cycles appears in Figure 6.2.8. As can be seen in this picture there are some slip bands in a few grains. Subjecting the specimen to more cyclic loading results in a larger number of deformed grains (i.e. grains in which slip bands have appeared), as well as an increase in the number of slip bands in each grain.

As cycling continued, more and more slip bands are produced, which eventually resulted in the appearance of fine cracks. Figure 6.2.9 displays a typical portion of the microstructure of this specimen after 2,000,000 cycles. There were evidences of some slip bands in the ferrite grains and some fatigue microcracks along some of the slip bands.

With more cycling the number of cracks increases until the specimen finally fails. The microstructure of this specimen after failure (6,266,000 reversals) is shown in Figure 6.2.10 which consists of two ferrite and one pearlite grain. Well-developed fatigue microcracks can be seen in the left ferrite grain.

Specimens B.S.22 and B.S.25 were subjected to 0.095 and 0.1 percent of cyclic strain, respectively. Typical microstructures of these specimens are shown in Figures 6.2.11 to 6.2.14. Examination of the gage sections of these two specimens showed extensive slip band activ-

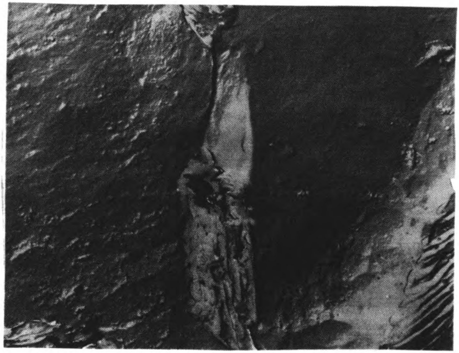

Figure 6.2.7 Microstructure of B.S.27 After 500,000 Cycles (4500X)

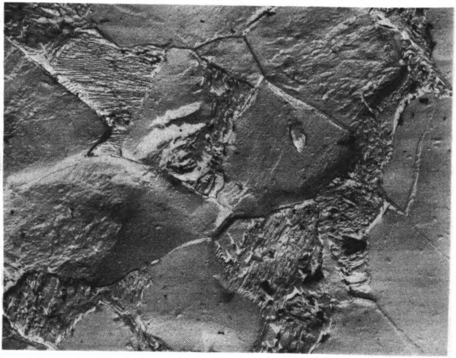

Figure 6.2.8 Microstructure of B.S.27 After 1,000,000 Cycles (2000X)

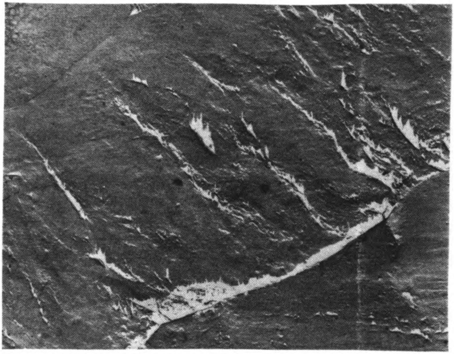

Figure 6.2.9 Microstructure of B.S.27 After 2,000,000 Cycles (3000X)

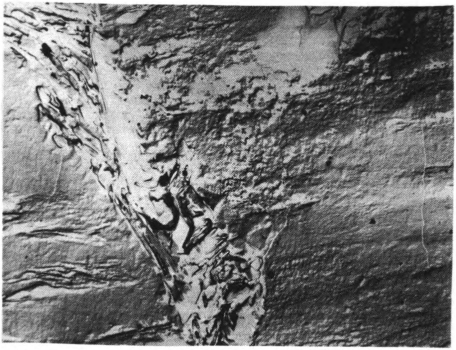

Figure 6.2.10 Microstructure of B.S.27 After Failure (4500X)

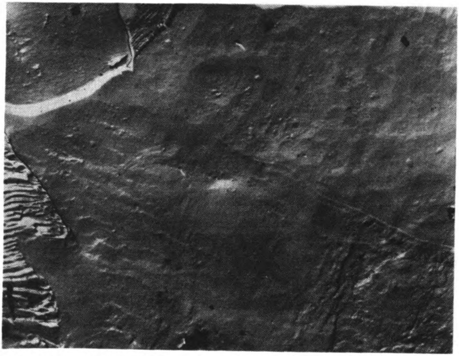

Figure 6.2.11 Microstructure of B.S.22 After 100,000 Cycles (3000X)

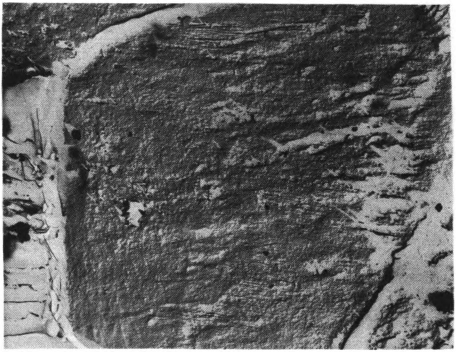

Figure 6.2.12 Microstructure of B.S.22 After 500,000 Cycles (7000X)

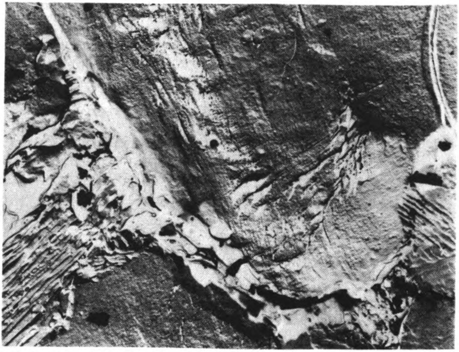

Figure 6.2.13 Microstructure of B.S.25 After 100,000 Cycles (4500X)

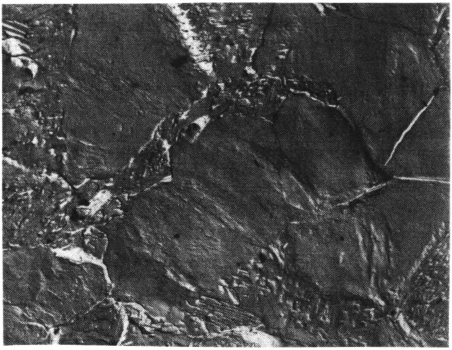

Figure 6.2.14 Microstructure of B.S.25 After 500,000 Cycles (2000X)

ity. The slip band structures of these specimens were extremely dense and they appeared earlier in the test compared with specimen B.S.27, as can be seen in Figure 6.2.12 and 6.2.14. Comparison of these two specimens (even though they were subjected to strain amplitudes close to each other) reveals that slip bands of specimen B.S.25 which was subjected to a relatively higher strain is coarser than those of specimen B.S.22. Figure 6.2.13 shows microcracks in developed slip bands after 100,000 cycles.

Comparison of the results of these three specimens revealed that: specimens subjected to a higher strain range have a significantly higher slip band density than those subjected to a lower strain range. Coarse grains in these specimens undergo more deformation than fine grains. Transmission electron microscope examination of the replicas of these specimens shows more extensive slip band activity in coarse grains than in the finer ones. This may be due to the existence of more favorable orientations for slip or areas of high stress concentration in these grains.

The structure of a 1020 sheet steel specimen that was subjected to 0.1 percent strain of constant amplitude only (specimen T.S.16) is presented in Figures 6.2.15 to 6.2.18. In Figures 6.2.15 and 6.2.16 the successive growth of slip bands from 100,000 to 500,000 cycles is displayed. These micrographs are taken from large grains to demonstrate this phenomenon more clearly. The same phenomenon is observed in small grains. In Figure 6.2.15 which was taken at 3000X, slip

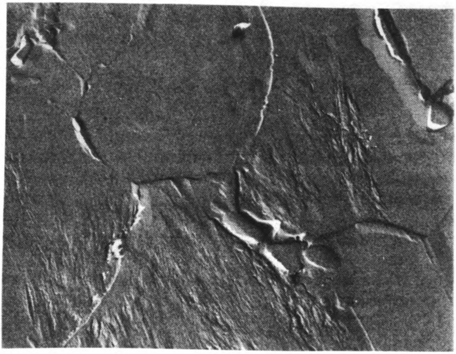

Figure 6.2.15 Microstructure of T.S.16 After 100,000 Cycles (3000X)

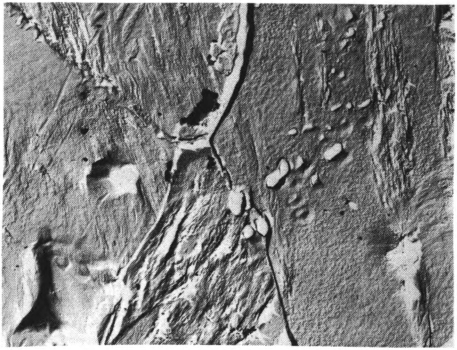

Figure 6.2.16 Microstructure of T.S.16 After 500,000 Cycles (4500X)

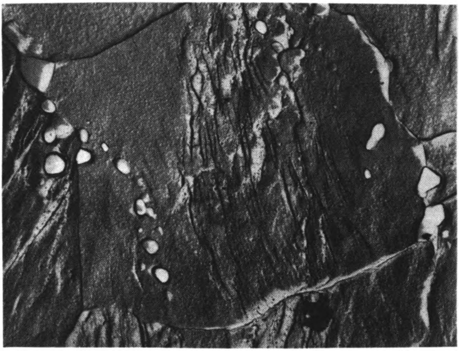

Figure 6.2.17 Microstructure of T.S.16 After Failure (4500X)

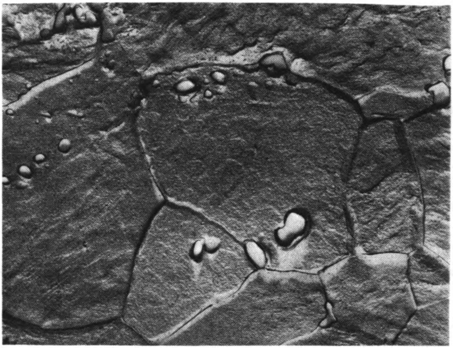

Figure 6.2.18 Microstructure of T.S.18 After 5,000,000 Cycles (3000X)

bands have formed in three adjacent grains while the rest of the grains in this micrograph has no slip bands. This micrograph was taken at this relatively low magnification in order to show more grains.

As the number of cycles increases, slip bands develop very slowly. While the favored direction for the development of the slip lines is usually the longitudinal one, the band sources are activated almost parallel to the primary bands. This formation of new bands, parallel to the primary ones, reduces the band separation and ultimately results in blurring of the bands. Figure 6.2.17 shows the microstructure of this specimen after failure (3,220,000 reversals), which exhibits microcracks in highly developed slip bands and their blockage by grain boundaries. These features (with the exception of the density of slip lines) were also easily observable under optical microscopy.

As can be seen in the photos in most cases, the only sources of blockage that could be detected within each grain were the grain boundaries. This is not unexpected, since these boundaries are saturated with foreign atoms and foreign phase precipitates, i.e. carbide particles in case of 1020 specimens, and thus provide very strong barriers to the bands. This is shown very clearly in Figure 6.2.16 and 6.2.17.

For a thin sheet steel specimen tested at a strain of 0.085 percent (specimen T.S.18) grain boundaries prove to be the ultimate barrier. No slip could be detected in neighboring grains, even after 5,000,000 cycles. Figure 6.2.18 shows a picture taken after 5,000,000 cycles from this specimen. Very fine slip bands can be seen in almost all grains of this specimen at this stage. This specimen failed after 12,695,000 reversals and very few microcracks were observed in a small number of scattered grains. The data of T.S.15 and T.S.17 were disregarded, since they failed as a result of material defects rather than fatigue damage.

Specimen F.S.4, which was made of 1030 steel, was subjected to 0.1 percent strain. Replicas were taken after every 100,000 cycles. These are shown in Figures 6.2.19 to 6.2.24. Close examination shows that there are no slip bands in the gage section up to 300,000 cycles. As the cycling is continued, however, slip bands are found on some grains. Figures 6.2.20 and 6.2.21 show the gage surface after 400,000 and 500,000 cycles, respectively. Again, in order to show more grains in the micrograph, the magnification was reduced. Some fine slip bands in a coarse ferrite grain can be seen in these pictures. As one would expect, the density of slip bands has increased with increased cycling number.

If the cyclic loading is continued, the slip bands give rise to microcracks, which then propagate and finally cause the rupture of the specimen. The appearance of microcracks on the edge of some slip bands can be seen in Figures 6.2.22 and 6.2.23. These were taken from

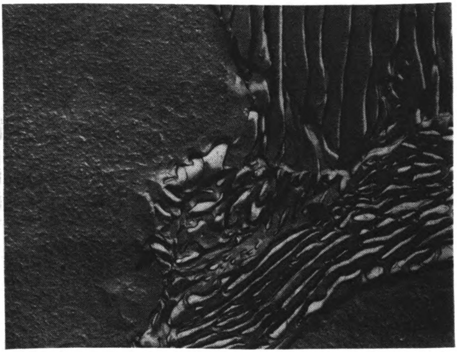

Figure 6.2.19 Microstructure of F.S.4 After 300,000 Cycles (4500X)

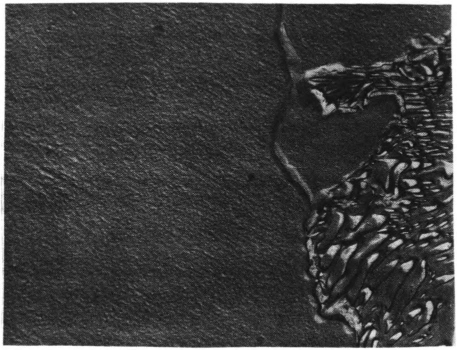

Figure 6.2.20 MIcrostructure of F.S.4 After 400,000 Cycles (3000X)

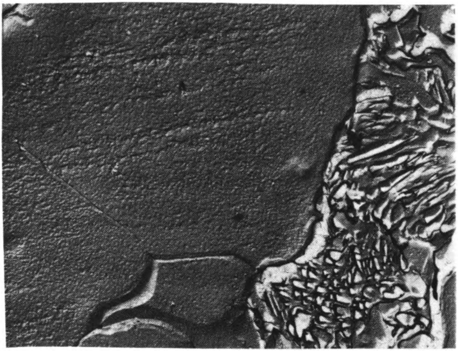

Figure 6.2.21 Microstructure of F.S.4 After 500,000 Cycles (3000X)

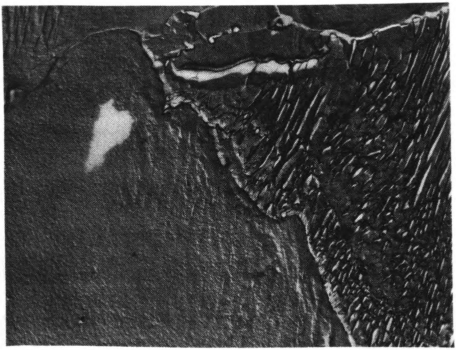

Figure 6.2.22 Microstructure of F.S.4 After Failure (4500X)

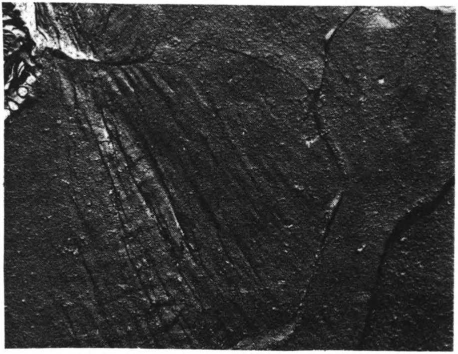

Figure 6.2.23 Microstructure of F.S.4 After Failure (4500X)

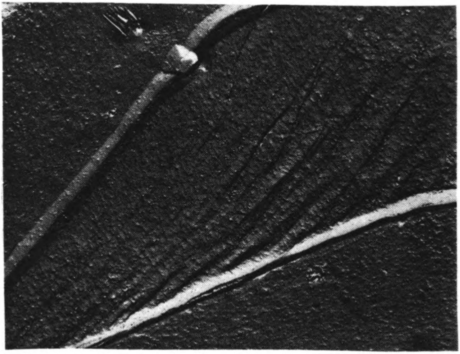

Figure 6.2.24 Microstructure of F.S.11 After 50,000 Cycles (4500X)

different areas of the gage surface of the specimen after failure (1,644,000 reversals).

Figures 6.2.24 to 6.2.26 show the microstructure of specimen F.S.11, which has been subjected to a cyclic load with a slightly higher amplitude (0.13 percent strain). In this case the slip band networks in most areas were moderate to sparse, with some slip bands near grain boundaries in isolated areas. Figure 6.2.25 which has taken at a slightly lower magnification (3000X) shows that even though there exist coarse and well developed slip bands in some grains, still there are other grains without slip bands.

Typical microstructures of the specimens cycled at a constant strain amplitude of 0.2 percent (F.S.10) after failure (127,000 reversals) are displayed in Figure 6.2.26. Microcracks in highly developed slip bands and their blockage by grain boundaries are evident in this picture. Slip bands were observed in most of the grains. The distances between slip bands in this case were greater than in the case of F.S.11.

The obvious conclusion of this part of experiment is that the formation of the slip bands depends on the plastic deformation. In all these samples, small damage in the form of slip bands was always visible around the grain boundaries.

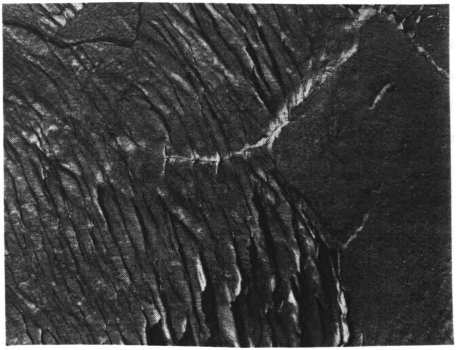

Figure 6.2.25 Microstructure of F.S.11 After Failure (3000X)

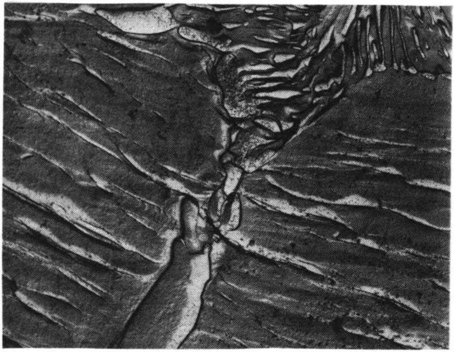

Figure 6.2.26 Microstructure of F.S.10 After Failure (4500X)

6.2.3 INITIAL OVERSTRAINING

Specimens B.S.20, B.S.16 and B.S.12 (of the 1018 bar steel) were subjected to initial overstrains. After overstraining, these specimens were cycled at a constant strain of 0.097, 0.085 and 0.1 percent, rspectively, until they failed. A typical microstructure of these specimens after initial overstraining is shown in Figure 6.2.27. In all the replicas that were taken after initial overstraining on this material, some coarse slip bands were observed at grain boundaries and in the interior of some grains.

It should be mentioned here that all materials used for this investigation, namely 1018, 1020 and 1030 steels, showed cyclic hardening when subjected to overstrain. This was expected, since all of these materials were in annealed conditions.

The behavior of specimen B.S.16 was somewhat anomalous. After this specimen was overloaded and subjected to 5,000,000 cycles, the number of slip bands observed was very small and increased very slowly. After 5,000,000 cycles this specimen was periodically overstrained (this was a break in the standard test program) after every 100,000 cycles 10 times. As a result, some rough slip bands did appear, but the rate of increase was very slow. This specimen did not break and the test was stopped after 6,000,000 cycles. The microtructure of this specimen after initial overstraining is shown in Figure 6.2.27. This micrograph shows a few coarse slip bands in a grain in

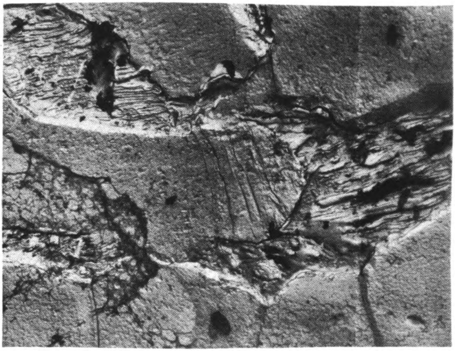

Figure 6.2.27 Microstructure of B.S.16 After Initial Overstrain (3000X)

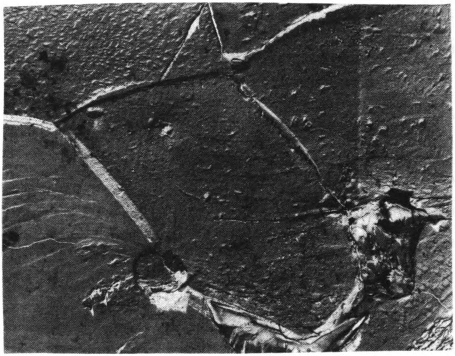

Figure 6.2.28 Microstructure of B.S.16 After 5,200,000 Cycles (3000X)

the center of the picture. Examination of the replicas taken from the gage sections of this specimen showed the existence of some slip bands right after overstraining. Most of these slip bands were found on coarse grains, but as cycling continued -after overstraining- some lines were observed on the finer grains too.

As in the case of no overstrain, the number of slip bands per grain increased with the number of cycles. However, the density of slip bands was higher in the present case. Figure 6.2.28 shows the microstructure and appearance of this specimen after 5,200,000 cycles at 3000X. This micrograph shows some desperse slip bands in some grains. Figure 6.2.29 which was taken after 5,400,000 cycles at 7000X clearly shows well developed slip bands in neighboring grains that were blocked by grain boundaries.

The deformation resulting from the larger strain amplitude after initial overstraining (specimen B.S.20) is shown in Figures 6.2.30 and 6.2.31. It can be seen that the deformation is completely homogeneous, with slip bands present throughout the entire grain (Figure 6.2.30). Close examination of Figures 6.2.30 and 6.2.31 reveals that the slip bands are not uniform, being coarser in the interior of the grain. Microstructures of specimen B.S.12 after 100,000 and 500,000 cycles are shown in Figures 6.2.32 to 6.2.33. As can be seen in Figures 6.2.31 and 6.2.33, there is not much difference between this specimen and specimen B.S.20.

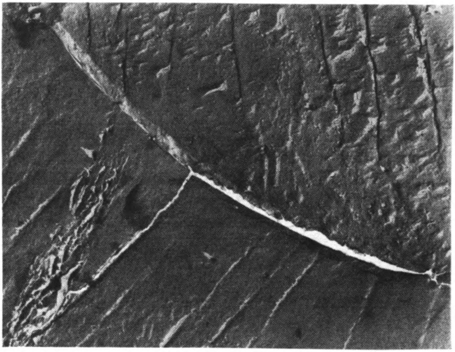

Figure 6.2.29 Microstructure of B.S.16 After 5,400,000 Cycles (7000X)

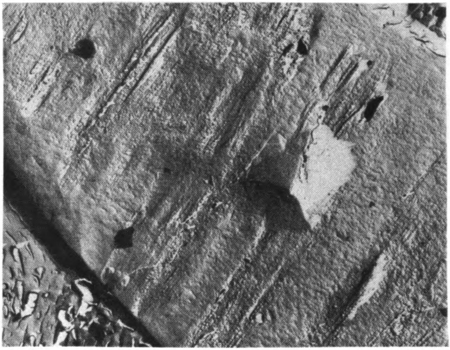

Figure 6.2.30 Microstructure of B.S.20 After 100,000 Cycles (7000X)

Figure 6.2.31 Microstructure of B.S.20 After 800,000 Cycles (2000X)

Figure 6.2.32 Microstructure of B.S.12 After 100,000 Cycles (2000X)

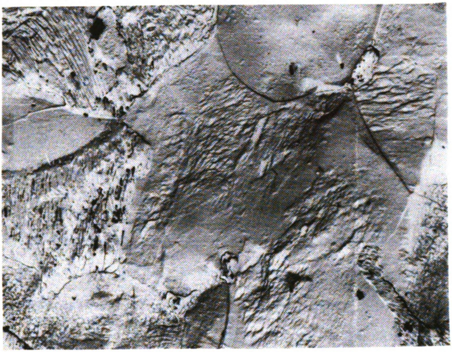

Figure 6.2.33 Microstructure of B.S.12 After 500,000 Cycles (2000X)

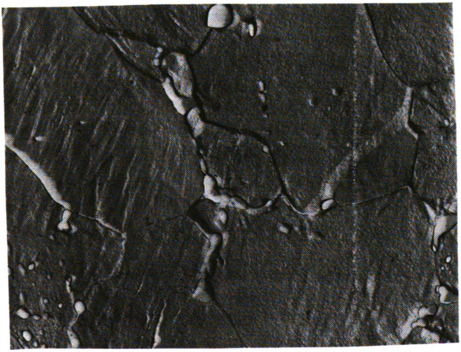

Figure 6.2.34 Microstructure of T.S.19 After Initial Overstrain

(3000X)

From the 1020 sheet steel specimens, specimens T.S.19 and T.S.10 were chosen for microstructural examinations during the fatigue test. These specimens were first overstrained. The replicas, which were taken just after overstraining, showed that slip bands had developed in some coarse grains. Figure 6.2.34 shows several grains of the specimen number T.S.19 after overstraining. Slip bands are observed only in a grain located on the left side of this micrograph.

After overstraining, specimen T.S.19 was subjected to 0.1 percent and specimen T.S.10 to 0.085 percent strain. Examination of the electron micrographs of the replicas taken from the gage sections shows that the number of grains in which slip bands have developed increased with the number of cycles, and the rate of increase was higher than in the case of no overstraining. Some micrographs of gage surfaces of specimen T.S.19 after 200,000 cycles and after failure are shown in Figures 6.2.35 and 6.2.36, respectively. Figure 6.2.37 and 6.2.38 show the development of slip bands in specimen T.S.10 after 200,000 cycles and after failure, respectively. As can be seen in these pictures, slip bands and some fatigue microcracks almost always cover the entire deformed grains, while in the non-overstrain case slip bands mostly cover the centeral portion of deformed grains (see Figure 6.2.17).

From 1030 flat specimens which had been overstrained, specimens F.S.20, F.S.16 and F.S.21, which were strained at 0.09, 0.1 and 0.11 percent, respectively, were selected for microstructural examination.

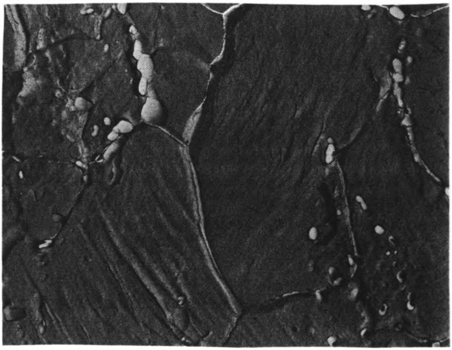

Figure 6.2.35 Microstructure of T.S.19 After 200,000 Cycles (3000X)

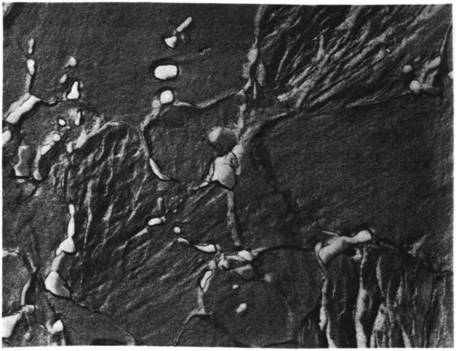

Figure 6.2.36 Microstructure of T.S.19 After Failure (3000X)

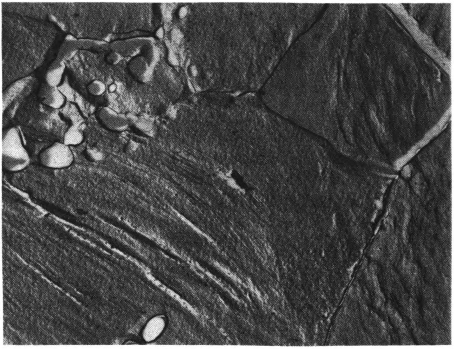

Figure 6.2.37 Microstructure of T.S.10 After 200,000 Cycles (4500X)

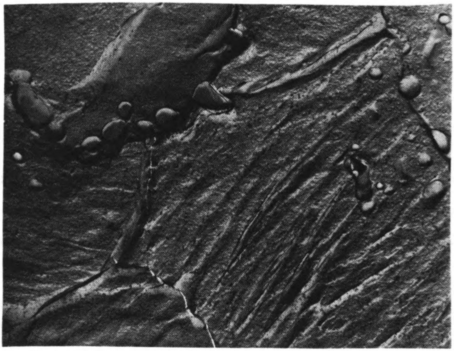

Figure 6.2.38 Microstructure of T.S.10 After Failure (4500X)

The examination showed that the behavior of slip bands in this material was slightly different in comparison with the other two materials studied. Figures 6.2.39 to 6.2.45 show different parts of gage section of these specimens. This material showed more sensitivity to overstrain than the other two. As a result of overstraining, large numbers of coarse slip bands were formed on some grains (Figure 6.2.39). Cycling this specimen after initial overstraining at the abovementioned strain level caused the slip bands, which were produced by overstrain, to enlarge and resulted in some fine microcracks to appear along them. Figure 6.2.40 shows the fine microcracks along the slip bands in a ferrite grain, while Figure 6.2.41 shows well developed microcracks along slip bands and some fine microcracks around the boundary of two ferrite grains. Figures 6.2.42–6.2.45 are other examples of formations of slip bands and microcracks on some grains of this material after cycling at different strain amplitudes.

In the initial overstraining case it is observed that slip bands appear at a relatively low rate if the overstrainig is followed by low strain amplitude cycling. On the other hand, if the overstraining is followed by a high strain amplitude cycling, the rate of appearance of the slip bands is also higher. Comparing the results of initial overstraining, with that of no overstraining, one finds that initial overstraining accelerates the appearance of the slip bands. More specifically, if in a specimen subjected to cyclic loading of a given amplitude, the slip bands appear after a certain number of cycles, the same phenomenon in an overstrained specimen subjected to the same

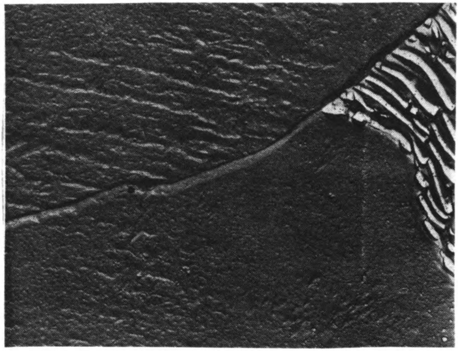

Figure 6.2.39 Microstructure of F.S.20 After Initial Overstrain

(4500X)

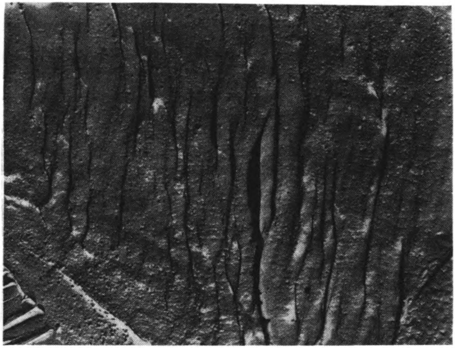

Figure 6.2.40 Microstructure of F.S.20 After 1,000,000 Cycles (7000X)

Figure 6.2.41 Microstructure of F.S.20 After 12,206,494 Cycles (3000X)

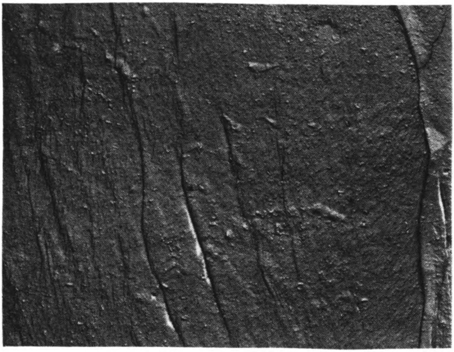

Figure 6.2.42 Microstructure of F.S.16 After 300,000 Cycles (3000X)

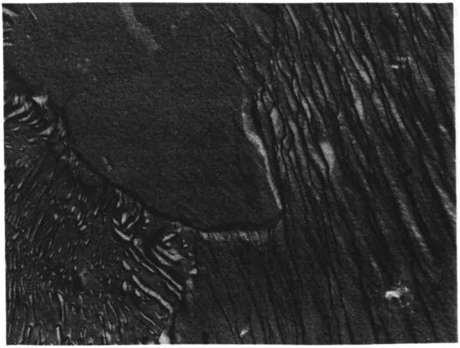

Figure 6.2.43 Microstructure of F.S.16 After Failure (3000X)

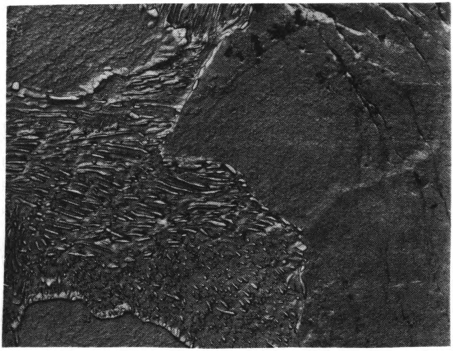

Figure 6.2.44 Microstructure of F.S.13 After 100,000 (3000X)

Figure 6.2.45 Microstructure of F.S.13 After Failure (4500X)

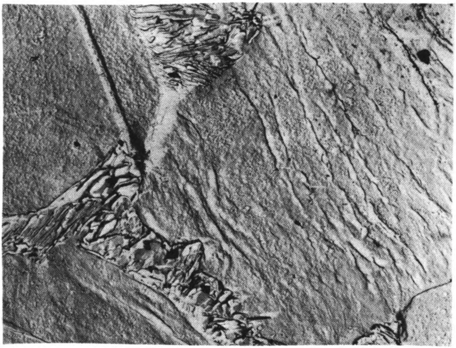

Figure 6.2.46 Microstructure of B.S.5 After Third Overstrain (3000X)

cyclic loading occurs much earlier.

In some cases the life of initially overstrained specimens was longer than those specimens which had not been overstrained at all. The reason for this increasing fatigue life could be both the dispersion hardening effect of the carbids and the smaller grain size.

6.2.4 PERIODIC OVERSTRAINING

The following specimens were chosen for metallographic examination in the periodically overstrained test series: Specimens B.S.3 ,B.S.5, B.S.19 and B.S.23 from the bar steel specimens; specimens T.S.21 and T.S.23 from the sheet steel specimens; and specimens F.S.17, F.S.18 and F.S.12 from the thick sheet steel specimens. These specimens were overstrained after each 100,000 cycles. The constant strain that each specimen was subjected to during the fatigue test is shown in Tables 6.2.8 - 6.2.16. Figures 6.2.46 to 6.2.66 show the microstructure of these overstrained specimens after certain numbers of overstraining. The microscopic structure of these specimens after the first overstraining is not shown here, since it is identical to the case of initial overstrain.

The microstructures of specimen B.S.5, which was subjected to .093 percent strain, after different degrees of overstraining are shown in Figures 6.2.46 to 6.2.48. The slip bands within the grains of this specimen after the third, seventh, and sixteenth overload can

Figure 6.2.47 Microstructure of B.S.5 After Seventh Overstrain

(2000X)

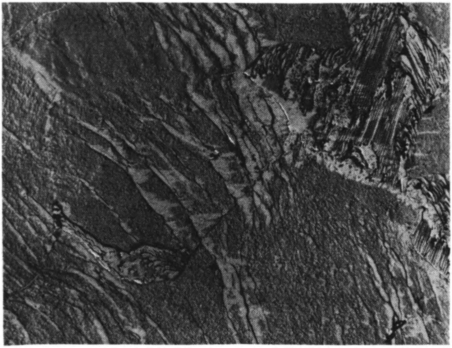

figure 6.2.48 Microstructure of B.S.5 After Sixteenth Overstrain

(3000X)

be seen clearly in these figures. These micrographs were taken at relatively low magnification in order to show more grains. As can be seen clearly in these photos, slip bands are evenly distributed over the ferrite grains, and, as the number of overstrain blocks increase, in some grains they get denser, especially along the grain boundaries.

Figures 6.2.49 to 6.2.51 show the microstructure of specimen B.S.23, which was tested at 0.0102 percent strain, after the second, fourth and sixth overstraining. The extremely dense slip band structure of this specimen is clearly evident from these pictures. Similar results were also observed from the specimen B.S.3 which was tested at 0.095 percent strain. Photographs of this specimen are not shown.

The microstructure of specimen T.S.23 after different numbers of overstraining appears in Figures 6.2.52 to 6.2.56. As can be seen from these photos most slip bands are coarse. Furthermore, as the number of overstrain blocks is increased, the number of these slip bands and their length also increases. Very few fine slip bands can be found in any of these pictures. However, after the second overstraining, well developed fatigue slip bands and microcracks can be seen in most areas of the gage sections. Since specimen T.S.21 had a life which was much shorter than what was predicted, the data it provided was not considered here.

Tests with 1030 steel show that this material is highly sensitive to overstrain. In particular, the fatigue life is shortened by over-

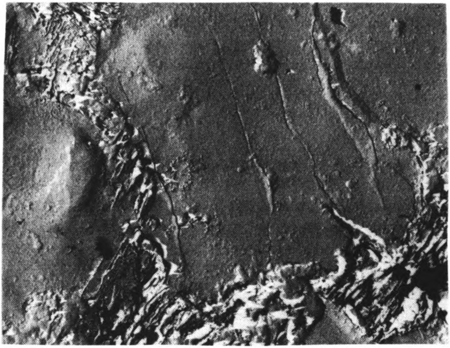

Figure 6.2.49 Microstructure of B.S.23 After Second Overstrain

(3000X)

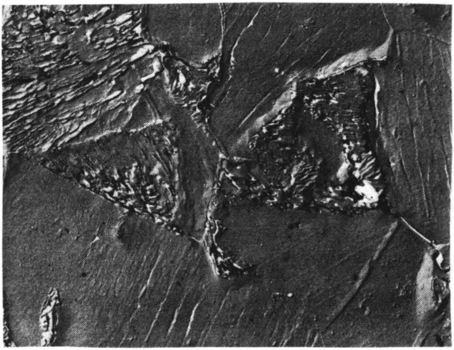

Figure 6.2.50 Microstructure of B.S.23 After Fourth Overstrain

(2000X)

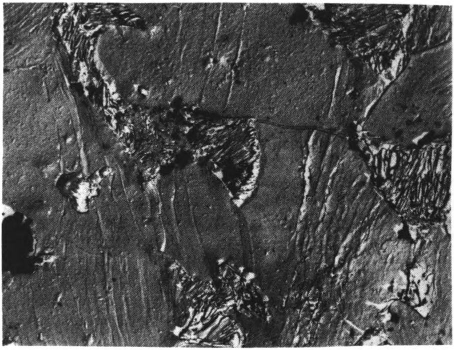

Figure 6.2.51 Microstructure of B.S.23 After Sixth Overstrain (1500X)

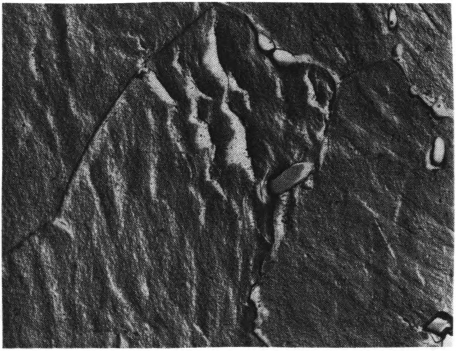

Figure 6.2.52 Microstructure of T.S.23 After Second Overstrain

(4500X)

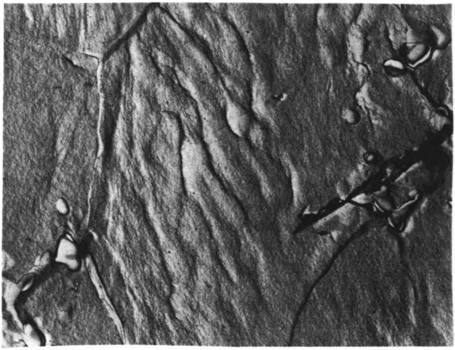

Figure 6.2.53 Microstructure of T.S.23 After Fourth Overstrain (4500X)

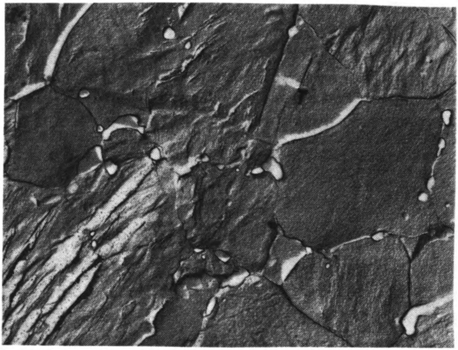

Figure 6.2.54 Microstructure of T.S.23 After Sixth Overstrain (3000X)

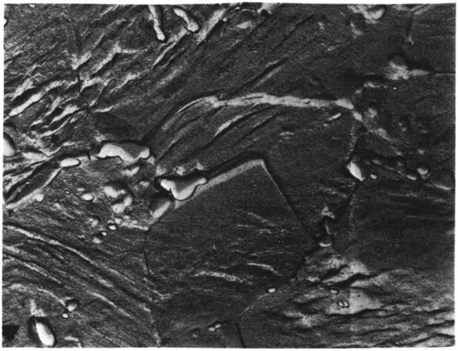

Figure 6.2.55 Microstructure of T.S.23 After Seventh Overstrain

(3000X)

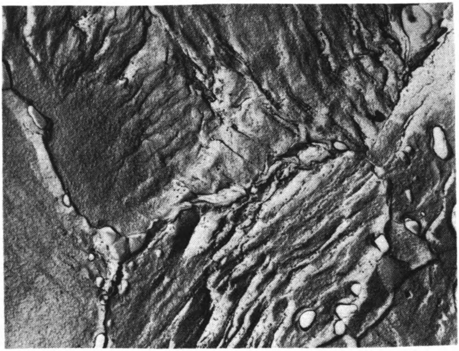

figure 6.2.56 Microstructure of T.S.23 After Failure ((4500X)

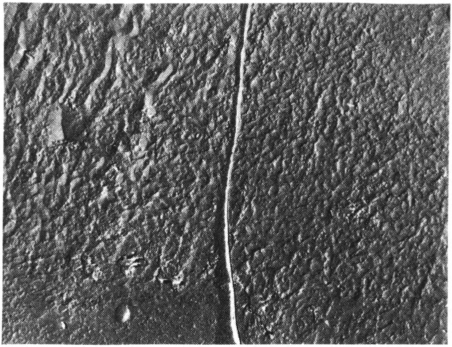

Figure 6.2.57 Microstructure of F.S.17 After Second Overstrain

(7000X)

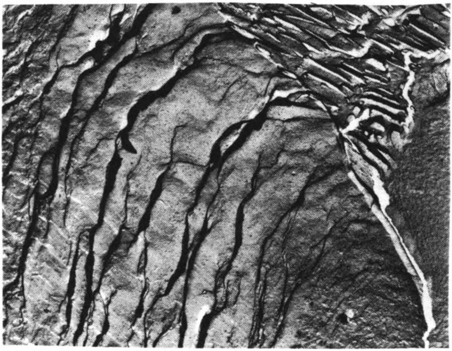

Figure 6.2.58 Microstructure of F.S.17 After Tenth Overstrain (4500X)

Figure 6.2.59 Microstructure of F.S.17 After Failure (4500X)

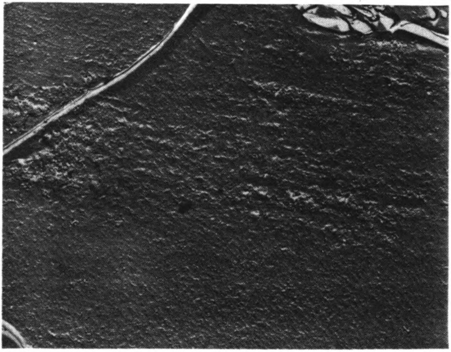

Figure 6.2.60 Microstructure of F.S.18 After Second Overstrain

(4500X)

strain. Figures 6.2.57–6.2.59, show the microstructure of F.S.17 after second, and tenth overstraining, and failure (2,336,000 reversals). Comparison of these micrographs reveals the damages (slip bands and microcracks) that were caused by successive overstraining. Figures 6.2.60 - 6.2.62 show microstructures of specimen F.S.18. Successive growth of slip bands and fatigue microcracks are clearly evident in these photographs. Figures 6.2.63 - 6.2.65 display the microstructure of specimen F.S.12 after the second and third overstrain. Figure 6.2.65 shows a magnified section of the micrograph shown in Figure 6.2.64 (upper left portion). In this micrograph simultaneous interpenetration of two different slip bands is shown. This phenomenon was not observed for the other two materials. Comparison of the micrographs taken between two successive overstrains during the fatigue test shows that the appearance of slip bands for this material was faster than those for 1018 and 1020.

Another interesting feature of the 1030 specimens is that specimens which were subjected to initial overstraining had a longer life compared with specimens subjected to periodic overstraining. This may be because of non-uniformity of the grain size of this material.

Examination of replicas taken from the gage section of overstrained specimens after a certain period (usually after each overstraining) reveals that overstraining gives rise to a large number of well-developed slip bands. Slip bands first started to appear on the coarse grains, and the density in these grains was higher. A sim-

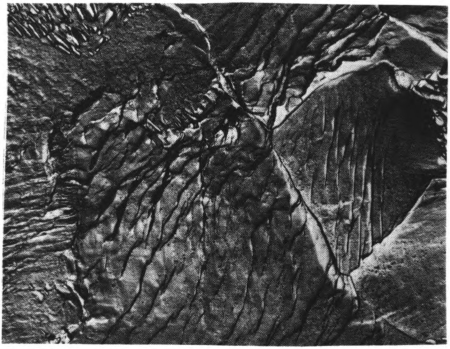

Figure 6.2.61 Microstructure of F.S.18 After Fifth Overstrain (3000X)

Figure 6.2.62 Microstructure of F.S.18 After Failure (7000X)

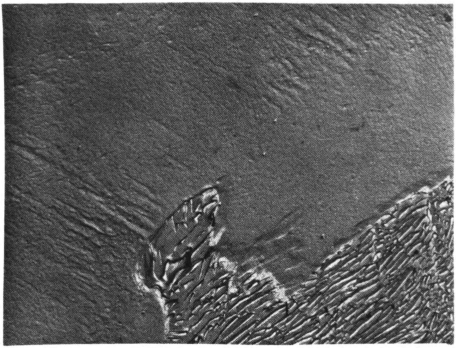

Figure 6.2.63 Microstructure of F.S.12 After Second Overstrain

(3000X)

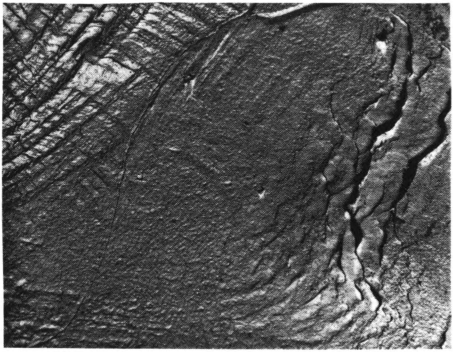

Figure 6.2.64 Microstructure of F.S.12 After Third Overstrain (3000X)

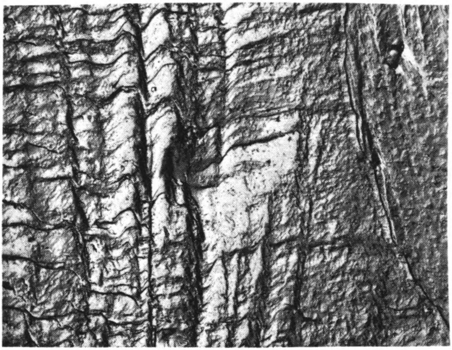

Figure 6.2.65 The same as 6.2.64 but higher Magnification (7000X)

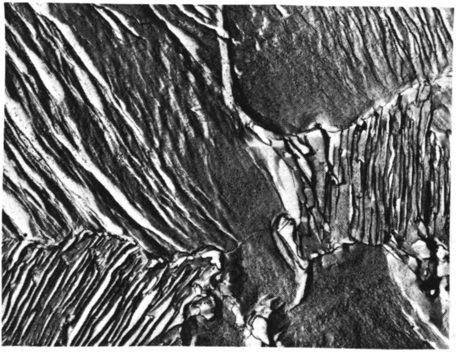

Figure 6.2.66 Microstructure of F.S.12 After Failure (3000X)

ilar phenomenon was observed in the case of initial overstraining. As can be seen in Figures 6.2.46 - 6.2.66, a large number of well-developed slip bands were present in some grains. At the beginning of overstraining, the density of these slip bands was low, but increased as the cycling continued.

While an increase in the number of overstrains during a test resulted in an increase in the slip band density, it seems reasonable to conclude that the development of the slip bands is solely due to overstraining, and cycling between two overstrains seems only to eliminate the hardening which is caused by overstraining.

Overstraining results in the hardening of the specimens. It also causes coarse slip bands in the weak grains of the specimens. Periodic overstraining prevents the development of fine slip bands, which usually appear when a specimen is cycled with a small amplitude. Moreover, it results in an increase in the number of coarse slip bands and microcracks as well as the extension of existing microcracks.

In general, it can be said that continued cyclic loading leads to an increased slip band activity resulting in microcracks which, in turn, propagate until the specimen fails. An increased strain amplitude accelerates the development of slip bands, it also makes them denser and coarser. If the specimen experiences an initial overstraining the formation of slip bands occurs at a faster rate which causes a large number of coarse slip bands to form. The susceptibility to overstrain for 1030 specimens is higher than for the other two materials. Both the periodic overstraining itself and a rise in its frequency increase the density of the slip bands. While the formation of slip bands can be attributed to overstraining only, the hardening caused by it is neutralized by cycling between the overstrains. For all three types of loading, grain boundaries serve as the sources of blockage within each grain.

As mentioned in the previous section, the extent of the effect of overloading differs for different materials. Changes which occured in microstructures due to cycling were very much dependent on the history of the specimens and the materials.

The following recommendations resulted from this study: first, tests (either initial or periodic overstraining) should be performed on pure materials, second, it could be useful to study the structural damage in layers close to the surface of specimens. This should be done on thin enough specimens to enable the making of thin foil samples for electron microscopy examination without the need of slicing the gage section or any other usage of a mechanical device.

CHAPTER 7

SUMMARY AND CONCLUSIONS

In this investigation more than 75 plain carbon steel specimens of three different geometries were tested under one of the following conditions: no overstrain, initial overstrain, and periodic overstrain.

Each overstrain block consisted of 20 decreasing cycles with a maximum strain of ±1 percent. All tests were performed under completely reversed strain control. For thin sheet specimens, axial strain was calculated from the axial stress and transverse strain, and then used to control the test. During each fatigue test, hysteresis loops were recorded to show cyclic behavior and for correlation with microstructural data. Among these loops the stable ones were chosen as representative loops and cyclic stress-strain properties were determined from them. Fatigue properties of each material were determined from the same stress-strain data that were used to determine the cyclic stress-strain properties.

To study the microstructure of the specimens and to detect slip bands and fatigue microcracks, some of the specimens of each kind were polished and then etched to obtain a fine smooth surface. Plastic replicas were then made from the whole gage sections of these specimens after every 100,000 cycles and after each overstraining. A series of replicas formed a permanent record of the (surface) microstructure of the specimen during its fatigue life.

These three steels exhibited cyclic softening at low strain amplitudes and cyclic hardening at higher amplitudes. Furthermore they never become completely stable under any strain amplitude. The instability observed seems to be cycle dependent. In general the fatigue test results showed the pattern characteristic of mild steels.

For all of these steels, cyclic overstraining resulted in a small amount of hardening which in turn reduced the amount of plastic strain. When the specimen was cycled continuously at a constant amplitude it softened and returned to its stable condition. For 1018 cylindrical specimens, periodic overstraining resulted in a fatigue life which was appreciably higher than when the specimens received only an initial overstrain. This can be attributed to the strain hardening of the material during the overstrain and also the uniform microstructure of the material. (Recall that the 1018 steel has finer and more uniform grains.) On the other, hand constant amplitude cycling of specimens of this material yielded a fatigue life only slightly higher than that of periodically overstrained specimens.

Overstraining of the 1020 thin sheet specimens did not produce any significant change in the fatigue life, whereas periodic cyclic overstrain had a noticeable effect. Initial overstraining of 1030 sheet specimens was found to have no appreciable effect on fatigue life of these specimens, whereas periodic overstraining caused a sharp decrease in the fatigue life. This is almost entirely due to the nonuniformity of the grains of this material.

For all the materials which were used, the structural deformation (i.e. the appearance of slip bands, initiation of microcracks, etc.) was found to be inhomogeneous and history dependent. As expected, slip bands appeared in weaker grains (coarse ferrite grains) first. No slip bands were observed in the pearlite grains. As for microcracks, in all cases they initiated within the grains and not along the grain boundaries as has sometimes been reported.

In general the mechanical properties of the material seemed to be affected by local plastic strain and fatigue damage resulting from the application of cyclic strain.

REFERENCES

[1]. Koterazawa, R., "Fatigue Crack Propagation under Periodic Overstressing , Int. Journal of Fracture, Vol.12, No. 1, (1976), pp.169-171.

[2]. Belyaev, V. I., Problems of Metal Fatigue, Daniel Davey and Co., Inc., New York, 1963.

[3]. Watson, P., and Topper, T. H., "Fatigue-damage Evaluation for Mild Steel Incorporating Mean Stress and Overload Effects", Experimental Mechanics, Vol.12, No.1, 1972,pp.11-17.

[4]. Ditschun, A., Cyclic Fatigue Behaviour of Ferrovac E, mimeographed notes prepared for Faculty of Mech. Eng. University of Waterloo, Waterloo, Ontario, January 5, 1976.

[5]. Schijve, J., "Cumulative Damage Problems in Aircraft Structures and Materials , Journal of Aeronautical, Vol.74, No. 714, 1970, pp.517-531.

[6]. Topper, T. H. and Sandor, B. I., "Effects of Environment and Complex Loading History on Fatigue Life , ASTM STP 462, American

Society for Testing and Materials, 1970, pp.93-104.

[7]. Kocanda, S., Fatigue Failure of Metals, Sijthoff and Noordoff International Publishers, 1978.

[8]. Dowling, N. E., "Fatigue Failure Predictions for Complicated Stress- Strain History", Journal of Materials, JMLSA, Vol.7, No.1, March 1972, pp.71-87.

[9]. Topper, T. H., Sandor, B. I. and Morrow, J.,"Cumulative Fatigue Damage under Cyclic Strain Control", presented at the 70th Anual Meeting, American Society for Testing and Materials, Boston, Mass., June 1967.

[10]. Kommers, H. J., "The Effect of Overstressing and Understressing in Fatigue", Proceedings, American Society for Testing and Materials, Vol.38, 1938, pp.249-268.

[11]. Kommers, H. J., "The Effect of Overstressing and Understressing in Fatigue", Proceedings, American Society for Testing and Materials, Vol.43, 1943, pp.749-762.

[12]. Kommers, H. J., "The Effect of Overstress in Fatigue on the Endurance life of Steel", Proceedings, American Society for Testing Materials Vol.45, 1945, pp.532-543.

[13]. Watson, P. and Topper, T. H. "The Effects of Overstrain on the Fatigue Behaviour of Five Steels", Presented at the 1970 Fall Meeting of the Metallurgical Society, Oct. 1970, Cleveland, Ohio.

[14]. Watson, P., Hoddinott, D. S. and Norman, J. P., "Periodic Overstrains and Random Fatigue Behavior", ASTM STP 519, American Society for Testing and Materials, 1973,pp. 271-284.

[15]. Bennett, J. A., "A Study of the Damage Effect of Fatigue Stressing on X4130 Steel", Proceedings, American Society for Testing Materials, Vol.46, 1946, pp.693-711.

[16]. Dolan, T. J., Richart, Jr., F. E., and Work, C. E., "The Influence of Fluctuations in Stress Amplitude on the Fatigue of Metals", Proceedings, American Society for Testing and Materials, Vol.49, 1949, pp.646-679.

[17]. Landgraf, R. W., and LaPointe, N. R., "Cyclic Stress- Strain Concepts Applied to Component Fatigue Life Prediction", SAE Paper 740221, Society of Automotive Engineers, Vol.83, 1974, pp. 1198-1207

[18]. Dowling, N. E., "Fatigue Life and Inelastic Strain under Complex Histories for an Alloy Steel", Journal of Testing and Evaluation, JTEVA, Vol.1, No. 4, July 1973, pp. 271-287.

[19]. Forsyth, P. J. E., The Physical Basis of Metal Fatigue,

Blackie and Son Limited, London and Glasgow, 1969.

[20]. Reed Hill R. E., Physical Metallurgy Principles, Van Nostrand Reinhold Company, 1970.

[21]. Fuchs, H. O. and Stephens, R. I., Metal Fatigue in Engineering, John Wiley and Sons, Inc., New york, 1980.

[22]. Kennedy, A. J., Processes of Creep and Fatigue in Metals, John-Wiley and Sons, Inc., New York, 1963.

[23]. Laird, C.,"Fatigue", Materials Science and Engineering, Vol.25, 1976, pp.187-191.

[24]. Miner, M. A.,"Cumulative Damage in Fatigue", Journal of Applied Mechanics, Vol.12, No.3, Sep. 1945, pp.A-159-164.

[25]. Sandor, B. I., Fundamentals of Cyclic Stress and Strain, The University of Wisconsin Press, 1972.

[26]. Socie, D. F., Mitchell, M. R., and Caulfield, E. M., Fundamentals of Modern Fatigue Analysis, FCP Report No.26, College of Engineering, University of Illinois, Urbana, Illinois, April, 1977.

[27]. Morrow, J., "Cyclic Elastic Strain Energy and Fatigue of

Metals", ASTM STP 378, American Society for Testing and Materials, 1964, pp.45-84.

[28]. Martin, J. F., "Cyclic Stress-Strain and Fatigue Properties of Sheet Steels As Affected by Load Spectra", Journal of Testing and Evaluation, JTEVA, Vol.11, No. 1, Jan.1983.

[29]. Raske, D. T. and Morrow, JoDean, Mechanics of Materials in Low Cycle Fatigue Testing, Manual on Low Cyclic Fatigue Testing, ASTM STP 465, American Society for Testing and Materials, 1969, pp.1-25.

[30]. Goodhew, P. J., Specimen Preparation in Materials Science, North-Holland Publishing Company, 1972.